1 2  9 0

UNIVERSIDADE D
COIMBRA

Hugo Peña Gómez

Coupling Light Propagation and Diffusion in Drug Delivery: A Mathematical Approach

Tese no âmbito do Programa Interuniversitário de Doutoramento em Matemática, orientada pelos Professores Doutor José Augusto Mendes Ferreira e Doutor Luis Miguel Dias Pinto e apresentada ao Departamento de Matemática da Faculdade de Ciências e Tecnologia da Universidade de Coimbra.

Julho de 2023

COUPLING LIGHT PROPAGATION AND DIFFUSION IN DRUG DELIVERY: A MATHEMATICAL APPROACH

Hugo Peña Gómez

UNIVERSIDADE D COIMBRA

U.PORTO

UC|UP Joint PhD Program in Mathematics

Programa Interuniversitário de Doutoramento em Matemática

PhD Thesis | Tese de Doutoramento

Julho 2023

Abstract

This work aims to study numerical methods for systems of partial differential equations (PDEs) that arise in light-controlled drug delivery. Because of its noninvasive nature, ease of application, and temporal and spatial control, light has been called a magic tool for controlled drug delivery. We can classify light-responsive polymeric drug carriers into photochemical and photothermal, depending on the nature of the links between the drug particles and the polymeric chains. In this work, we consider photochemical drug carriers. Due to photon scattering, we can use a diffusion equation to describe light propagation through polymeric structures and live tissue. Consequently, we can model drug release from a light-responsive polymer using a system of PDEs that describes light propagation, bound and unbound drug dynamics, and drug transport.

The numerical schemes investigated in this work rely on space discretizations based on finite differences methods that, under appropriate integration rules, can be written as piecewise linear finite element methods. The stability and convergence analysis of the proposed numerical schemes are the main objectives of this work. We remark that the proof of stability requires the uniform boundedness of the numerical solution with respect to the mesh's step sizes. Such boundedness is determined using error estimates established for smooth and nonsmooth solutions. Numerical experiments illustrate the main theoretical results and the model's applicability to light-controlled drug delivery.

Resumo

Neste trabalho estudamos métodos numéricos para sistemas de equações com derivadas parciais que surgem no contexto da libertação controlada de fármacos ativada por luz. Devido à sua natureza não invasiva, fácil utilização, e controlo espacial e temporal, a luz é considerada uma ferramenta mágica para a libertação controlada de fármacos. Sistemas poliméricos fotossensíveis para a libertação controlada de fármacos podem ser classificados em sistemas fotoquímicos e sistemas fototérmicos, dependendo da natureza das ligações entre as partículas de fármaco e as cadeias poliméricas. Neste trabalho consideramos sistemas fotoquímicos. Atendendo ao espalhamento dos fotões, podemos utilizar uma equação parabólica para modelar a propagação da luz em polímeros e tecido vivo. Consequentemente, modelamos a libertação controlada de fármacos a partir de uma estrutura polimérica fotossensível por um sistema de equações de derivadas parciais que descreve a propagação da luz, a dinâmica entre fármaco ligado e livre e o transporte do fármaco livre.

Os esquemas numéricos investigados neste trabalho assentam em discretizações espaciais baseadas em métodos de diferenças finitas que, utilizando fórmulas de quadratura adequadas, podem ser escritos como métodos de elementos finitos segmentados lineares. A análise da estabilidade e convergência dos esquemas numéricos propostos é o principal objetivo deste trabalho. Notamos que o estudo da estabilidade requer a limitação uniforme da solução numérica relativamente ao tamanho das malhas. Esta propriedade é demonstrada utilizando as estimativas de erro estabelecidas para soluções regulares e não regulares. Simulações numéricas ilustram os principais resultados teóricos e a aplicabilidade do modelo no contexto da libertação controlada de fármacos recorrendo a polímeros fotossensíveis.

Acknowledgements

First, I thank my advisors, Professor José Augusto Ferreira and Researcher Luis Pinto, for all the support, knowledge, and kindness they shared with me so this thesis could be fulfilled. I have the privilege of meeting with them and enjoying their endless positive energy in mathematics and academic work. To them, my deepest gratitude.

Next, I would like to thank my classmates from the Ph.D. program for their help and companionship. I wish all of them the best.

To Ana, Carla, Herman, and Igor, I have to say that I appreciate very much all those moments around Coimbra, running days, and dinners. Especially those dinners during the pandemic. Thanks for your friendship; I am going to miss you.

I gratefully acknowledge the support of my friends and colleagues in Costa Rica. It was not an easy task for me to detach myself from all my other projects to start the Ph.D. program; however, my friends always assisted me with everything they could.

I would also like to thank Ayk, Vincenzo, and Geovan for the shared moments playing football. I also thank all the wonderful people I met in Coimbra who helped me to enjoy my time in Portugal even more.

I must mention that during all the time that I have been in Portugal, my family has given me all the support they could, as they always have. It has been a joy to count on them unconditionally. To them, I am very grateful. Particularly thanks to Carla, with whom I have had the opportunity to share much of my life in Coimbra.

I thankfully acknowledge the financial support from the Portuguese Foundation for Science and Technology through the Ph.D. fellowship PD/BD/150551/2019. Also, a special thanks to the Center for Mathematics of the University of Coimbra for hosting me and financing my participation in academic events.

Table of contents

List of figures

List of tables

Chapter 1

Introduction

1.1 Drug delivery enhanced by light

Conventional drug delivery systems, such as tablets, capsules, ointments, syrups, suppositories, are characterized by repeated high doses, concentration fluctuations in the plasma, poor bioavailability, and poor absorption by the target sites. Due to the repeated applications, oscillatory behavior of the concentration in the target is observed, with a possible accumulation of drug above the toxic level leading to side effects. Controlled drug delivery systems were designed to keep the drug concentration within the therapeutic window, thus avoiding undesirable side effects. The drug and the excipient's properties play an essential role in the sustained release of the drug. Examples of controlled drug delivery systems are eye implants and stents. Eye implants are used in the anterior eye chamber to treat diseases like glaucoma [9] or in the posterior eye chamber to treat diseases like uveitis, diabetic macular edema, and retinitis pigmentosa [10], while stents are used to treat atherosclerosis [11].

According to the World Health Organization, cancer is a leading cause of death worldwide, and the most common cancers are breast, lung, colon, rectum and prostate. Cancer treatment usually includes surgery, radiotherapy, and/or systemic therapy (chemotherapy, hormonal treatments, and targeted biological therapies).

The most traditional cancer treatment is the chemotherapy, usually administered systemically. The chemotherapeutic drugs attack the tumor cells in different phases of their life cycle, altering their ability to grow and/or to proliferate, leading to their death. However, the chemical agents are not selective, interfering with the life cycle of non-cancer cells, leading to severe side effects and life quality deterioration of the cancer patients. Chemotherapy is also limited by high-dose drug requirements, the formation of drug resistance, and non-specific drug targeting [12–14].

To avoid some of these disadvantages, it is crucial to develop techniques that allow the localized and controlled delivery of chemotherapeutic drugs to the target, thereby preventing severe side effects caused by drug interactions with healthy cells. The localized release is crucial to minimize undesirable side effects induced by drugs with high toxicity, while the controlled release is crucial to maintain the drug concentration in its therapeutic window. The importance of the therapeutic window is twofold: first, when the maximum safety range is exceeded, undesirable side effects can occur; second, failure to reach the minimum therapeutic range leads to no therapeutic effect and increases the risk of drug resistance by the tumor [12–14].

The development of nanotechnology contributed tremendously to find new solutions to protect healthy cells from the aggressiveness of chemotherapeutic drugs. Nanocarriers were proposed to entrap the drugs, and carry their load to the target, and thus protect the healthy tissues and maintain the drug properties. To tune the drug release from the nanocarriers, endogenous (pH, redox, enzymes) and exogenous (temperature, ultrasound, light, electric fields, magnetic fields) stimuli are being explored ([15–20]). Some of the stimuli-responsive drug nanocarriers being studied include dendrimers, liposomes, micelles, metal particles, polymeric nanoparticles, carbon nanotubes, and hydrogels ([19, 21–23]).

Hydrogels are polymeric materials that can store large amounts of water or biological fluids, which makes them highly biocompatible. The physical and chemical properties of these polymers are also highly tunable, and properties like temperature and degradation rate can be controlled by an external stimulus. These properties make hydrogels an ideal candidate for controlled and localized drug delivery ([21, 24, 25]). In this work, we focus our discussion on near infrared (NIR) light as an enhancer of the drug release. NIR light is characterized by wavelengths between 760nm and 1500nm and has two appealing properties: minimal adverse effects on human tissue and relatively deep tissue penetration. Light is also easy to operate, and several parameters like intensity, duration and wavelength can be manipulated to fine-tune the drug release rate ([13, 14, 18, 22, 24–29]).

Once a drug-loaded NIR light-responsive hydrogel is in contact with the target tissue, the drug entrapped in the polymeric matrix can be released by light radiation. The breakage of the links of the drug particles with polymeric chains occurs due to radiation absorption, photochemical reaction, or increase in temperature generated by light, photothermal reaction. In what follows, we consider photochemical reactions. The drug transport through the polymeric structure can be induced by different factors: temperature rise, hydrogel swelling due to increased osmotic pressure, or disintegration of the polymeric matrix (i.e., photocleavage) ([30]). Moreover, such processes are reversible, meaning that diffusion is controlled and regulated over time. The desired release rates are obtained by manipulating light parameters (e.g., intensity and duration) and hydrogel composition ([21, 24, 26, 27]).

One of the objectives of this thesis is the mathematical modeling and numerical simulation of drug release from hydrogels. We believe that this work can be helpful for the design of an in silico laboratory to test drug delivery devices responsive to light. Our main mathematical contribution is the convergence and stability analysis of numerical methods for modeling controlled drug delivery. Such properties allow accurate numerical simulations. In silico laboratories are powerful tools that can be used to test multiple scenarios by changing the parameters governing the interaction between hydrogel, bounded drug, and light. The numerical simulation provides new insights into the design of new drug carriers that give rise to optimal target drug release profiles, maximizing drug efficiency and minimizing undesirable side effects ([12, 13, 31]).

1.2 Outline

Light propagation

In this thesis, we study, from a numerical point of view, systems of partial differential equations that can be used to describe drug release from a NIR light-responsive polymeric structure. We assume

that a polymeric platform, loaded with a drug linked by cleavable bonds with the polymeric chains, is exposed to NIR light irradiation. Due to the light absorption, the links between the polymeric chains and the drug particles break. The bound drug is converted into a free drug that is allowed to diffuse according to Fick's law.

A main ingredient in our problem is the mathematical description of the light propagation. It is well known that light propagation through a scattering and absorption medium can be described by the radiative transfer equation ([32]). Let I (W/cm^2) be the light intensity. Then the radiative transfer equation can be written in the following form

$$\frac{1}{\beta}\frac{\partial I}{\partial t} + \mu_t I + \gamma \nabla I = \mu_s F_{sc}(I) + F_s(I), \tag{1.1}$$

where β (cm/s) denotes the light propagation speed through the medium Ω, $\mu_t = \mu_a + \mu_s$, μ_a (cm^{-1}) and μ_s (cm^{-1}) are the absorption and the scattering coefficients, respectively, $\mu_s F_{sc}$ and F_s denote the scattering and the source light terms, and γ denotes a unit vector in the direction of particle motion.

Depending on the magnitude of the absorption and scattering coefficients, μ_a and μ_s, we can consider different approaches to replace the radiative transport equation (1.1). The most basic mathematical law for the evolution of light intensity I is the so called Beer-Lambert law. This law is established by assuming that $\mu_a \gg \mu_s$; the light incidence is orthogonal to the plane where the material lies and the material is homogeneous ([33–35]):

$$\frac{dI}{dx} = -\mu_a I, \quad x \in \Omega. \tag{1.2}$$

Equation (1.2) is obtained from (1.1) considering the stationary state and $F_{sc} = F_s = 0$.

In [36], a system of partial differential equation is established to replace (1.1). Let J be the current density (W^2/cm^2). In the domain $\Omega \times (0,T]$, the authors propose the following system

$$\begin{cases} \dfrac{1}{\beta}\dfrac{\partial I}{\partial t} + \mu_a I + \nabla \cdot J = 0, & (1.3) \\ \dfrac{1}{\beta}\dfrac{\partial J}{\partial t} + (\mu_a + \mu_s) J + \dfrac{1}{3}\nabla I = 0. & (1.4) \end{cases}$$

From (1.3), assuming that the time derivative of the current density is negligible, more precisely $\dfrac{1}{\beta(\mu_a+\mu_s)}\dfrac{\partial J}{\partial t} \approx 0$, then the diffusion approximation for the current density is established

$$J = -D_\ell \nabla I, \tag{1.5}$$

with $D_\ell = \frac{1}{3(\mu_a+\mu_s)}$. Consequently, for the light intensity is deduced from the following diffusion equation

$$\frac{1}{\beta}\frac{\partial I}{\partial t} + \mu_a I = D_\ell \Delta I. \tag{1.6}$$

Other approaches can be used to replace (1.3) and (1.4). In what follows, we consider the drug release from a polymeric structure enhanced by light following two different approaches for the mathematical description of the light propagation: Beer-Lambert law (1.2) and the diffusion equation

(1.6), respectively, in Chapter 3 - *Beer–Lambert approach for light*, and Chapter 4-*Diffusion approach for light*.

Chapter 2: Beer-Lambert approach for light

In this chapter, we consider an isotropic cube hydrogel $(0,1)^3$ where the light incidence is orthogonal to a cube face. We assume that the drug is homogeneously distributed and the properties of the polymer-drug mixture are the same at all points of the same transversal section orthogonal to the light incidence direction. These assumptions allow us to replace the 3D spatial domain with a one-dimensional $\Omega = (0,1)$. Let $t \in [0,T]$, for a fixed $T > 0$.

From (1.2), considering that the light intensity is known at the incidence face, we have

$$I(x) = I_0 \exp(-\beta x), \quad x \in \Omega. \tag{1.7}$$

In what concerns the bound (c_b) and free (c_f) drug dynamics, the bound drug is converted into free drug due to the absorption of light energy through the breakage of the links between the polymeric chains and the drug particles. Let F be the reaction term depending on bound and free drug as well as on the light intensity I that defines the conversion of the bound drug into the free drug. Let F and S be the reaction terms for the free drug and bound drug, respectively. From (1.7), in the Beer-Lambert context, I is known for every point in the domain, then we can consider F and S depending only on the unknowns c_f and c_b.

The mathematical problem that we study in chapter 2 is the initial boundary value problem (IBVP)

$$\frac{\partial c_f}{\partial t} = \frac{\partial}{\partial x}\left(D(c_f)\frac{\partial c_f}{\partial x}\right) + F(c_f, c_b), \tag{1.8}$$

$$\frac{\partial c_b}{\partial t} = S(c_f, c_b), (x,t) \in \Omega \times (0,T], \tag{1.9}$$

$$c_b(x,0) = c_{b,0}(x), \quad c_f(x,0) = 0, \quad x \in \Omega, \tag{1.10}$$

$$c_f(a,t) = c_f(b,t) = 0, \quad t \in (0,T], \tag{1.11}$$

where $F, S : \mathbb{R}^2 \to \mathbb{R}$ are suitable reaction functions and $D : \mathbb{R} \to \mathbb{R}$ is a diffusion coefficient that is allowed to depend on c_f. Here, for simplicity, we have dropped the dependency on x and t. In system (1.8)-(1.11), we assume that the bound initial drug distribution is known and no free drug exists at initial time.

A simple choice for the reaction term F is obtained by considering that the unbinding reaction term is proportional to the light intensity and the bound drug concentration, that is $F = \phi I c_b$ and $S = -\phi I c_b$, where the parameter ϕ ($cm^2/(Ws)$) is the conversion rate of the bound drug to free drug in presence of NIR light with intensity I.

This chapter is focused on the study of numerical methods for the IBVP (1.8)-(1.11). Several numerical methods have been proposed for similar problems to this IBVP, particularly for the semilinear case with nonlinear reaction and linear diffusion. Fully nonlinear equations/systems were analyzed, e.g., in [37–40]. In [37], a coupled reaction-diffusion system was considered in the context of heat transport. A finite difference method (FDM) was proposed and optimal error estimates in discrete L^2 and H^1 norms were obtained by considering uniform grids. Optimal convergence estimates in

the L^2-norm were also obtained in [38] for a general class of nonlinear reaction-diffusion equations discretized by mixed finite elements. Finite volume schemes with high order of accuracy were developed in [39] for general nonlinear advection-diffusion-reaction equations. Stability analysis for discontinuous Galerkin methods applied to the same class of equations was the subject of [40]. Let us also mention that FDMs for other type of problems have been previously investigated by some of the authors of this work ([41–43]).

In [44, 45], IMEX (implicit-explicit) methods are used in the numerical approximation for reaction-diffusion problems. The stiff term (the diffusion term) is discretized implicitly, and the nonlinear reaction terms are discretized explicitly. Compared to a fully discrete scheme, this approach avoids a restrictive time step condition associated with the diffusion term. On the other hand, compared to a fully implicit scheme, it avoids the solution of non-linear systems associated with the reaction terms. The advantage of IMEX methods to deal with reaction-diffusion equations is discussed in [45].

Ideally, an IMEX approach should have better stability properties than a fully explicit scheme and reduce the computational cost associated with a fully implicit scheme, which requires the solution of nonlinear systems at each time level. IMEX methods have been recently used in [46, 47] to compute the numerical solutions of wave equations containing terms with different time scales (fast and slow), where the slow terms are approximated explicitly and the fast terms are approximated implicitly. The results show that IMEX methods have similar accuracy to a fully implicit method but with much faster performance.

A comparison between the second order Runge-Kutta-Chebyshev (RKC) methods and Runge-Kutta-IMEX (RK-IMEX) methods for time integration of reaction-diffusion-convection equations was recently described in [48]. Combined with second order centered finite difference operators for the space discretization, the author found that RK-IMEX methods are more accurate than the RKC methods, and in many cases RK-IMEX outperform RKC methods.

In this chapter, we propose finite difference methods defined in nonuniform meshes that can be seen as fully discrete in space piecewise linear finite element methods, and the stability and convergence analysis will be stated. Following the MOL approach (method of lines approach), we start by considering semi-discrete approximation methods, that is, we discretize the spatial derivatives in (1.8) reducing the IBVP (1.8)-(1.11) to an ordinary differential system. Fully discrete methods will be also considered integrating the last problem using an IMEX approach.

As we are dealing with nonlinear differential problems, stability is a local property in the sense that is established around a fixed numerical solution, see [49, 50]. The proof of the stability requires the uniform boundedness, in time and mesh size, of the fixed numerical solution. To prove such boundedness, we use the convergence properties. Consequently, the stability will be concluded if its initial condition belongs to a certain ball centered in the restriction of the initial condition of the continuous solution with a mesh size-dependent radius.

In what concerns the convergence analysis, and looking at the proposed methods as finite difference methods, the corresponding spatial truncation errors are only of first order with respect to the norm $\|\cdot\|_\infty$. Nevertheless, we prove that the correspondent spatial global errors are of second order with respect to norms that can be seen as discrete versions of the usual H^1-norm. These results will be proved for smooth and nonsmooth solutions. For nonsmooth solutions, the approach introduced

in [51] plays an important role for the one-dimensional case; similarly, [41] is important for the two-dimensional case.

This approach is based on Bramble-Hilbert Lemma ([52]) which allows us to reduce the smoothness assumptions usually imposed when the convergence analysis is based on the use of Taylor expansion, and was followed for instance in [17, 43, 53, 54]. In the finite difference context, this phenomenon is called supraconvergence and was observed in the literature using different techniques, for instance in [55–61]. In the finite element context, the results proved in this chapter can be seen as superconvergence results in the sense that the piecewise linear finite element approximation is first order convergent in the usual H^1-norm, and we show that a fully discrete in space approximation is second order convergent with respect to a discrete version of the usual H^1-norm for smooth and nonsmooth solutions.

Chapter 3: Diffusion approximation for light

Here we consider $\Omega = (0,1)^2$, $\partial\Omega$ denotes its boundary, and $t \in [0,T]$ for a fixed $T > 0$. We assume that $\partial\Omega = \overline{\Gamma}_l \cup \overline{\Gamma}_u \cup \overline{\Gamma}_r \cup \overline{\Gamma}_d$ where Γ_l, Γ_r denote the left and right sides of Ω, respectively, and Γ_d, Γ_u are the bottom and upper sides of Ω, respectively (see Figure (3.1)).

For the light propagation we consider the diffusion approximation (1.6). Consequently, the light intensity I, the free drug concentration c_f and the bound drug concentration c_b are defined by the following differential system

$$\begin{cases} \dfrac{1}{\beta}\dfrac{\partial I}{\partial t} = \nabla \cdot (D_I \nabla I) + G(I), & (1.12) \\ \dfrac{\partial c_f}{\partial t} = \nabla \cdot (D_d \nabla c_f) + F(I, c_f, c_b), & (1.13) \\ \dfrac{\partial c_b}{\partial t} = S(I, c_f, c_b), & (1.14) \end{cases}$$

for $x \in \Omega, t \in (0,T]$. In (1.12)-(1.14), D_I and D_d are diagonal matrices defined in $\overline{\Omega} \times (0,T]$, given by

$$D_I = \begin{pmatrix} D_{I,11} & 0 \\ 0 & D_{I,22} \end{pmatrix} \quad \text{and} \quad D_d = \begin{pmatrix} D_{d,11} & 0 \\ 0 & D_{d,22} \end{pmatrix},$$

where the diagonal entries are bounded from below by a positive constant.
To close the system (1.12)-(1.14) we assume the initial conditions

$$I(x,0) = 0, \quad c_f(x,0) = 0, \quad c_b(x,0) = c_{b,0}(x), \quad x \in \Omega, \tag{1.15}$$

and the boundary conditions

$$I(x,t) = I_0(t), \quad x \in \Gamma_l, t \in (0,T], \tag{1.16}$$
$$\nabla I(x,t) \cdot \eta = 0, \quad x \in \partial\Omega - \overline{\Gamma}_l, t \in (0,T], \tag{1.17}$$
$$\nabla c_f(x,t) \cdot \eta = 0, \quad x \in \partial\Omega - \overline{\Gamma}_r, t \in (0,T], \tag{1.18}$$
$$c_f(x,t) = 0, \quad x \in \Gamma_r, t \in (0,T], \tag{1.19}$$

where η denotes the unitary exterior normal. Boundary condition (1.16) and (1.17) means that the light intensity is known at the left side of Ω and propagates through $\partial\Omega - \overline{\Gamma}_l$. For the free drug, the boundary condition (1.19) means that all the free drug particles that reach Γ_r are immediately removed. The remaining boundary of Ω is not permeable to the drug particles (1.18).

Our main goal is to propose a numerical method for the IBVP (1.12)-(1.19) constructed using the MOL approach: the spatial discretization followed by the time integration. In what concerns the spatial discretization, we consider a finite difference discretization defined in a nonuniform rectangular grid that extends the one considered in chapter 2. The method can be seen as a fully discrete in space piecewise linear finite element discretization where the triangulation is generated by the finite difference nonuniform rectangular grid. Fully discrete methods in time and space will be suggested and obtained by discretizing the semi-discrete initial value problem corresponding to the spatial discretization using a Crank-Nicolson approach. The theoretical stability and the convergence support are provided using the approach presented in Chapter 2.

Let us consider the free drug equation (1.14) and its variational formulation

$$\left(\frac{\partial c_f}{\partial t}, w\right)_{L^2} + (D_d \nabla c_f, \nabla w)_{[L^2]^2} = (F(I, c_f, c_b), w)_{L^2}, \forall w \in H^1_{0,r}(\Omega), \tag{1.20}$$

where $H^1_{0,r}(\Omega) = \{v \in H^1(\Omega) : v = 0 \text{ on } \Gamma_r\}$. In (1.20), $(\cdot,\cdot)_{L^2}$ denotes the usual inner product in $L^2(\Omega)$ and $(\cdot,\cdot)_{[L^2]^2}$ represents the usual inner product in $L^2(\Omega) \times L^2(\Omega)$.

We remark that this equality is established by considering the compatibility between (1.13) and (1.18). In the construction of the numerical methods proposed here, the main tool is the discrete version of (1.20). This discrete version is obtained by considering a convenient set of fictitious points as well as convenient discrete inner products for different grid function spaces and the corresponding norms. In the convergence analysis for a smooth solution, the global error does not have homogeneous boundary conditions. To get the desired error estimate, a discrete version of the so-called trace inequality ([62]) will play an important role. The literature is not very fruitful on numerical methods for IBVP with Neumann or Robin boundary conditions. We mention for instance [63] for a one-dimensional and [64] for the Laplace operator considering a square. In both cases, the authors assume smooth solutions. The extension of the results obtained here for nonsmooth solutions is a challenge that we intend to study in the near future.

We remark that we do not address the existence and uniqueness of the solution of the IBVP discussed in Chapters 2 and 3. For more details on the global existence and uniqueness of solutions for more general IBVP than those discussed here, see [65–67].

Chapter 4: Drug delivery enhanced by light

Chapter 4 focuses on the numerical simulation of drug delivery controlled by light in two scenarios: drug release from a hydrogel and transdermal drug delivery. In the first scenario, we consider Beer-Lambert law for light propagation and $S = -F$ with $F(I, c_f, c_s) = \phi I c_b$. Simulation results reveal a good agreement with laboratory experiments taken from [26]. In the second scenario, we consider a polymeric patch in contact with the skin. The drug release occurs in response to a light stimulus, and we take the diffusion approach for the mathematical description of light propagation. We model the

coupling between the drug release from the patch and its propagation through the skin. Simulation results show good agreement with in vivo results taken from [68].

In the context of transdermal delivery, we present a computational tool for optimizing NIR light stimulus protocols. We assume that a NIR light protocol consists of several identical cycles characterized by three parameters: laser power, laser-on period, and laser-off period. We formulate a minimization problem to find the optimal NIR light protocol, i.e., the optimal set of parameters that lead to a prescribed drug absorption profile. The minimization problem is solved numerically using the classic Nelder-Mead downhill method.

Conclusions

Here, we present some conclusions and we introduce a significant set of open problems that we would like to address in the near future.

Main outputs

To conclude this introduction, we would like to highlight that some of the results included in this thesis were published in the following works:

1. *A mathematical model for NIR light protocol optimization in controlled transdermal drug delivery*, J.A. Ferreira, H. Gómez, L. Pinto, Applied Mathematical Modelling, 112 (2022), 1–17;

2. *A numerical scheme for a partial differential system motivated by light-triggered drug delivery*, J.A. Ferreira, H. Gómez, L. Pinto, Applied Numerical Mathematics, 184 (2023), 101–120;

3. *Numerical simulation and validation of a nonlinear differential system for drug release boosted by light*, J.A. Ferreira, H. Gómez, L. Pinto, to appear in International Conference on Mathematical Analysis and Applications in Science and Engineering, Porto, Portugal, June 27- July 1, 2022, to be published by Springer.

4. *Numerical analysis and numerical simulation in light responsive drug delivery systems*, J.A. Ferreira, H. Gómez, L. Pinto, submitted.

Chapter 2

Beer-Lambert approach for light

2.1 Introduction

Let $\Omega \subset \mathbb{R}$ be the space domain, $\Omega = (a,b)$, and $[0,T]$ the time domain, $T > 0$. Our aim is to introduce stable and convergent numerical methods to approximate the solution (c_f, c_b) of the initial boundary value problem (IBVP)

$$\begin{cases} \dfrac{\partial c_f}{\partial t} = \dfrac{\partial}{\partial x}\left(D(c_f)\dfrac{\partial c_f}{\partial x}\right) + F(c_f, c_b), & \text{in } \Omega \times (0,T], \quad (2.1) \\ \dfrac{\partial c_b}{\partial t} = S(c_f, c_b), & \text{in } \Omega \times (0,T], \quad (2.2) \\ c_b(x,0) = c_{b,0}(x), \;\; c_f(x,0) = c_{f,0}(x), & \text{in } \Omega, \quad (2.3) \\ c_f(x,t) = 0, & \text{on } \partial\Omega \times (0,T], \quad (2.4) \end{cases}$$

where $F, S : \mathbb{R}^2 \to \mathbb{R}$ and $D : \mathbb{R} \to \mathbb{R}$ are suitable functions.

The structure of this chapter is as follows, in Section 2.2 we introduce the notations and the basic definitions. Next, the main two sections are presented, Section 2.3 and Section 2.4. The first is focused in the semi-discrete approximation for the IBVP (2.1)-(2.4) defined by (2.6)-(2.9), and in the later, we study fully discrete in time and space numerical methods (2.20)-(2.23) constructed using MOL approach-spatial discretization followed by a time integration using an implicit-explicit Euler method where the diffusion and the reaction terms are treated explicitly. Finally, in Section 2.5 we include some numerical experiments to illustrate the convergence results.

The numerical schemes presented in this chapter are based on finite difference methods that, under appropriate integration rules, can be written as piecewise linear finite element methods. For the finite difference formulation of the method we study the stability (propagation in time of perturbations of the initial data around a fixed numerical solution) and convergence.

The summary of the approach used to prove such properties is the next: consider the semi-discrete case. Let $c_{f,h}(t), c_{b,h}(t)$ be the fixed numerical solution. From Proposition 2.3.2 we conclude stability if a certain quantity depending on $c_{f,h}(t)$ is uniformly bounded for the space and time step size. As we realise that such boundedness can be concluded from convenient error estimates, we study the convergence and then we return to the stability and we impose a convenient smoothness assumption

of the spatial grids (condition (2.65)). The steps to conclude stability and convergence for the fully-discrete approximation are similar.

For the semi-discrete approximation (2.6)-(2.9), the main results of this chapter are: Proposition 2.3.2 for stability, and for convergence Theorems 2.3.1 and 2.3.2, respectively, for smooth and nonsmooth solutions. The fully discrete version of these results are the stability result- Proposition 2.4.2, and the convergence result - Theorem 2.4.1.

The stability and convergence analysis of the methods introduced in this chapter are established assuming some smoothness on the reaction F and S as well as on the diffusion coefficient D:

$$D(x) \geq D_0 > 0, \tag{HD_0}$$
$$|D(x) - D(\tilde{x})| \leq C_D|x-\tilde{x}|, \tag{HD_ℓ}$$
$$|F(x,y)| \leq C_F(|x|+|y|), \tag{HF}$$
$$|S(x,y)| \leq C_S(|x|+|y|), \tag{HS}$$
$$|F(x,y) - F(\tilde{x},\tilde{y})| \leq C_{F_\ell}(|x-\tilde{x}|+|y-\tilde{y}|), \tag{HF_ℓ}$$
$$|S(x,y) - S(\tilde{x},\tilde{y})| \leq C_{S_\ell}(|x-\tilde{x}|+|y-\tilde{y}|), \tag{HS_ℓ}$$

where $x, y, \tilde{x}, \tilde{y} \in \mathbb{R}$, and $C_D, C_F, C_S, C_{F_\ell}$ and C_{S_ℓ} are positive constants.

2.2 Definitions and notations

Let Λ be a sequence of vectors $h = (h_1, \ldots, h_N)$ with positive entries such that $\sum_{i=1}^{N} h_i = b - a$ and $h_{max} = \max_{i=1,\ldots,N} h_i \to 0$. For $h \in \Lambda$, we introduce in $\overline{\Omega} = [a,b]$ the nonuniform grid

$$\overline{\Omega}_h = \{x_i, i = 0, \ldots, N, \;\; a = x_0, \;\; x_N = b, \;\; x_i = x_{i-1} + h_i, i = 1, \ldots, N\}.$$

Let W_h be the space of grid functions defined in $\overline{\Omega}_h$ and let $W_{h,0}$ denote the subspace of W_h of the grid functions null on the boundary $\partial\Omega_h$. Let also $\widehat{W}_h$ be the space of grid functions defined in $\Omega_h = \overline{\Omega}_h \cap (a,b)$. In $W_{h,0}$, we define the inner product

$$(u_h, v_h)_h = \sum_{i=1}^{N-1} h_{i+1/2} u_h(x_i) v_h(x_i),$$

with $h_{i+1/2} = \frac{h_i + h_{i+1}}{2}$ and $u_h, v_h \in W_{h,0}$. Let $\|\cdot\|_h$ be the norm induced by $(\cdot,\cdot)_h$. Let us also define

$$(u_h, v_h)_+ = \sum_{i=1}^{N} h_i u_h(x_i) v_h(x_i), \quad u_h, v_h \in W_h,$$

with $\|u_h\|_+ = \sqrt{(u_h, u_h)_+}$, for $u_h \in W_h$. We also introduce the average operator

$$M_x u_h(x_i) = \frac{u_h(x_i) + u_h(x_{i-1})}{2},$$

and the finite difference operators

$$D_{-x}u_h(x_i) = \frac{u_h(x_i) - u_h(x_{i-1})}{h_i}, \quad D_x^* u_h(x_i) = \frac{u_h(x_{i+1}) - u_h(x_i)}{h_{i+1/2}}.$$

We observe that holds the following: for $u_h \in W_{h,0}$ we have

$$\|u_h\|_\infty \leq \sqrt{b-a}\|D_{-x}u_h\|_+, \tag{2.5}$$

where $\|u_h\|_\infty = \max_{i=1,\ldots,N-1} |u_h(x_i)|$. In fact, since $u_h(x_i) = \sum_{j=1}^{i} h_j D_{-x}u_h(x_j)$ for $i = 1,\ldots,N$, we obtain

$$|u_h(x_i)| \leq \sqrt{b-a}\|D_{-x}u_h\|_+.$$

In what follows we introduce the two numerical approximations for the solution of the IBVP (2.1)-(2.4) that will be studied in this chapter: the semi-discrete approximation and the discrete in time and space approximation.

The semi-discrete finite difference approximation for the solution of the IBVP (2.1)-(2.4) is solution of the following ordinary differential problem: find $c_{f,h}(t) \in W_{h,0}$, $c_{b,h}(t) \in \hat{W}_h$ such that

$$\begin{aligned}
c'_{f,h}(t) &= D_x^*(D(M_x c_{f,h}(t))D_{-x}c_{f,h}(t)) + F(c_{f,h}(t), c_{b,h}(t)), && \text{in } \Omega_h \times (0,T], && (2.6)\\
c'_{b,h}(t) &= S(c_{f,h}(t), c_{b,h}(t)), && \text{in } \Omega_h \times (0,T], && (2.7)\\
c_{f,h}(0) &= R_h c_{f,0}, \quad c_{b,h}(0) = R_h c_{b,0}, && \text{in } \Omega_h, && (2.8)\\
c_{f,h}(a,t) &= c_{f,h}(b,t) = 0, && \text{for } t \in (0,T]. && (2.9)
\end{aligned}$$

In (2.8), $R_h : C([a,b]) \to W_h$ denotes the restriction operator $R_h u(x_i) = u(x_i), i = 0,\ldots,N$.

The system (2.6)-(2.9) can be written in the variational form:

$$\begin{aligned}
(c'_{f,h}(t), u_h)_h &= -(D(M_x c_{f,h}(t))D_{-x}c_{f,h}(t), D_{-x}u_h)_+ + (F(c_{f,h}(t), c_{b,h}(t)), u_h)_h, && (2.10)\\
(c'_{b,h}(t), v_h)_h &= (S(c_{f,h}(t), c_{b,h}(t)), v_h)_h, && (2.11)\\
(c_{f,h}(0), u_h)_h &= (R_h c_{f,0}, u_h), && (2.12)\\
(c_{b,h}(0), v_h)_h &= (R_h c_{b,0}, v_h)_h, && (2.13)
\end{aligned}$$

for $u_h \in W_{h,0}$, $v_h \in \widehat{W}_h$ and $t \in (0,T]$.

We notice that (2.6)-(2.9) is equivalent to discrete variational system (2.10)-(2.12). To prove this, consider first $(c_{f,h}(t), c_{b,h}(t))$ a solution to the IBVP (2.6)-(2.9). Let $u_h \in W_{h,0}$ and $v_h \in \widehat{W}_h$. Applying inner product $(\cdot,\cdot)_h$ to equation (2.6) with u_h and using summation by parts we get

$$(c'_{f,h}(t), u_h)_h = -(D(M_x c_{f,h}(t))D_{-x}c_{f,h}(t), D_{-x}u_h)_+ + (F(c_{f,h}(t), c_{b,h}(t)), u_h)_h, \qquad t \in (0,T].$$

Analogously, from (2.7) we deduce

$$(c'_{b,h}(t), v_h)_h = (S(c_{f,h}(t), c_{b,h}(t)), v_h)_h, \qquad t \in (0,T].$$

Equations (2.10) and (2.11) are complemented by the initial conditions

$$(c_{f,h}(0),u_h)_h = (R_h c_{f,0},u_h)_h, \quad u_h \in W_{h,0},$$
$$(c_{b,h}(0),v_h)_h = (R_h c_{b,0},v_h)_h, \quad v_h \in \widehat{W}_h.$$

Conversely, assume that $(c_{f,h}(t),c_{b,h}(t))$ satisfy the variational system (2.10)-(2.12). Using summation by parts in equation (2.10) we can obtain

$$(c'_{f,h}(t) - D_x^*(D(M_x c_{f,h}(t))D_{-x}c_{f,h}(t)) - F(c_{f,h}(t),c_{b,h}(t)),u_h)_h = 0, \tag{2.14}$$

for all $u_h \in W_{h,0}$. Then, from (2.14), we obtain (2.6).

Analogously, it can be shown that (2.11) and (2.12) lead to (2.7) and (2.8), respectively.

We remark that (2.10)-(2.12) defines a fully discrete in space variational problem that allows the computation of a solution for the IBVP (2.1)-(2.4).

Remark 2.2.1. *We show now that (2.10)-(2.12) can be seem as a fully discrete in space finite element method. Let $\hat{u}_h = P_h u_h$ be the piecewise linear interpolator of $u_h \in W_{h,0}$, and, for $u_h \in \hat{W}_h$, let $\tilde{u}_h = Q_h u_h$ denote the piecewise constant interpolator defined by*

$$\tilde{u}_h(x) = Q_h u_h(x) = u_h(x_i), \;\; x \in \left(x_i - \frac{h_i}{2}, x_i + \frac{h_{i+1}}{2}\right), \;\; i = 1,\cdots,N-1. \tag{2.15}$$

The finite element solution $\hat{c}_{f,h}(t) = P_h c_{f,h}(t) \in H_0^1(\Omega), \tilde{c}_{b,h}(t) = Q_h c_{b,h}(t) \in L^2(\Omega)$ is solution of the following system of equations for $\forall w_h \in W_{h,0}$, $\forall v_h \in \hat{W}_h$, and $t \in (0,T]$

$$\left(\frac{\partial \hat{c}_{f,h}}{\partial t}(t), P_h u_h\right) = -\left(D(\hat{c}_{f,h}(t))\frac{\partial \hat{c}_{f,h}}{\partial x}(t), \frac{\partial P_h u_h}{\partial x}\right) + \left(F(\hat{c}_{f,h}(t),\tilde{c}_{b,h}(t)), P_H u_H\right), \tag{2.16}$$
$$\left(\frac{\partial \hat{c}_{b,h}}{\partial t}(t), Q_h v_h\right) = (S(\hat{c}_{f,h}(t),\tilde{c}_{b,h}(t)), Q_h w_h), \tag{2.17}$$
$$(\hat{c}_{f,h}(0), P_h u_h) = (\hat{c}_{f,0}, P_h u_h), \tag{2.18}$$
$$(\tilde{c}_{b,h}(0), Q_h v_h) = (\tilde{c}_{b,0}, Q_h v_h)_h, \tag{2.19}$$

where $\hat{c}_{f,0} = P_h R_h c_{f,0}$ and $\tilde{c}_{b,0} = Q_h R_h c_{b,0}$.

Considering in (2.16) the following quadrature rule

$$\begin{aligned}\int_{x_i-\frac{h_i}{2}}^{x_i+\frac{h_{i+1}}{2}} \frac{\partial \hat{c}_{f,h}}{\partial t}(t) P_h u_h dx &\simeq \frac{1}{2}(h_i+h_{i+1})\frac{\partial \hat{c}_{f,h}}{\partial t}(x_i,t) P_h u_h(x_i) \\ &= \frac{1}{2}(h_i+h_{i+1})\frac{\partial c_{f,h}}{\partial t}(x_i,t) u_h(x_i), i = 1,\ldots,N-1,\end{aligned}$$
$$\int_{x_0}^{x_0+\frac{h_1}{2}} \frac{\partial \hat{c}_{f,h}}{\partial t}(t) P_h u_h dx \approx 0,$$
$$\int_{x_N-\frac{h_N}{2}}^{x_N} \frac{\partial \hat{c}_{f,h}}{\partial t}(t) P_h u_h dx \approx 0,$$

$$\int_{x_i}^{x_{i+1}} D(\hat{c}_{f,h}(t))\frac{\partial \hat{c}_{f,h}}{\partial x}(t)\frac{\partial P_h u_h}{\partial x}dx \approx \int_{x_i}^{x_{i+1}} D\left(\frac{(c_{f,h}(x_i,t)+c_{f,h}(x_{i+1},t))}{2}\right)\frac{\partial \hat{c}_{f,h}}{\partial x}(t)\frac{\partial P_h u_h}{\partial x}dx,$$
$$= D\left(\frac{1}{2}(c_{f,h}(x_i,t)+c_{f,h}(x_{i+1},t))\right)D_{-x}c_{f,h}(x_{i+1},t)D_{-x}u_h(x_{i+1}),$$

for $i = 0,\ldots,N-1$, *and*

$$\int_{x_i-\frac{h_i}{2}}^{x_i+\frac{h_{i+1}}{2}} F(\hat{c}_{f,h}(t)\tilde{c}_{b,h}(t))P_h u_h dx \approx \frac{1}{2}(h_i+h_{i+1})F(\hat{c}_{f,h}(x_i,t),\tilde{c}_{b,h}(x_i,t))P_h u_h(x_i)$$
$$= \frac{1}{2}(h_i+h_{i+1})F(c_{f,h}(x_i,t),c_{b,h}(x_i,t))u_h(x_i), i = 1,\ldots,N-1,$$
$$\int_{x_0}^{x_0+\frac{h_1}{2}} F(\hat{c}_{f,h}(t),\tilde{c}_{b,h}(t))P_h u_h dx \approx 0,$$
$$\int_{x_N-\frac{h_N}{2}}^{x_N} \frac{\partial \hat{c}_{f,h}}{\partial t}(t)P_h u_h dx \approx 0,$$

we obtain (2.10). Analogously, considering in (2.17) convenient quadrature rule, we deduce (2.11).

To define the discrete in time and space approximation for the solution of the IBVP (2.1)-(2.4), we introduce in $[0,T]$ uniform grid $\{t_m, m = 0,\ldots,M\}$ with $t_0 = 0$, $t_M = T$, and $t_{m+1} = t_m + \Delta t$, for $m = 0,\ldots,M-1$. The discrete solution is then solution of the following discrete problem: find $c^m_{f,h} \in W_{h,0}$, $c^m_{b,h} \in \hat{W}_h$ such that for $m = 1,\ldots,M$

$$D_{-t}c^m_{f,h} = D^*_x\left(D(M_x c^{m-1}_{f,h})D_{-x}c^m_{f,h}\right) + F(c^{m-1}_{f,h},c^{m-1}_{b,h}), \quad \text{in } \Omega_h, \tag{2.20}$$
$$D_{-t}c^m_{b,h} = S(c^{m-1}_{f,h},c^{m-1}_{b,h}), \quad \text{in } \Omega_h, \tag{2.21}$$
$$c^0_{f,h} = R_h c_{f,0}, \quad c^0_{b,h} = R_h c_{b,0}, \quad \text{in } \Omega_h, \tag{2.22}$$
$$c^m_{f,h}(x_0) = c^m_{f,h}(x_N) = 0, \quad \text{on } \partial\Omega_h, \tag{2.23}$$

In (2.20), D_{-t} denotes the backward finite difference operator

$$D_{-t}u^m_h = \frac{u^m_h - u^{m-1}_h}{\Delta t}.$$

We avoid the need to solve a nonlinear system of equations in each time step by using an explicit discretization for the diffusion coefficient D and the nonlinear terms F and S. We observe that IMEX methods are often considered for nonlinear reaction-diffusion problems ([45]). Note that the discrete equations (2.20) and (2.21) can be rewritten, for $m = 1,\ldots,M$, as

$$(I - \Delta t A)\, c^m_{f,h} = c^{m-1}_{f,h} + \Delta t F(c^{m-1}_{f,h},c^{m-1}_{b,h}),$$
$$c^m_{b,h} = c^{m-1}_{b,h} + \Delta t S(c^{m-1}_{f,h},c^{m-1}_{b,h}),$$

where I is an $(N-1)\times(N-1)$ identity matrix and $A=\{a_{i,j}\}_{i,j=1}^{N-1}$ is a tridiagonal matrix with entries

$$
\begin{aligned}
a_{i,i-1} &= \frac{1}{h_{i+1/2}} D\left(\frac{c_{f,h}^{m-1}(x_i)+c_{f,h}^{m-1}(x_{i-1})}{2}\right)\frac{1}{h_{i-1}}, \quad i=2,\dots,N-1,\\
a_{i,i} &= -\frac{1}{h_{i+1/2}}\left(D\left(\frac{c_{f,h}^{m-1}(x_{i+1})+c_{f,h}^{m-1}(x_i)}{2}\right)\frac{1}{h_i}\right.\\
&\qquad \left. -D\left(\frac{c_{f,h}^{m-1}(x_i)+c_{f,h}^{m-1}(x_{i-1})}{2}\right)\frac{1}{h_{i-1}}\right), \quad i=1,\dots,N-1,\\
a_{i+1,i} &= \frac{1}{h_{i+1/2}} D\left(\frac{c_{f,h}^{m-1}(x_{i+1})+c_{f,h}^{m-1}(x_i)}{2}\right)\frac{1}{h_i}, \quad i=1,\dots,N-2.
\end{aligned}
$$

We remark that for all $v_h\in W_{h,0}$ and $w_h\in\widehat{W}_h$, the fully discrete FDM (2.20)-(2.23) can be rewritten in the equivalent variational form

$$(D_{-t}c_{f,h}^m, v_h)_h = -(D(M_x c_{f,h}^{m-1})D_{-x}c_{f,h}^m, D_{-x}v_h)_+ + (F(c_{f,h}^{m-1}, c_{b,h}^{m-1}), v_h)_h, \tag{2.24}$$

$$(D_{-t}c_{b,h}^m, w_h)_h = (S(c_{f,h}^{m-1}, c_{b,h}^{m-1}), w_h)_h, \tag{2.25}$$

$$(c_{f,h}^0, v_h)_h = (R_h c_{f,0}, v_h)_h, \tag{2.26}$$

$$(c_{b,h}^0, w_h)_h = (R_h c_{b,0}, w_h)_h, \tag{2.27}$$

for $m=1,\dots,M$.

As in semi-discrete case, it can be shown that (2.20)-(2.23) is equivalent to the fully discrete in time and space variational system (2.24)-(2.27).

In what follows, we study the stability and convergence properties of the semi-discrete in space FDM (2.6)-(2.9) and the fully discrete scheme (2.20)-(2.23).

2.3 The semi-discrete FDM

In this section we analyze the semi-discrete approximation defined by (2.6)-(2.9). First, to study the boundedness of the semi-discrete approximations we assume the hypothesis (HD_0)-(HS), in particular, we ask the functions F and S to be bounded by a linear function. Secondly, to prove stability, we replace the boundedness conditions by the Lipschitz properties (HF_ℓ) and (HS_ℓ). Because of the nonlinearity of the problem, we study the stability of a fixed solution $c_{f,h}(t)\in W_{h,0}$, $c_{b,h}(t)\in\hat{W}_h$, $t\in[0,T]$, that is, for any $\rho_\varepsilon>0$ we would like to fix $B_{\rho_0}(c_{f,h}(0))$ and $B_{\rho_0}(c_{b,h}(0))$ such that, for all $\tilde{c}_{f,h}(0)\in B_{\rho_0}(c_{f,h}(0))$, $\tilde{c}_{b,h}(0)\in B_{\rho_0}(c_{b,h}(0))$, we have

$$\|c_{f,h}(t)-\tilde{c}_{f,h}(t)\|_h<\rho_\varepsilon,\ \|c_{b,h}(t)-\tilde{c}_{b,h}(t)\|_h<\rho_\varepsilon,\ t\in[0,T]. \tag{2.28}$$

From Proposition 2.3.2, we realize that to conclude equation (2.28) we need first to show the uniform bound

$$\int_0^t \|D_{-x}c_{f,h}(s)\|_\infty^2\le C,\quad h\in\Lambda,\ t\in[0,T]. \tag{2.29}$$

For this purpose, we use the following inequalities that hold for $i = 1, \cdots, N-1$

$$|D_{-x}c_{f,h}(x_i,t)|^2 \leq 2\Big(|D_{-x}E_{f,h}(x_i,t)|^2 + |D_{-x}R_h c_f(x_i,t)|^2\Big), \tag{2.30}$$

$$|D_{-x}E_{f,h}(x_i,t)|^2 \leq \frac{1}{h_{min}}\|D_{-x}E_{f,h}(t)\|_+^2, \tag{2.31}$$

where the error $E_{f,h}(x_i,t) = R_h c_{f,h}(x_i,t) - c_{f,h}(x_i,t)$ is involve. Therefore, it is convenient to study the convergence of the semi-discrete scheme (2.6)-(2.9) (Section 2.3.2), from where we can prove that $\int_0^t \|D_{-x}E_{f,h}(s)\|_+^2 ds$ is bounded and then, we finally are able to conclude the desired stability result (2.28).

2.3.1 Stability

We start by proving the uniform boundedness of $c_{f,h}(t), t \in [0,T], h \in \Lambda$.

Proposition 2.3.1. *Let $c_{f,h}(t) \in W_{h,0}$, $c_{b,h}(t) \in \widehat{W}_h$, be defined by* (2.6)-(2.9) *with initial conditions $c_{f,h}(0) \in W_{h,0}$, $c_{b,h}(0) \in \widehat{W}_h$. If the assumptions (HD_0), (HF), and (HS) hold, then there exists a positive constant C, independent of h and t, such that*

$$\|c_{f,h}(t)\|_h^2 + \|c_{b,h}(t)\|_h^2 + 2D_0\int_0^t e^{C(t-s)}\|D_{-x}c_{f,h}(s)\|_+^2 ds \leq e^{Ct}\Big(\|c_{f,h}(0)\|_h^2 + \|c_{b,h}(0)\|_h^2\Big), \tag{2.32}$$

for $t \in [0,T], h \in \Lambda$.

Proof: From (2.10) and (2.11) with $u_h = c_{f,h}(t)$, $v_h = c_{b,h}(t)$ and considering the smoothness assumptions (HD_0), (HF), and (HS) we easily get

$$\begin{aligned}\frac{1}{2}\frac{d}{dt}\Big(\|c_{f,h}(t)\|_h^2 + \|c_{b,h}(t)\|_h^2\Big) + D_0\|D_{-x}c_{f,h}(t)\|_+^2 & \\ \leq (\|c_{f,h}(t)\|_h + \|c_{b,h}(t)\|_h)(C_F\|c_{f,h}(t)\|_h + C_S\|c_{b,h}(t)\|_h) & \\ \leq 2\max\{C_F,C_S\}(\|c_{f,h}(t)\|_h^2 + \|c_{b,h}(t)\|_h^2). &\end{aligned}$$

The last inequality leads to (2.32) with $C = 4\max\{C_F,C_S\}$. ∎

As corollary of the last result we conclude the following uniform boundedness result which is consequence of inequality (2.5).

Corollary 2.3.1. *Under the conditions of Proposition 2.3.1, there exists a positive constant C, independent of h and t, such that*

$$\int_0^t \|c_{f,h}(s)\|_\infty^2 ds \leq C,$$

for $t \in [0,T]$, $h \in \Lambda$, provided that $\|c_{f,h}(0)\|_h^2 + \|c_{b,h}(0)\|_h^2$, $h \in \Lambda$, is bounded.

Proposition 2.3.2. *Let $c_{f,h}(t), \tilde{c}_{f,h}(t) \in W_{h,0}$, $c_{b,h}(t), \tilde{c}_{b,h}(t) \in \widehat{W}_h$, be defined by* (2.6)-(2.9) *with initial conditions $c_{f,h}(0)$, $\tilde{c}_{f,h}(0) \in W_{h,0}$, $c_{b,h}(0)$, $\tilde{c}_{b,h}(0) \in \widehat{W}_h$. If the assumptions (HD_0), (HD_ℓ), (HF_ℓ), and (HS_ℓ) hold, then, for $\omega_{f,h}(t) = c_{f,h}(t) - \tilde{c}_{f,h}(t)$ and $\omega_{b,h}(t) = c_{b,h}(t) - \tilde{c}_{b,h}(t)$ we have*

$$\|\omega_{f,h}(t)\|_h^2+\|\omega_{b,h}(t)\|_h^2+2(D_0-\varepsilon^2)\int_0^t e^{\int_s^t\gamma(\mu)d\mu}\|D_{-x}\omega_{f,h}(s)\|_+^2ds \\ \leq e^{\int_0^t\gamma(s)\,ds}\Big(\|\omega_{f,h}(0)\|_h^2+\|\omega_{b,h}(0)\|_h^2\Big), \tag{2.33}$$

for $t\in[0,T], h\in\Lambda$, *where*

$$\gamma(s)=\max\left\{\frac{1}{2\varepsilon^2}C_D^2\|D_{-x}c_{f,h}(s)\|_\infty^2, 4\max\{C_{F_\ell},C_{S_\ell}\}\right\}, \tag{2.34}$$

and $\varepsilon\neq 0$ *is an arbitrary constant.*

Proof: It can be shown that for $\omega_{f,h}(t)$ and $\omega_{b,h}(t)$ we have

$$\frac{1}{2}\frac{d}{dt}\Big(\|\omega_{f,h}(t)\|_h^2+\|\omega_{b,h}(t)\|_h^2\Big)+(D(M_x\tilde{c}_{f,h}(t))D_{-x}\omega_{f,h}(t),D_{-x}\omega_{f,h}(t))_+ \\ \leq((D(M_x\tilde{c}_{f,h}(t))-D(M_xc_{f,h}(t)))D_{-x}c_{f,h}(t),D_{-x}\omega_{f,h}(t))_+ \\ +(F(c_{f,h}(t),c_{b,h}(t))-F(\tilde{c}_{f,h}(t),\tilde{c}_{b,h}(t)),\omega_{f,h}(t))_h \\ +(S(c_{f,h}(t),c_{b,h}(t))-S(\tilde{c}_{f,h}(t),\tilde{c}_{b,h}(t)),\omega_{b,h}(t))_h. \tag{2.35}$$

Using in (2.35) the assumptions (HD_0), (HD_ℓ), (HF_ℓ) and, (HS_ℓ) we get

$$\frac{1}{2}\frac{d}{dt}\Big(\|\omega_{f,h}(t)\|_h^2+\|\omega_{b,h}(t)\|_h^2\Big)+D_0\|D_{-x}\omega_{f,h}(t)\|_+^2 \\ \leq C_D\|D_{-x}c_{f,h}(t)\|_\infty\|\omega_{f,h}(t)\|_h\|D_{-x}\omega_{f,h}(t)\|_+ \\ +C_{F_\ell}(\|\omega_{f,h}(t)\|_h+\|\omega_{b,h}(t)\|_h)\|\omega_{f,h}(t)\|_h \\ +C_{S_\ell}(\|\omega_{f,h}(t)\|_h+\|\omega_{b,h}(t)\|_h)\|\omega_{b,h}(t)\|_h. \tag{2.36}$$

From inequality (2.36), we obtain

$$\frac{d}{dt}\Big(\|\omega_{f,h}(t)\|_h^2+\|\omega_{b,h}(t)\|_h^2\Big)+2(D_0-\varepsilon^2)\|D_{-x}\omega_{f,h}(t)\|_+^2 \\ \leq\gamma(t)\Big(\|\omega_{f,h}(t)\|_h^2+\|\omega_{b,h}(t)\|_h^2\Big), \tag{2.37}$$

with $\gamma(t)$ defined by (2.34) and $\varepsilon\neq 0$ an arbitrary constant. Inequality (2.33) follows from (2.37).

■

From (2.28), the semi-discrete in space FDM (2.6)-(2.6) is local stable in the solution $c_{f,h}(t)\in W_{h,0}$, $c_{b,h}(t)\in\hat{W}_h$, $t\in[0,T]$, $h\in\Lambda$, provided we fix ρ_0 by

$$\rho_0\leq\frac{\sqrt{2}}{2}\sqrt{\rho_\varepsilon}e^{-\frac{T}{2}\max\limits_t\gamma(t)},\ \ t\in[0,T], \tag{2.38}$$

and (2.29) holds. To conclude (2.29) we study in what follows the convergence of the semi-discrete problem (2.6)-(2.6).

2.3.2 Convergence

Convergence for smooth solution and non-smooth solution is proved in this section. In the first approach use a Taylor representation of the spatial truncation error and consequently we assume that $c_f(t) \in C^4(\overline{\Omega})$ and $c_b(t) \in C(\Omega)$. In the second part we use the Bramble-Hilbert lemma that allow us to reduce the smoothness on $c_f(t)$ and $c_b(t)$.

Let $(c_f(t), c_b(t))$ be a solution of the system (2.1)-(2.4). We define the errors $E_{f,h}(t)$ and $E_{b,h}(t)$ by

$$E_{f,h}(t) = R_h c_f(t) - c_{f,H}(t), \quad E_{f,h}(t) = R_h c_b(t) - c_{b,H}(t),$$

where $R_h c_f(t)$ and $R_h c_b(t)$ are, respectively, the restriction of $c_f(t)$ and $c_b(t)$ to the mesh Ω_h.

Convergence for smooth solutions

In what follows, C is a positive constant which is independent of t and the mesh parameter h, and which may have different values in different equations.

We observe that for $E_{f,h}(t)$ we have

$$\begin{aligned}\frac{dE_{f,h}}{dt}(t) = {} & D_x^*(D(M_h R_h c_f(t))D_{-x}R_h c_f(t)) - D_x^*(D(M_h c_{f,h}(t))D_{-x}c_{f,h}(t)) \\ & + F(R_h c_f(t), R_H c_b(t)) - F(c_{f,h}(t), c_{b,h}(t)) + T_h(t), \quad \text{in } \Omega_h, \end{aligned} \tag{2.39}$$

for $t \in (0,T]$, where

$$T_h(x_i,t) = T_1(x_i,t) + T_r(x_i,t), \tag{2.40}$$

being T_1 and T_r such that for $i = 1,\dots,N-1$ and $t \in (0,T]$, we have

$$\begin{aligned} T_1(x_i,t) &= (h_{i+1} - h_i)s(x_i,t), \\ |T_r(x_i,t)| &\le C\|J_{1,c_f}(t)\|_{C^4(\overline{\Omega})}h_{max}^2, \end{aligned}$$

where s and J_{1,c_f} are smooth functions depending on the spatial derivatives of order lees or equal to three and less or equal to four, respectively. In the next Theorem 2.3.1, we prove the convergence of the approximations $c_{f,h}(t)$ and $c_{b,h}(t)$.

Theorem 2.3.1. *Let $(c_f(t), c_b(t))$ be a solution of the system* (2.1)-(2.4)*, and denote a solution of the FDM* (2.6)-(2.9) *by $(c_{f,h}(t), c_{b,h}(t))$. Assume that $c_f(t) \in C^4(\overline{\Omega})$, $c_b(t) \in C(\Omega)$, F, S satisfy conditions (HF), (HS) respectively. Assume also that D satisfies (HD_0).*

Then, for $E_{f,h}(t)$ and $E_{b,h}(t)$, holds the following

$$\begin{aligned} &\|E_{f,h}(t)\|_h^2 + \|E_{b,h}(t)\|_h^2 + 2(D_0 - \varepsilon_0^2 - \varepsilon_1^2)\int_0^t e^{\int_s^t \hat{\gamma}(\mu)d\mu}\|D_{-x}E_{f,h}(s)\|_+^2 ds \\ &\le e^{\int_0^t \hat{\gamma}(s)ds}\left(\|E_{f,h}(0)\|_h^2 + \|E_{b,h}(0)\|_h^2\right) + \int_0^t e^{\int_s^t \hat{\gamma}(\mu)d\mu}\hat{T}(s)ds, \end{aligned} \tag{2.41}$$

for $t \in [0,T]$. In (2.41), $\hat{\gamma}$ and $\hat{T}$ are such that

$$\hat{\gamma}(t) = \max\left\{\frac{C_D^2}{\varepsilon_0^2}\|D_{-x}R_h c_f(t)\|_\infty^2 + 3(\varepsilon_1^2+\varepsilon_2^2) + 3C_{F_\ell} + C_{F_\ell},\ \ C_{F_\ell} + 3C_{S_\ell}\right\}, \tag{2.42}$$

and

$$\hat{T}(t) \le Ch_{\max}^4\left(\frac{1}{2\varepsilon_1^2}+\frac{1}{2\varepsilon_2^2}\right)\|c_f(t)\|_{C^4(\overline{\Omega})}^{p_f}, \tag{2.43}$$

where $\varepsilon_i \neq 0, i = 0,1,2$ and p_f is a positive integer.

Proof: From (3.72) we get

$$\begin{aligned}(E'_{f,h}(t), E_{f,h}(t))_H = &-(D(M_hR_hc_f(t))D_{-x}R_hc_f(t) - D(M_hc_{f,h}(t))D_{-x}c_{f,h}(t), D_{-x}E_{f,h}(t))_+\\ &+(F(R_hc_f(t),R_hc_b(t)) - F(c_{f,h}(t),c_{b,h}(t)), E_{f,h}(t))_h + (T_1(t), E_{f,h}(t))_h.\end{aligned}$$

As

$$\begin{aligned}&-(D(M_hR_hc_f(t))D_{-x}R_hc_f(t) - D(M_hc_{f,h}(t))D_{-x}c_{f,h}(t), D_{-x}E_{f,h}(t))_+\\ &\quad= -((D(M_hR_hc_f(t)) - D(M_hc_{f,h}(t)))D_{-x}R_Hc_f(t), D_{-x}E_{f,h}(t))_+\\ &\qquad - D(M_hc_{f,h}(t)))D_{-x}E_{f,h}(t), D_{-x}E_{f,h}(t))_+\\ &\qquad\le C_D\|D_{-x}R_hc_f(t)\|_\infty\|E_{f,h}(t)\|_h\|D_{-x}E_{f,h}(t)\|_+ - D_0\|D_{-x}E_{f,h}(t)\|_+^2\\ &\qquad\le C_D^2\frac{1}{4\varepsilon_0^2}\|D_{-x}R_hc_f(t)\|_\infty^2\|E_{f,h}(t)\|_h^2 + (\varepsilon_0^2 - D_0)\|D_{-x}E_{f,h}(t)\|_+^2,\end{aligned}$$

where $\varepsilon_0 \neq 0$, and

$$(F(R_hc_f(t),R_hc_b(t)) - F(c_{f,h}(t),c_{b,h}(t)), E_{f,h}(t))_h \le C_{F_\ell}\Big(\|E_{f,h}(t)\|_h^2 + \|E_{b,h}(t)\|_h\|E_{f,h}(t)\|_h\Big),$$

we conclude

$$\begin{aligned}&\frac{1}{2}\frac{d}{dt}\|E_{f,h}(t)\|_H + (D_0 - \varepsilon_0^2)\|D_{-x}E_{f,h}(t)\|_+^2\\ &\qquad\le \Big(C_D^2\frac{1}{2\varepsilon_0^2}\|D_{-x}R_hc_f(t)\|_\infty^2 + C_{F_\ell}\Big)\|E_{f,h}(t)\|_h^2 + C_{F_\ell}\|E_{b,h}(t)\|_h\|E_{f,h}(t)\|_h\\ &\qquad + (T_h(t), E_{f,h}(t))_h.\end{aligned} \tag{2.44}$$

Now we establish a bound for $(T_h(t), E_{f,h}(t)_H)$. By taking inner product of $T_1(t)$ with $E_{f,h}(t)$, one has

$$(T_1(t), E_{f,h}(t))_h = \sum_{i=1}^{N-1} h_{i+1/2}T_1(x_i,t)E_{f,h}(x_i,t) \tag{2.45}$$

$$= \frac{1}{2}\sum_{i=1}^{N} h_i^2\big(s(x_{i-1},t)E_{f,h}(x_{i-1},t) - s(x_i,t)E_{f,h}(x_i,t)\big) \tag{2.46}$$

$$= -\frac{1}{2}\sum_{i=1}^{N} h_i^3 s(x_{i-1},t)D_{-x}E_{f,h}(x_i,t)$$

$$-\frac{1}{2}\sum_{i=1}^{N} h_i^2 \int_{x_{j-1}}^{x_j} \frac{\partial s}{\partial x}(x,t)dx E_{f,h}(x_i,t),$$

that leads to

$$(T_1(t),E_{f,h}(t))_h \leq \frac{C}{4\varepsilon_1^2} h_{max}^4 \|s(t)\|^2_{C^1(\overline{\Omega})} + \frac{3}{2}\varepsilon_1^2\big(\|E_{f,h}(t)\|_+^2 + \|D_{-x}E_{f,h}(t)\|_+^2\big), \tag{2.47}$$

where $\varepsilon_1 \neq 0$. On the other hand, we also have

$$(T_2(t),E_{c_f}(t))_h \leq \frac{C}{4\varepsilon_2^2} h_{max}^4 \|J_{1,c_f}(t)\|^2_{C(\overline{\Omega})} + \varepsilon_2^2\|E_{f,h}(t)\|_h^2,$$

where $\varepsilon_2 \neq 0$, we obtain

$$\begin{aligned}(T_h(t),E_{f,h}(t))_h \leq & C\Big(\frac{1}{4\varepsilon_1^2}+\frac{1}{4\varepsilon_2^2}\Big)h_{max}^4\left(\|s(t)\|^2_{C^1(\overline{\Omega})} + \|J_{1,c_f}(t)\|^2_{C^1(\overline{\Omega})}\right)\\ &+\frac{3}{2}\big(\varepsilon_1^2+\varepsilon_2^2\big)\|E_{f,h}(t)\|_h^2 + \frac{3}{2}\varepsilon_1^2\|D_{-x}E_{f,h}(t)\|_+^2.\end{aligned} \tag{2.48}$$

Inserting the upper bound (2.48) in (2.44) we have

$$\begin{aligned}&\frac{1}{2}\frac{d}{dt}\|E_{f,h}(t)\|_h^2 + (D_0-\varepsilon_0^2-\frac{3}{2}\varepsilon_1^2)\|D_{-x}E_{f,h}(t)\|_+^2\\ &\quad\leq \Big(C_D^2\frac{1}{2\varepsilon_0^2}\|D_{-x}R_H c_f(t)\|_\infty^2 + \frac{3}{2}(\varepsilon_1^2+\varepsilon_2^2)+C_{F_\ell}\Big)\|E_{f,h}(t)\|_h^2 + C_{F_\ell}\|E_{b,h}(t)\|_h\|E_{f,h}(t)\|_h\\ &\quad+C\Big(\frac{1}{4\varepsilon_1^2}+\frac{1}{4\varepsilon_2^2}\Big)h_{max}^4\left(\|s(t)\|^2_{C^1(\overline{\Omega})} + \|J_{1,c_f}(t)\|^2_{C^1(\overline{\Omega})}\right).\end{aligned} \tag{2.49}$$

Analogously, we also have

$$\frac{1}{2}\frac{d}{dt}\|E_{b,h}(t)\|_h^2 \leq C_{S_\ell}\|E_{b,h}(t)\|_h^2 + C_{S_\ell}\|E_{f,h}(t)\|_h\|E_{b,h}(t)\|_h. \tag{2.50}$$

Finally, from (2.49) and (2.51)

$$\begin{aligned}\frac{1}{2}\frac{d}{dt}\big(\|E_{f,h}(t)\|_h^2+\|E_{b,h}(t)\|_h^2\big) + (D_0-\varepsilon_0^2-\frac{3}{2}\varepsilon_1^2)\|D_{-x}E_{f,h}(t)\|_+^2&\\ \leq \hat{\gamma}(t)\big(\|E_{f,h}(t)\|_h^2+\|E_{b,h}(t)\|_h^2\big)+\hat{T}(t),&\end{aligned} \tag{2.51}$$

where $\hat{\gamma}$ and $\hat{T}$ are defined by (2.42) and (2.43) respectively.

Finally, inequality (2.51) leads to (2.41). ■

Corollary 2.3.2. *Under the conditions of Theorem* (2.3.1)*, there exists a positive constant C independent of h and t, such that*

$$\|E_{f,h}(t)\|_h^2 + \|E_{b,h}(t)\|_h^2 + \int_0^t \|D_{-x}E_{f,h}(s)\|_+^2 ds \leq C\Big(h_{max}^4 + \|E_{f,h}(0)\|_h^2 + \|E_{b,h}(0)\|_h^2\Big),$$

for $t \in [0,T]$ *and* $h \in \Lambda$.

From the previous result, if we consider $c_{f,h}(0) = R_h c_f(0)$ and $c_{b,h}(0) = R_h c_b(0)$ then

$$\|E_{f,h}(t)\|_h^2 + \|E_{b,h}(t)\|_h^2 + \int_0^t \|D_{-x}E_{f,h}(s)\|_+^2 ds \leq Ch_{max}^4.$$

Convergence for non-smooth solutions

The Taylor-based error estimate (2.41), requires that $c_f(t) \in C^4(\overline{\Omega})$. Based on the approach introduced in [51] we establish an error bound for the solution of the scheme (2.1)-(2.4) considering $c_f(t) \in H^3(\Omega) \cap H_0^1(\Omega)$.
Let $x_{i-1/2} = x_i - \frac{h_i}{2}$ and $x_{i+1/2} = x_i + \frac{h_{i+1}}{2}$. Moreover, define

$$(g)_h(x_i) = \frac{1}{h_{i+1/2}} \int_{x_{i-1/2}}^{x_{i+1/2}} g(x)dx, \quad i = 1, \ldots, N-1,$$
$$\widehat{R}_h g(x_i) = g(x_{i-1/2}), \quad i = 1, \ldots, N.$$

To get an estimate for $E_{f,h}(t)$ we start by noting that

$$\begin{aligned}(E'_{f,h}(t), E_{f,h}(t))_h = &((\frac{\partial c_f}{\partial t}(t))_h, E_{f,h}(t))_h + (R_h \frac{\partial c_f}{\partial t}(t) - (\frac{\partial c_f}{\partial t}(t))_h, E_{f,h}(t))_h \\ &+ (D(M_x c_{f,h}(t))D_{-x}c_{f,h}(t), D_{-x}E_{f,h}(t))_+ - (F(c_{f,h}(t), c_{b,h}(t)), E_{f,h}(t))_h.\end{aligned}$$

We have

$$\begin{aligned}\left((\frac{\partial c_f}{\partial t}(t))_h, E_{f,h}(t)\right)_h &= \left((\frac{\partial}{\partial x}(D(c_f(t))\frac{\partial c_f}{\partial x}(t)) + F(c_f(t), c_b(t)))_h, E_{f,h}(t)\right)_h \\ &= -(D(\widehat{R}_h c_f(t))\widehat{R}_h \frac{\partial c_f}{\partial x}(t), D_{-x}E_{f,h}(t))_+ \\ &\quad + (D(M_x R_h c_f(t))D_{-x}R_h c_f(t), D_{-x}E_{f,h}(t))_+ \\ &\quad - (D(M_x R_h c_f(t))D_{-x}R_h c_f(t), D_{-x}E_{f,h}(t))_+ \\ &\quad + ((F(c_f(t), c_b(t)))_h - F(R_h c_f(t), R_h c_b(t)), E_{f,h}(t))_h \\ &\quad + (F(R_h c_f(t), R_h c_b(t)), E_{f,h}(t))_h \\ &= \sum_{\ell=1}^{2} T_{h,\ell}(t) - (D(M_x R_h c_f(t))D_{-x}R_h c_f(t), D_{-x}E_{f,h}(t))_+ \\ &\quad + (F(R_h c_f(t), R_h c_b(t)), E_{f,h}(t))_h,\end{aligned}$$

where

$$T_{h,1}(t) = +(D(M_x R_h c_f(t))D_{-x}R_h c_f(t), D_{-x}E_{f,h}(t))_+ - (D(\widehat{R}_h c_f(t))\widehat{R}_h \frac{\partial c_f}{\partial x}(t), D_{-x}E_{f,h}(t))_+, \tag{2.52}$$

and

$$T_{h,2}(t) = ((F(c_f(t), c_b(t)))_h - F(R_h c_f(t), R_h c_b(t)), E_{f,h}(t))_h. \tag{2.53}$$

Then, for $(E'_{f,h}(t), E_{f,h}(t))_h$ we deduce the following representation

$$\begin{aligned}(E'_{f,h}(t), E_{f,h}(t))_h = &-(D(M_x R_h c_f(t)) D_{-x} R_h c_f(t), D_{-x} E_{f,h}(t))_+ \\ &+ (D(M_x c_{f,h}(t)) D_{-x} c_{f,h}(t), D_{-x} E_{f,h}(t))_+ \\ &+ (F(R_h c_f(t), R_h c_b(t)) - F(c_{f,h}(t), c_{b,h}(t)), E_{f,h}(t))_h \\ &+ \sum_{\ell=1}^{3} T_{h,\ell}(t), \end{aligned} \tag{2.54}$$

where

$$T_{h,3}(t) = (R_h \frac{\partial c_f}{\partial t}(t), E_{f,h}(t))_h - ((\frac{\partial c_f}{\partial t}(t))_h, E_{f,h}(t))_h. \tag{2.55}$$

From (2.54), taking into account the assumptions (HD_0), (HD_ℓ), and (HF_ℓ), we easily get

$$\begin{aligned}\frac{1}{2}\frac{d}{dt}\|E_{f,h}(t)\|_h^2 \leq &-D_0 \|D_{-x} E_{f,h}(t)\|_+^2 \qquad (2.56)\\ &+ C_{D_\ell} \|D_{-x} R_h c_f(t)\|_\infty \|E_{f,h}(t)\|_h \|D_{-x} E_{f,h}(t)\|_+ \\ &+ C_{F_\ell}(\|E_{f,h}(t)\|_h + \|E_{b,h}(t)\|_h)\|E_{f,h}(t)\|_h \\ &+ \sum_{\ell=1}^{3} T_{h,\ell}(t), \qquad (2.57)\end{aligned}$$

For the error $E_{b,h}(t)$, we have

$$(E'_{b,h}(t), E_{b,h}(t))_h = (S(R_h c_f(t), R_h c_b(t)) - S(c_{f,h}(t), c_{b,h}(t)), E_{b,h}(t))_h,$$

and considering the assumption (HS_ℓ), we obtain

$$\frac{1}{2}\frac{d}{dt}\|E_{b,h}(t)\|_h^2 \leq C_{S_\ell}(\|E_{f,h}(t)\|_h + \|E_{b,h}(t)\|_h)\|E_{b,h}(t)\|_h. \tag{2.58}$$

In what follows, we establish upper bounds for the terms $T_{h,\ell}(t), \ell = 1,2,3$. The results presented in [51] for elliptic equations have a central role here.

Proposition 2.3.3. *Let $T_{h,1}(t)$ be defined by* (2.52)*. If $c_f(t) \in H^3(\Omega) \cap H_0^1(\Omega)$ and (HD_ℓ) holds, then there exists a positive constant C_{T_1}, independent of h and t, such that*

$$|T_{h,1}(t)| \leq C_{T_1} \frac{1}{\varepsilon^2}\Big(C_D^2 \|\frac{\partial c_f}{\partial x}(t)\|_\infty^2 + \|D\|_\infty^2\Big)\|c_f(t)\|_{H^3(\Omega)}^2 h_{max}^4 + 2\varepsilon^2 \|D_{-x} E_{f,h}(t)\|_+^2, \tag{2.59}$$

for $t \in (0,T], h \in \Lambda$, and with $\varepsilon \neq 0$ an arbitrary constant.

Proof: As

$$\begin{aligned}T_{h,1}(t) = &-((D(\widehat{R}_h c_f(t)) - D(M_x R_h c_f(t)))\widehat{R}_h \frac{\partial c_f}{\partial x}(t), D_{-x} E_{f,h}(t))_+ \\ &+ (D(M_x R_h c_f(t))(\widehat{R}_h \frac{\partial c_f}{\partial x}(t) - D_{-x} R_h c_f(t), D_{-x} E_{f,h}(t))_+,\end{aligned}$$

we have

$$\begin{aligned}|T_{h,1}(t)| &\leq \|\frac{\partial c_f}{\partial x}(t)\|_\infty C_D \|\widehat{R}_h c_f(t) - M_x R_h c_f(t)\|_+ \|D_{-x}E_{f,h}(t)\|_+ \\ &\quad + \|D\|_\infty \|\widehat{R}_h \frac{\partial c_f}{\partial x}(t) - D_{-x}R_h c_f(t)\|_+ \|D_{-x}E_{f,h}(t)\|_+ \\ &:= T_{h,1}^{(1)}(t) + T_{h,1}^{(2)}(t),\end{aligned}$$

with

$$T_{h,1}^{(1)}(t) = \|\frac{\partial c_f}{\partial x}(t)\|_\infty C_D \|\widehat{R}_h c_f(t) - M_x R_h c_f(t)\|_+ \|D_{-x}E_{f,h}(t)\|_+$$

and

$$T_{h,1}^{(2)}(t) = \|D\|_\infty \|\widehat{R}_H \frac{\partial c_f}{\partial x}(t) - D_{-x}R_H c_f(t)\|_+ \|D_{-x}E_{f,h}(t)\|_+.$$

Considering Theorem 1 of [51], it can be shown that there exist two positive constants C_1 and C_2, independent of h and t, such that

$$|T_{h,1}^{(1)}(t)| \leq C_1 \|\frac{\partial c_f}{\partial x}(t)\|_\infty C_D \Big(\sum_{i=1}^{N} h_i^4 \|c_f(t)\|^2_{H^2(x_{i-1},x_i)} \Big)^{1/2} \|D_{-x}E_{f,h}(t)\|_+. \tag{2.60}$$

and

$$|T_{h,1}^{(2)}(t)| \leq C_2 \|D\|_\infty \Big(\sum_{i=1}^{N} h_i^4 \|c_f(t)\|^2_{H^3(x_{i-1},x_i)} \Big)^{1/2} \|D_{-x}E_{f,h}(t)\|_+. \tag{2.61}$$

Inequalities (2.60) and (2.61) easily lead to (2.59). ■

The next two propositions give estimates for $T_{h,2}(t)$ and $T_{h,3}(t)$. The proofs also follow from Theorem 1 of [51].

Proposition 2.3.4. *Let $T_{h,2}(t)$ be defined by* (2.53)*. If $F(c_f(t), c_b(t)) \in H^2(\Omega)$, then there exists a positive constant C_{T_2}, independent of h and t, such that*

$$|T_{h,2}(t)| \leq C_{T_2} \frac{1}{\varepsilon^2} \|F(c_f(t), c_b(t))\|^2_{H^2(\Omega)} h_{max}^4 + \varepsilon^2 \|D_{-x}E_{f,h}(t)\|^2_+,$$

for $t \in (0,T], h \in \Lambda$, and with $\varepsilon \neq 0$ an arbitrary constant.

Proposition 2.3.5. *Let $T_{h,3}(t)$ be defined by* (2.55)*. If $\frac{\partial c_f}{\partial t}(t) \in H^2(\Omega)$, then there exists a positive constant C_{T_3}, independent of h and t, such that*

$$|T_{h,3}(t)| \leq C_{T_3} \frac{1}{\varepsilon^2} \|c_f'(t)\|^2_{H^2(\Omega)} h_{max}^4 + \varepsilon^2 \|D_{-x}E_{f,h}(t)\|^2_+,$$

for $t \in (0,T], h \in \Lambda$, and with $\varepsilon \neq 0$ an arbitrary constant.

Using the estimates of Propositions 2.3.3-2.3.5, we are able to obtain an upper bound for $\|E_{f,h}(t)\|_h^2 + \|E_{b,h}(t)\|_h^2 + \int_0^t \|D_{-x}E_{f,h}(s)\|_+^2 ds$. We start by noting that from (2.56),(2.58) it can be shown that holds the following

$$\frac{d}{dt}\Big(\|E_{f,h}(t)\|_h^2 + \|E_{b,h}(t)\|_h^2 \Big) + 2(D_0 - 5\varepsilon^2) \|D_{-x}E_{f,h}(t)\|_+^2$$

$$\leq \frac{1}{2\varepsilon^2}C_D^2\|D_{-x}R_hc_f(t)\|_\infty^2\|E_{f,h}(t)\|_h^2 + 4\max\{C_{F_\ell},C_{S_\ell}\}(\|E_{f,h}(t)\|_h^2+\|E_{b,h}(t)\|_h^2)+\widehat{T}_h(t), \tag{2.62}$$

where

$$\widehat{T}_h(t) = C_{\widehat{T}}\frac{1}{\varepsilon^2}\Big(\Big(C_D^2\|\frac{\partial c_f}{\partial x}(t)\|_\infty^2+\|D\|_\infty^2\Big)\|c_f(t)\|_{H^3(\Omega)}^2 + \|F(c_f(t),c_b(t))\|_{H^2(\Omega)}^2+\|c_f'(t)\|_{H^2(\Omega)}^2\Big)h_{max}^4, \tag{2.63}$$

being $C_{\widehat{T}} = 2\max\limits_{i=1,2,3}\{C_{T_i}\}$. Using (2.62), we can prove the main result of this section.

Theorem 2.3.2. *Let $c_f \in L^2(0,T,H^3(\Omega)\cap H_0^1(\Omega))\cap C^1([0,T],C(\overline{\Omega}))\cap H^1(0,T,H^2(\Omega))$ and $c_b \in C^1([0,T],C(\Omega))$ be solution of the system* (2.1)-(2.4)*, with D, F, and S satisfying the assumptions (HD_0), (HD_ℓ), (HF_ℓ), and (HS_ℓ). Let $c_{f,h}\in C^1([0,T],W_{h,0})$, $c_{b,h}\in C^1([0,T],\widehat{W}_h)$ be defined by the FDM* (2.6)-(2.9)*. Then*

$$\|E_{f,h}(t)\|_h^2+\|E_{b,h}(t)\|_h^2+2(D_0-5\varepsilon^2)\int_0^t e^{\int_s^t\gamma(\mu)d\mu}\|D_{-x}E_{f,h}(s)\|_+^2\,ds \leq \int_0^t e^{\int_s^t\gamma(\mu)d\mu}\widehat{T}_h(s)\,ds + e^{\int_0^t\gamma(\mu)d\mu}\Big(\|E_{f,h}(0)\|_h^2+\|E_{b,h}(0)\|_h^2\Big), \tag{2.64}$$

for $t\in[0,T], h\in\Lambda$, with $\varepsilon\neq 0$ an arbitrary constant, γ defined by

$$\gamma(t) = \max\left\{\frac{1}{2\varepsilon^2}C_D^2\|D_{-x}R_hc_f(t)\|_\infty^2, 4\max\{C_{F_\ell},C_{S_\ell}\}\right\},$$

and $\widehat{T}_h(t)$ given by (2.63).

Choosing in (2.64) ε conveniently and considering $\|E_{f,h}(0)\|_h = \|E_{b,h}(0)\|_h = 0$, we obtain the following corollary.

Corollary 2.3.3. *Under the assumptions of Theorem 2.3.2, there exists a positive constant C_e, independent of h and t, such that*

$$\|E_{f,h}(t)\|_h^2+\|E_{b,h}(t)\|_h^2+\int_0^t\|D_{-x}E_{f,h}(s)\|_+^2\,ds\leq C_eh_{max}^4,\quad t\in[0,T], h\in\Lambda.$$

2.3.3 Concluding stability

Let us consider $c_{f,h}(t)\in W_{h,0}, c_{b,h}(t)\in\hat{W}_h$ solutions of (2.1)-(2.4). Let $\tilde{c}_{f,h}(t)\in W_{h,0}, \tilde{c}_{b,h}(t)\in\hat{W}_h$ be another solution of the same problem but with initial conditions $\tilde{c}_{f,h}(0)\in B_{\rho_0}(c_{f,h}(0))$ and $\tilde{c}_{b,h}(0)\in B_{\rho_0}(c_{b,h}(0))$. As we mentioned before, to conclude that (2.28) holds it is enough to show that $\int_0^t\|D_{-x}E_{f,h}(s)\|_+^2ds$ is bounded for $t\in[0,T]$ and $h\in\Lambda$, however, this result follows from Corollary 2.3.3 and therefore we conclude the stability for the IBVP (2.1)-(2.4).

Let us suppose that Ω_h for $h\in\Lambda$ satisfies

$$\exists C_G>0: \frac{h_{max}^p}{h_{min}}\leq C_G,\ h\in\Lambda,\ \text{with } h_{max}\text{ small enough.} \tag{2.65}$$

1. If $p=1$, then to get stability of (2.1)-(2.4) in $c_{f,h}(t)\in W_{h,0}, c_{b,h}(t)\in \hat{W}_h$ it is enough to assume that the correspondent initial conditions verify

$$\|E_{f,h}(0)\|_h \leq C\sqrt{h_{max}},\ \ \|E_{b,h}(0)\|_h \leq C\sqrt{h_{max}}.$$

2. If $p=2$, and the initial condition $c_{f,h}(0)\in W_{h,0}, c_{b,h}(0)\in \hat{W}_h$ are such that

$$\|E_{f,h}(0)\|_h \leq Ch_{max},\ \ \|E_{b,h}(0)\|_h \leq Ch_{max},$$

then we conclude the stability of (2.1)-(2.4) in $c_{f,h}(t)\in W_{h,0}, c_{b,h}(t)\in \hat{W}_h$.

We observe that in the last case we consider a weaker smoothness condition for the spatial grid but we need to consider the initial conditions $c_{f,h}(0)\in W_{h,0}, c_{b,h}(0)\in \hat{W}_h$ closer of $R_h c_f(0)$ and $R_h c_b(0)$, respectively. This fact means that there is compromise between the smoothness of the spatial grid and the set of solutions of (2.1)-(2.4) where we can state the stability.

2.4 An Implicit-Explicit Euler method

In this section, we analyze the fully discrete scheme (2.20)-(2.23). The structure is similar to the previous section, we study stability, then convergence and finally the main result on stability is established.

2.4.1 Stability

From (2.24)-(2.27) with $v_h = c^m_{f,h}, w_h = c^m_{b,h}$ and considering the assumptions (HD_0), (HF), and (HS), we obtain

$$\|c^m_{f,h}\|^2_h \leq \|c^{m-1}_{f,h}\|^2_h - 2\Delta t D_0 \|D_{-x}c^m_{f,h}\|^2_+ + 2\Delta t C_F(\|c^{m-1}_{f,h}\|_h + \|c^{m-1}_{b,h}\|_h)\|c^m_{f,h}\|_h, \tag{2.66}$$

$$\|c^m_{b,h}\|^2_h \leq \|c^{m-1}_{b,h}\|^2_h + 2\Delta t C_S(\|c^{m-1}_{f,h}\|_h + \|c^{m-1}_{b,h}\|_h)\|c^m_{b,h}\|_h, \tag{2.67}$$

for $m=1,\ldots,M$. Inequalities (2.66),(2.67) allow us to obtain

$$(1-2\Delta t\max\{C_F,C_S\})\Big(\|c^m_{f,h}\|^2_h + \|c^m_{b,h}\|^2_h\Big) + 2\Delta t D_0\|D_{-x}c^m_{f,h}\|^2_+ \\ \leq (1+2\Delta t\max\{C_F,C_s\})\Big(\|c^{m-1}_{f,h}\|^2_h + \|c^{m-1}_{b,h}\|^2_h\Big),$$

which leads to

$$\|c^m_{f,h}\|^2_h + \|c^m_{b,h}\|^2_h + 2\Delta t D_0 \sum_{\ell=1}^{m}\|D_{-x}c^\ell_{f,h}\|^2_+ \leq \left(\frac{1+2\Delta t\max\{C_F,C_s\}}{1-2\Delta t\max\{C_F,C_S\}}\right)^m \Big(\|c^0_{f,h}\|^2_h + \|c^0_{b,h}\|^2_h\Big),$$

provided that

$$1-2\Delta t\max\{C_F,C_S\} > 0.$$

From the previous inequality, we can conclude the following result.

Proposition 2.4.1. *Let $c^m_{f,h} \in W_{h,0}$, $c^m_{b,h} \in \widehat{W}_h$, be defined by* (2.24)-(2.27) *with the initial conditions $c^0_{f,h} \in W_{h,0}$, $c^0_{b,h} \in \widehat{W}_h$. If (HD$_0$), (HF), and (HS) hold, then*

$$\|c^m_{f,h}\|^2_h + \|c^m_{b,h}\|^2_h + 2\Delta t D_0 \sum_{\ell=1}^{m} \|D_{-x}c^\ell_{f,h}\|^2_+ \le e^{m\Delta t\theta}\Big(\|c^0_{f,h}\|^2_h + \|c^0_{b,h}\|^2_h\Big),$$

for $m = 1,\dots,M, h \in \Lambda$, and $\Delta t \in (0,\Delta t_0]$, where

$$\theta = \frac{4\max\{C_F, C_S\}}{1 - 2\Delta t_0 \max\{C_F, C_S\}},$$

and Δt_0 is such that

$$1 - 2\Delta t_0 \max\{C_F, C_S\} > 0.$$

The fully discrete scheme (2.24)-(2.27) is stable in the solution $c^m_{f,h} \in W_{h,0}$, $c^m_{b,h} \in \widehat{W}_h$, $m = 0,\dots,M$, if for all $\rho_\varepsilon > 0$, there exists $\rho_0 > 0$ such that, for all solutions $\tilde{c}^m_{f,h}, \tilde{c}^m_{f,h} \in W_{h,0}$, $c^m_{b,h}, \tilde{c}^m_{b,h} \in \widehat{W}_h$, $m = 0,\dots,M$, of (2.24)-(2.27) with initial conditions $\tilde{c}^0_{f,h}, \tilde{c}^0_{b,h}$ satisfying $\|\omega^0_{i,h}\|_h \le \rho_0$, $i = f,b$, we have

$$\|\omega^m_{i,h}\|_h \le \rho_\varepsilon, \quad i = f,b,$$

for $m = 1,\dots,M$, $h \in \Lambda$.

In the next proposition we establish an upper bound for $\|\omega^m_{i,h}\|_h, i = f,b$.

Proposition 2.4.2. *Let $c^m_{f,h}, \tilde{c}^m_{f,h} \in W_{h,0}$, $c^m_{b,h}, \tilde{c}^m_{b,h} \in \widehat{W}_h$ be defined by* (2.24)-(2.27) *with initial conditions $c^0_{f,h} \in W_{h,0}$, $c^0_{b,h} \in \widehat{W}_h$. If the assumptions (HD$_0$), (HD$_\ell$), (HF$_\ell$), and (HS$_\ell$) hold, then for $\omega^m_{f,h} = c^m_{f,h} - \tilde{c}^m_{f,h}$ and $\omega^m_{b,h} = c^m_{b,h} - \tilde{c}^m_{b,h}$ we have*

$$\|\omega^m_{f,h}\|^2_h + \|\omega^m_{b,h}\|^2_h + \Delta t D_0 \sum_{j=1}^{m} \|D_{-x}\omega^j_{f,h}\|^2_+ \le e^{m\Delta t \max\limits_{j=1,\dots,M}\sigma(j)}\Big(\|\omega^0_{f,h}\|^2_h + \|\omega^0_{b,h}\|^2_h\Big), \tag{2.68}$$

for $m = 1,\dots,M$, $h \in \Lambda$, and $\Delta t \in (0,\Delta t_0]$, with

$$1 - 2\Delta t_0 \max\{C_{F_\ell}, C_{S_\ell}\} > 0,$$

and

$$\sigma(j) = \frac{\max\{\frac{1}{D_0}C_D^2\|D_{-x}c^j_{f,h}\|^2_\infty, 2\max\{C_{F_\ell}, C_{S_\ell}\}\} + \max\{C_{F_\ell}, C_{S_\ell}\}}{1 - 2\Delta t_0 \max\{C_{F_\ell}, C_{S_\ell}\}}. \tag{2.69}$$

Proof: Taking into account the assumptions (HF$_\ell$) and (HS$_\ell$), it can be proved that

$$\begin{aligned}
\|\omega^m_{f,h}\|^2_h \le{}& \|\omega^{m-1}_{f,h}\|^2_h - 2\Delta t\big(D(M_x c^{m-1}_{f,h})D_{-x}c^m_{f,h} - D(M_x\tilde{c}^{m-1}_{f,h})D_{-x}\tilde{c}^m_{f,h}, D_{-x}\omega^m_{f,h}\big)_+ \\
&+ 2\Delta t C_{F_\ell}(\|\omega^{m-1}_{f,h}\|_h + \|\omega^{m-1}_{b,h}\|_h)\|\omega^m_{f,h}\|_h, \\
\|\omega^m_{b,h}\|^2_h \le{}& \|\omega^{m-1}_{b,h}\|^2_h + 2\Delta t C_{S_\ell}(\|\omega^{m-1}_{f,h}\|_h + \|\omega^{m-1}_{b,h}\|_h)\|\omega^m_{b,h}\|_h.
\end{aligned} \tag{2.70}$$

Considering now the assumptions (HD$_0$) and (HD$_\ell$), we have successively

$$-\big(D(M_x c^{m-1}_{f,h})D_{-x}c^m_{f,h} - D(M_x\tilde{c}^{m-1}_{f,h})D_{-x}\tilde{c}^m_{f,h}, D_{-x}\omega^m_{f,h}\big)_+$$

$$
\begin{aligned}
&= -(D(M_x\tilde{c}_{f,h}^{m-1})D_{-x}\omega_{f,h}^m, D_{-x}\omega_{f,h}^m)_+ \\
&\quad -((D(M_xc_{f,h}^{m-1}) - D(M_x\tilde{c}_{f,h}^{m-1}))D_{-x}c_{f,h}^m, D_{-x}\omega_{f,h}^m)_+ \\
&\leq -D_0\|D_{-x}\omega_{f,h}^m\|_+^2 + C_D\|D_{-x}c_{f,h}^m\|_\infty\|\omega_{f,h}^{m-1}\|_h\|D_{-x}\omega_{f,h}^m\|_+.
\end{aligned}
$$

Using the previous upper bound in (2.70), we obtain

$$
\begin{aligned}
(1-2\Delta t\max\{C_{F_\ell},C_{S_\ell}\})\Big(\|\omega_{f,h}^m\|_h^2 + \|\omega_{b,h}^m\|_h^2\Big) + 2\Delta t(D_0-\varepsilon^2)\|D_{-x}\omega_{f,h}^m\|_+^2 \\
\leq \Delta t\frac{1}{2\varepsilon^2}C_D^2\|D_{-x}c_{f,h}^m\|_\infty^2\|\omega_{f,h}^{m-1}\|_h^2 \\
+ (1+2\Delta t\max\{C_{F_\ell},C_{S_\ell}\})(\|\omega_{f,h}^{m-1}\|_h^2 + \|\omega_{b,h}^{m-1}\|_h^2),
\end{aligned}
$$

that leads to

$$
\|\omega_{f,h}^m\|_h^2 + \|\omega_{b,h}^m\|_h^2 + 2\Delta t(D_0-\varepsilon^2)\|D_{-x}\omega_{f,h}^m\|_+^2 \leq (1+\Delta t\sigma(m))\Big(\|\omega_{f,h}^{m-1}\|_h^2 + \|\omega_{b,h}^{m-1}\|_h^2\Big), \quad (2.71)
$$

provided that

$$
1-2\Delta t\max\{C_{F_\ell},C_{S_\ell}\} > 0.
$$

In (2.71), $\sigma(m)$ is given by

$$
\sigma(m) = \frac{\max\left\{\frac{1}{2\varepsilon^2}C_D^2\|D_{-x}c_{f,h}^m\|_\infty^2, 2\max\{C_{F_\ell},C_{S_\ell}\}\right\}}{1-2\Delta t\max\{C_{F_\ell},C_{S_\ell}\}}.
$$

Let us fix $\varepsilon^2 = \frac{D_0}{2}$ then, from (2.71), we get

$$
\|\omega_{f,h}^m\|_h^2 + \|\omega_{b,h}^m\|_h^2 + \Delta tD_0\sum_{j=1}^m\|D_{-x}\omega_{f,h}^j\|_+^2 \leq \prod_{j=0}^{m-1}(1+\Delta t\sigma(j))\Big(\|\omega_{f,h}^0\|_h^2 + \|\omega_{b,h}^0\|_h^2\Big),
$$

where now $\sigma(j)$ is defined by (2.69). Then, we obtain

$$
\|\omega_{f,h}^m\|_h^2 + \|\omega_{b,h}^m\|_h^2 + \Delta tD_0\sum_{j=1}^m\|D_{-x}\omega_{f,h}^j\|_+^2 \leq (1+\Delta t\max_{j=1,\ldots,m}\sigma(j))^m\Big(\|\omega_{f,h}^0\|_h^2 + \|\omega_{b,h}^0\|_h^2\Big), \quad (2.72)
$$

and from inequality (2.72) we easily get (2.68). ■

Therefore, the local stability follows from Proposition 2.4.2, with

$$
\rho_0 \leq \frac{\sqrt{2}}{2}\sqrt{\rho_\varepsilon}e^{-\frac{1}{2}T\max\limits_{j=1,\ldots,M}\sigma(j)}.
$$

We remark that $\sigma(j)$ depends on $\|D_{-x}c_{f,h}^m\|_\infty$. Consequently, to obtain rho_0 independent of h, we need to establish the uniform boundedness

$$
\|D_{-x}c_{f,h}^m\|_\infty^2 \leq C, \quad m=1,\ldots,M, \Delta t\in(0,\Delta t_0], h\in\Lambda. \quad (2.73)
$$

In (2.73), C denotes a positive constant independent of h and Δt.

As in the semi-discrete stability analysis, to obtain the upper bound (2.73), we study the convergence properties of $c_{f,h}^m \in W_{h,0}, c_{b,h}^m \in \widehat{W}_h$, $m = 0,\ldots,M$, solution of (2.24)-(2.27).

2.4.2 Convergence

Theorem 2.4.1 is the main result of this section where we establish the an error bound that will be used to conclude inequality (2.73). This result considers only non-smooth solutions of the IBVP (2.1)-(2.4).

Theorem 2.4.1. *Let $c_f \in C([0,T],H^3(\Omega)\cap H_0^1(\Omega))\cap C^2([0,T],C(\overline{\Omega}))\cap C^1(0,T,H^2(\Omega))$ and $c_b \in C^2([0,T],C(\Omega))$ be solution of the IBVP* (2.1)-(2.4)*, with D, F, and S satisfying the assumptions (HD_0), (HD_ℓ), (HF_ℓ), and (HS_ℓ). Let $c_{f,h}^m \in W_{h,0}, c_{b,h}^m \in \widehat{W}_h$, be defined by the fully discrete scheme* (2.24)-(2.27) *with initial conditions $c_{f,h}^0 \in W_{h,0}$, $c_{b,h}^0 \in \widehat{W}_h$. Then, for the errors $E_{f,h}^m = R_h c_f(t_m) - c_{f,h}^m$, $E_{b,h}^m = R_h c_b(t_m) - c_{b,h}^m$, holds the following*

$$\begin{aligned}
&\|E_{f,h}^m\|_h^2 + \|E_{b,h}^m\|_h^2 + 2\Delta t(D_0 - 5\varepsilon^2)\Big(\sum_{j=1}^{m-1}\prod_{i=j+1}^{m}(1+\sigma(i))\|D_{-x}E_{f,h}^j\|_+^2 + \|D_{-x}E_{f,h}^m\|_+^2\Big)\\
&\qquad \le \prod_{j=1}^{m}(1+\Delta t\sigma(j))\Big(\|E_{f,h}^0\|_h^2 + \|E_{b,h}^0\|_h^2\Big)\\
&\qquad\qquad + \frac{\Delta t}{1-2\Delta t_0\max\{C_{F_\ell},2C_{S_\ell}\}}\Big(\sum_{j=1}^{m-1}\Big(\prod_{i=j+1}^{m}(1+\Delta t\sigma(i))\Big)T_h^j + T_h^m\Big),
\end{aligned} \tag{2.74}$$

for $m = 1,\ldots,M$, $h \in \Lambda$, and $\Delta t \in (0,\Delta t_0]$. In (2.74)*, $\sigma(j)$ is defined by*

$$\sigma(j) = \frac{\max\left\{\dfrac{1}{\varepsilon^2}C_{D_\ell}^2\|D_{-x}R_h c_f(t_j)\|_\infty^2, 2\max\{C_{F_\ell}C_{S_\ell}\}\right\} + \max\{C_{F_\ell},2C_{S_\ell}\}}{1-2\Delta t_0\max\{C_{F_\ell},2C_{S_\ell}\}}, \tag{2.75}$$

$\varepsilon \neq 0$ is an arbitrary constant such that $D_0 - 5\varepsilon^2 > 0$, Δt_0 is fixed by

$$1 - 2\Delta t_0\max\{C_{F_\ell},2C_{S_\ell}\} > 0, \tag{2.76}$$

and the error term T_h^j is given by

$$\begin{aligned}
T_h^j = C\frac{1}{2\varepsilon^2}\sum_{i=1}^{N}h_i^4\Big(&\|\frac{\partial c_f}{\partial t}(t_j)\|_{H^2(x_{i-1},x_i)}^2 + \|F(c_f(t_j),c_b(t_j))\|_{H^2(x_{i-1},x_i)}^2\\
&+ \|c_f(t_j)\|_{H^3(x_{i-1},x_i)}^2\Big) + \Delta t C\int_{t_{j-1}}^{t_j}\Big(\frac{1}{2\varepsilon^2}\|R_h\frac{\partial^2 c_f}{\partial t^2}(s)\|_h^2 + \frac{1}{C_{S_\ell}}\|R_h\frac{\partial^2 c_b}{\partial t^2}(s)\|_h^2\Big)ds,
\end{aligned} \tag{2.77}$$

$j = 1,\ldots,m$, with C a positive constant, h and Δt independent.

Proof: We start the proof by noting that

$$(D_{-t}E_{f,h}^m, E_{f,h}^m)_h = ((\frac{\partial c_f}{\partial t}(t_m))_h, E_{f,h}^m)_h - (D_{-t}c_{f,h}^m, E_{f,h}^m)_h + T_h^{(1)}(t_m), \tag{2.78}$$

where

$$T_h^{(1)}(t_m) = (D_{-t}R_h c_f(t_m) - (\frac{\partial c_f}{\partial t}(t_m))_h, E_{f,h}^m)_h.$$

We also have

$$\begin{aligned}((\frac{\partial c_f}{\partial t}(t_m))_h, E_{f,h}^m)_h &= -((D(\widehat{R}_h c_f(t_m))\widehat{R}_h \frac{\partial c_f}{\partial x}(t_m), D_{-x}E_{f,h}^m)_+ \\ &\quad + ((F(R_h c_f(t_m), R_h c_b(t_m)))_h, E_{f,h}^m)_h \\ &= -((D(M_x c_f(t_{m-1}))D_{-x}R_h c_f(t_m), D_{-x}E_{f,h}^m)_+ \\ &\quad + (F(R_h c_f(t_{m-1}), R_h c_b(t_{m-1})), E_{f,h}^m)_h \\ &\quad + T_h^{(2)}(t_m) + T_h^{(3)}(t_m),\end{aligned} \tag{2.79}$$

where

$$\begin{aligned}T_h^{(2)}(t_m) &= -(D(\widehat{R}_h c_f(t_m))\widehat{R}_h \frac{\partial c_f}{\partial x}(t_m), D_{-x}E_{f,h}^m)_+ \\ &\quad + ((D(M_x c_f(t_{m-1}))D_{-x}R_h c_f(t_m), D_{-x}E_{f,h}^m)_+\end{aligned}$$

and

$$T_h^{(3)}(t_m) = ((F(R_h c_f(t_m), R_h c_b(t_m)))_h - F(R_h c_f(t_{m-1}), R_h c_b(t_{m-1})), E_{f,h}^m)_h.$$

Using (2.79) in (2.78), we obtain

$$\begin{aligned}(D_{-t}E_{f,h}^m, E_{f,h}^m)_h &= -((D(M_x c_f(t_{m-1}))D_{-x}R_h c_f(t_m), D_{-x}E_{f,h}^m)_+ \\ &\quad + ((D(M_x c_{f,h}^{m-1})D_{-x}c_{f,h}^m, D_{-x}E_{f,h}^m)_+ \\ &\quad + (F(R_h c_f(t_{m-1}), R_h c_b(t_{m-1})), E_{f,h}^m)_h - (F(c_{f,h}^{m-1}, c_{b,h}^{m-1}), E_{f,h}^m)_h \\ &\quad + \sum_{\ell=1}^{3} T_h^{(\ell)}(t_m).\end{aligned} \tag{2.80}$$

From (2.80), considering the assumptions (HD_0), (HD_ℓ), and (HF_ℓ), one can get

$$\begin{aligned}&(1 - \Delta t C_{F_\ell})\|E_{f,h}^m\|_h^2 + 2\Delta t(D_0 - \varepsilon^2)\|D_{-x}E_{f,h}^m\|_+^2 \\ &\quad \le \Delta t \frac{1}{2\varepsilon^2} C_{D_\ell}^2 \|D_{-x}R_h c_f(t_m)\|_\infty^2 \|E_{f,h}^{m-1}\|_h^2 \\ &\qquad (1 + 2\Delta t C_{F_\ell})(\|E_{f,h}^{m-1}\|_h^2 + \|E_{b,h}^{m-1}\|_h^2) + 2\Delta t \sum_{j=1}^{3} T_h^{(j)}(t_m).\end{aligned} \tag{2.81}$$

Furthermore, we also have

$$(1 - \Delta t C_{S_\ell})\|E_{b,h}^m\|_h^2 \le (1 + 2\Delta t C_{S_\ell})(\|E_{f,h}^{m-1}\|_h^2 + \|E_{b,h}^{m-1}\|_h^2) + 2\Delta t T_h^{(4)}(t_m), \tag{2.82}$$

with

$$T_h^{(4)}(t_m) = (D_{-t}R_h c_b(t_m) - R_h \frac{\partial c_b}{\partial t}(t_{m-1}), E_{b,h}^m)_h.$$

From (2.81) and (2.82), we conclude

$$
\begin{aligned}
&(1-\Delta t C_{F_\ell})\|E^m_{f,h}\|^2_h+(1-\Delta t C_{S_\ell})\|E^m_{b,h}\|^2_h+2\Delta t(D_0-\varepsilon^2)\|D_{-x}E^m_{f,h}\|^2_+\\
&\quad\le\left(1+\Delta t\max\left\{\frac{1}{2\varepsilon^2}C^2_{D_\ell}\|D_{-x}R_hc_f(t_m)\|^2_\infty,2\max\{C_{F_\ell},C_{S_\ell}\}\right\}\right)\left(\|E^{m-1}_{f,h}\|^2_h+|||E^{m-1}_{b,h}\|^2_h\right)\\
&\qquad+2\Delta t\sum_{j=1}^{4}T^{(j)}_h(t_m).
\end{aligned}
\tag{2.83}
$$

In what follows we establish estimates for $T^{(j)}_h(t_m), j=1,\ldots,4$.

1. An estimate for $T^{(1)}_h(t_m)$: We observe that

$$
D_{-t}R_hc_f(t_m)-(\frac{\partial c_f}{\partial t}(t_m))_h=D_{-t}R_hc_f(t_m)-R_h\frac{\partial c_f}{\partial t}(t_m)+R_h\frac{\partial c_f}{\partial t}(t_m)-(\frac{\partial c_f}{\partial t}(t_m))_h,
$$

where, as in Proposition 2.3.3, we have

$$
|(R_h\frac{\partial c_f}{\partial t}(t_m)-(\frac{\partial c_f}{\partial t}(t_m))_h,E^m_{f,h})_h|\le C\Big(\sum_{i=1}^{N}h_i^4\|\frac{\partial c_f}{\partial t}(t_m)\|^2_{H^2(x_{i-1},x_i)}\Big)^{1/2}\|D_{-x}E^m_{f,h}\|_+,
\tag{2.84}
$$

for a positive constant C, independent of h and t.

The following representation holds

$$
D_{-t}R_hc_f(x_i,t_m)-\frac{\partial c_f}{\partial t}(x_i,t_m)=\frac{1}{\Delta t}\Big(\widehat{g}(1)-\widehat{g}(0)-\widehat{g}'(1)\Big),
$$

with $\widehat{g}(\xi)=c_f(x_i,t_{m-1}+\xi\Delta t)$. Let $\lambda:W^{2,1}(0,1)\to\mathbb{R}$ be defined by

$$
\lambda(g)=g(1)-g(0)-g'(1),\ g\in W^{2,1}(0,1).
$$

As $\lambda\in(W^{2,1}(0,1))'$ and $\lambda(g)=0$ for $g=1,\xi$, from Bramble-Hilbert lemma ([52]) we guarantee the existence of a positive constant C_λ, such that

$$
|\lambda(g)|\le C_\lambda\int_0^1|g''(\xi)|d\xi,\forall g\in W^{2,1}(0,1).
$$

Consequently,

$$
\begin{aligned}
|D_{-t}R_hc_f(x_i,t_m)-\frac{\partial c_f}{\partial t}(x_i,t_m)|&\le C_\lambda\int_{t_{m-1}}^{t_m}|\frac{\partial^2 c_f}{\partial t^2}(x_i,\xi)|d\xi\\
&\le C_\lambda\sqrt{\Delta t}\Big(\int_{t_{m-1}}^{t_m}(\frac{\partial^2 c_f}{\partial t^2}(x_i,\xi))^2d\xi\Big)^{1/2},
\end{aligned}
$$

that leads to

$$
|(D_{-t}R_hc_f(t_m)-\frac{\partial c_f}{\partial t}(t_m),E^m_{f,h})_h|\le C\sqrt{\Delta t}\Big\|\|R_h\frac{\partial^2 c_f}{\partial t^2}\|_{L^2((t_{m-1},t_m))}\Big\|_h\|D_{-x}E^m_{f,h}\|_+,
\tag{2.85}
$$

where C denotes a positive constant, independent of h and t.

Finally, from (2.84) and (2.85), we conclude

$$|T_h^{(1)}(t_m)| \leq C\frac{1}{4\varepsilon^2}\Big(\sum_{i=1}^{N} h_i^4 \|\frac{\partial c_f}{\partial t}(t_m)\|^2_{H^2(x_{i-1},x_i)} + \Delta t \int_{t_{m-1}}^{t_m} \|R_h \frac{\partial^2 c_f}{\partial t^2}(s)\|_h^2 ds\Big) + 2\varepsilon^2 \|D_{-x}E_{f,h}^m\|_+^2, \tag{2.86}$$

where $\varepsilon \neq 0$ is an arbitrary constant and C is a positive constant, independent of h and t.

2. An estimate for $T_h^{(2)}(t_m)$: As in Proposition 2.3.3, we have

$$|T_h^{(2)}(t_m)| \leq C\frac{1}{4\varepsilon^2}\sum_{i=1}^{N} h_i^4 \|c_f(t_m)\|^2_{H^3(x_{i-1},x_i)} + \varepsilon^2 \|D_{-x}E_{f,h}^m\|_+^2, \tag{2.87}$$

where $\varepsilon \neq 0$ is an arbitrary constant and C is a positive constant, independent of h and t.

3. An estimate for $T_h^{(3)}(t_m)$: As in Proposition 2.3.4, we have

$$|T_h^{(3)}(t_m)| \leq C\frac{1}{4\varepsilon^2}\sum_{i=1}^{N} h_i^4 \|F(c_f(t_m), c_b(t_m))\|^2_{H^2(x_{i-1},x_i)} + \varepsilon^2 \|D_{-x}E_{f,h}^m\|_+^2, \tag{2.88}$$

where $\varepsilon \neq 0$ is an arbitrary constant and C is a positive constant, independent of h and t.

4. An estimate for $T_h^{(4)}(t_m)$: Following the proof of (2.85), it can be shown that

$$\begin{aligned}|(D_{-t}R_h c_b(t_m) - \frac{\partial c_b}{\partial t}(t_m), E_{b,h}^m)_h| &\leq C\sqrt{\Delta t}\Big\| \|R_h \frac{\partial^2 c_b}{\partial t^2}\|_{L^2((t_{m-1},t_m))}\Big\|_h \|E_{b,h}^m\|_h \\ &\leq C\Delta t \frac{1}{4\alpha^2}\Big\| \|R_h \frac{\partial^2 c_b}{\partial t^2}\|_{L^2((t_{m-1},t_m))}\Big\|_h^2 + \alpha^2 \|E_{b,h}^m\|_h^2,\end{aligned}$$

where $\alpha \neq 0$ is an arbitrary constant. Fixing in the previous inequality $\alpha^2 = \frac{C_{S_\ell}}{2}$, we get

$$|T_h^{(4)}(t_m)| \leq C\Delta t \frac{1}{2C_{S_\ell}}\Big\| \|R_h \frac{\partial^2 c_b}{\partial t^2}\|_{L^2((t_{m-1},t_m))}\Big\|_h^2 + \frac{C_{S_\ell}}{2}\|E_{b,h}^m\|_h^2, \tag{2.89}$$

where C denotes a positive constant, independent of h and t.

Using the inequalities (2.86)-(2.89) in (2.83), we deduce

$$\begin{aligned}&\|E_{f,h}^m\|_h^2 + \|E_{b,h}^m\|_h^2 + 2\Delta t(D_0 - 5\varepsilon^2)\|D_{-x}E_{f,h}^m\|_+^2 \\ &\quad\leq (1+\Delta t\,\sigma(m))\Big(\|E_{f,h}^{m-1}\|_h^2 + \|E_{b,h}^{m-1}\|_h^2\Big) + \frac{\Delta t}{1-\Delta t\max\{C_{F_\ell}, 2C_{S_\ell}\}}T_h^m,\end{aligned} \tag{2.90}$$

where $\sigma(m)$ and T_h^m are defined by (2.75) and (2.77), respectively.

Finally, from (2.90) we easily get (2.74).

■

Fixing ε, and manipulating conveniently the inequality (2.74), we obtain the following corollary.

Corollary 2.4.1. *Under the assumptions of Theorem 2.4.1, there exist a positive constant C, independent of h and Δt, such that*

$$\|E_{f,h}^m\|_h^2 + \|E_{b,h}^m\|_h^2 + \Delta t \sum_{j=1}^{m} \|D_{-x}E_{f,h}^j\|_+^2 \leq C\Big(\Delta t^2 + h_{max}^4 + \|E_{f,h}^0\|_h^2 + \|E_{b,h}^0\|_h^2\Big), \tag{2.91}$$

for $m = 1,\ldots,M$, $h \in \Lambda$ and $\Delta t \in (0, \Delta t_0]$, with Δt_0 fixed by (2.76).

2.4.3 Concluding stability

In section 2.4.1 we conclude that local stability follows from proposition 2.4.2 provided that (2.73) holds.

We have

$$\|D_{-x}c_{f,h}^m\|_\infty^2 \leq 2\Big(\|D_{-x}E_{f,h}^m\|_\infty^2 + \|D_{-x}R_h c_f(t_m)\|_\infty^2\Big),$$

where

$$\begin{aligned}\|D_{-x}E_{f,h}^m\|_\infty^2 &\leq \tfrac{1}{h_{min}}\|D_{-x}E_{f,h}^m\|_+^2 \\ &\leq C\frac{1}{h_{min}\Delta t}\Delta t \sum_{j=1}^{m} \|D_{-x}E_{f,h}^j\|_+^2.\end{aligned}$$

We recall that from Corollary 2.4.1, (2.91) holds and consequently

$$\begin{aligned}\|D_{-x}E_{f,h}^m\|_\infty^2 &\leq C\frac{1}{h_{min}\Delta t}\Big(\Delta t^2 + h_{max}^4 + \|E_{f,h}^0\|_h^2 + \|E_{b,h}^0\|_h^2\Big) \\ &\leq C\Big(\frac{\Delta t}{h_{min}} + \frac{h_{max}^4}{h_{min}\Delta t} + \frac{1}{h_{min}\Delta t}\Big(\|E_{f,h}^0\|_h^2 + \|E_{b,h}^0\|_h^2\Big)\Big).\end{aligned}$$

Let us suppose that the sequence of grids $\Omega_h, h \in \Lambda$, and the time step size Δt satisfy the following

$$\frac{\Delta t}{h_{min}} \leq C_{G_1}, \quad \frac{h_{max}^{2p}}{h_{min}\Delta t} \leq C_{G_2}, \tag{2.92}$$

where p is positive and $C_{G_i}, i = 1,2$, are positive constant, independent of h and Δt. In (2.92) Δt and h_{max} are small enough.

If the initial conditions $c_{f,h}^0 \in W_{h,0}, c_{b,h}^0 \in \hat{W}_h$ are such that

$$\|E_{f,h}^0\|_h \leq Ch_{max}^p \quad \text{and} \quad \|E_{b,h}^0\|_h \leq Ch_{max}^p, \tag{2.93}$$

then (2.73) holds, and consequently we conclude the stability of (2.24)-(2.27) in $c_{f,h}^m \in W_{h,0}, c_{b,h}^m \in \hat{W}_h$, $m = 0,\ldots,M$.

Finally, we point out that as p increases, we reduce the smoothness of the space and time grids but we also reduce the set of solutions where we are able to conclude stability.

2.5 Numerical experiments

The goal of this section is to numerically illustrate the main result of this chapter - Theorem 2.4.1, or more precisely its corollary - Corollary 2.4.1 and the sharpness of the smoothness assumption imposed on the solution of the IBVP (2.1)-(2.4).

Following Corollary 2.4.1, we introduce the following notation

$$\text{Error}_h^2 = \max_{m=1,\dots,M} \left(\|E_{f,h}^m\|_h^2 + \|E_{b,h}^m\|_h^2 + \Delta t \sum_{k=1}^{m} \|D_{-x}E_{f,h}^m\|_+^2 \right). \tag{2.94}$$

Then the numerical convergence rate is given by

$$\text{Rate}_h = \log_2 \left(\frac{\text{Error}_h}{\text{Error}_{\frac{h}{2}}} \right),$$

where $\text{Error}_{\frac{h}{2}}$ denotes the error (2.94) defined by the numerical solution computed in the spatial mesh obtained by halving the intervals $[x_i, x_{i+1}], i = 0, \dots, N$, associated with the mesh Ω_h. The time step size Δt is chosen small enough (of the order of h_{max}^2) so that the spatial error dominates the time integration error.

Moreover, we measure the numerical time error introducing

$$\text{Error}_{\Delta t}^2 = \max_{m=1,\dots,M} \|E_{f,h}^m\|_h^2 + \|E_{b,h}^m\|_h^2$$

and the correspondent convergence rate $\text{Rate}_{\Delta t}$ defined as Rate_h.

Let $\overline{\Omega} = [0,1]$ and $t \in [0,1]$. We consider the IBVP (2.1)-(2.4) with $S(c_f, c_b) = 2c_f c_b^2$, $F(c_f, c_b) = c_f^2 c_b$, and $D(c_f) = 1 + c_f^2$, i.e.,

$$\begin{cases} \dfrac{\partial c_f}{\partial t} = \dfrac{\partial}{\partial x}\left((1 + c_f^2) \dfrac{\partial c_f}{\partial x} \right) + c_f^2 c_b + g_f(x,t), \\ \dfrac{\partial c_b}{\partial t} = 2c_f C_b^2 + g_b(x,t), \end{cases}$$

with homogeneous Dirichlet boundary conditions. The initial conditions and the functions $g_f(x,t)$ and $g_b(x,t)$ are such that

$$c_f(x,t) = \exp(t)|x - 0.5|^{\alpha}(x^2 - x),\ c_b(x,t) = \exp(t)\sin(\pi x),\ x,t \in [0,1].$$

The numerical approximation for c_f and c_g are then computed using the numerical method (2.24)-(2.27) where the initial numerical approximations coincide with the theoretical solution.

Firstly, we analyze the convergence rate in space. When $\alpha = 3.1$, the solution $c_f(t)$ belongs to $H^3(\Omega) \cap H_0^1(\Omega)$, and the regularity conditions of Theorem 2.4.1 are satisfied. However, when $\alpha = 2.1$, we have $c_f(t) \in H^2(\Omega) \cap H_0^1(\Omega)$.

The computed convergence rates Rate_h are included in Tables 2.1 and Table 2.2. We have second order convergence for $\alpha = 3.1$, see Table 2.1, and only first order convergence for $\alpha = 2.1$, see Table

2.2. These results illustrate that the regularity conditions imposed on the continuous solution are sharp.

N	h_{max}	Error_h	Rate_h
20	5.5249×10^{-2}	4.3243×10^{-3}	-
40	2.7625×10^{-2}	1.1690×10^{-3}	1.8872
80	1.3812×10^{-2}	2.9772×10^{-4}	1.9732
160	6.9061×10^{-3}	7.5112×10^{-5}	1.9868
320	3.4531×10^{-3}	1.8920×10^{-5}	1.9891

Table 2.1 Numerical space convergence rates for $\alpha = 3.1$.

N	h_{max}	Error_h	Rate_h
20	5.8156×10^{-2}	1.4089×10^{-2}	-
40	2.9078×10^{-2}	7.9888×10^{-3}	0.8185
80	1.4539×10^{-2}	3.8829×10^{-3}	1.0409
160	7.2695×10^{-3}	1.8877×10^{-3}	1.0405
320	3.6347×10^{-3}	9.0150×10^{-4}	1.0663

Table 2.2 Numerical space convergence rates for $\alpha = 2.1$.

Now we illustrate the time convergence rate established in Corollary 2.4.1. We fix the spatial mesh with $N = 320$ and $h_{max} = 3.5648 \times 10^{-3}$ and, in what concerns the time grids, we start by $\Delta t = 5 \times 10^{-1}$ and then we halve the time step size. The results obtained are included in Table 4.1. From these results we conclude first order convergence rate in time.

Δt	$\text{Error}_{\Delta t}$	$\text{Rate}_{\Delta t}$
5.0000×10^{-1}	2.7196×10^{-1}	-
2.5000×10^{-1}	1.3394×10^{-1}	1.0218
1.2500×10^{-1}	6.6789×10^{-2}	1.0039
6.2500×10^{-2}	3.3355×10^{-2}	1.0017
3.1250×10^{-2}	1.6607×10^{-2}	1.0061

Table 2.3 Numerical time convergence rate for $\alpha = 4$.

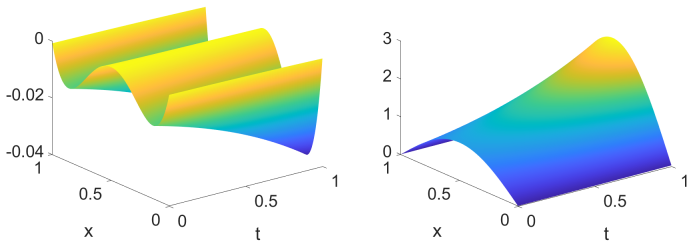

(a) $c_{f,h}$. (b) $c_{b,h}$.

Fig. 2.1 Numerical solution: c_f (on the left) and c_b (on the right).

Chapter 3

Diffusion approximation for light

3.1 Introduction

This chapter aims to study numerical methods for an IBVP defined in a two-dimensional domain that can be used to describe the drug release from a polymeric structure enhanced by light. While in Chapter 2, the Beer–Lambert law was used to describe the light propagation through the spatial domain, here we use the diffusion approach (1.6). This equation is deduced from system (1.3)-(1.4), assuming in the second equation that $\dfrac{1}{\beta(\mu_a+\mu_s)}\dfrac{\partial J}{\partial t}$ is neglected. Then the current density J is given by Fick's law (1.5), and consequently, for the light intensity I, the diffusion equation (1.6) is deduced.

As in Chapter 2, the polymeric structure is loaded with a drug whose molecules are linked with the polymeric chains through photochemical links. Due to the light absorption, the bound drug is converted into free drug that is able to diffuse and be released.

We consider $\Omega = (0,1)^2$ and its boundary $\partial\Omega$ is given by $\partial\Omega = \overline{\Gamma}_l \cup \overline{\Gamma}_u \cup \overline{\Gamma}_r \cup \overline{\Gamma}_d$ where $\Gamma_l = \{(0,y), y \in (0,1)\}$ being $\Gamma_j, j = d,r,u$, defined analogously. These sets are represented in Figure 3.1. For the light intensity I, free drug concentration c_f and bound drug concentration c_b, we consider the general differential system

$$\begin{cases} \dfrac{1}{\beta}\dfrac{\partial I}{\partial t} = \nabla\cdot(D_I\nabla I) + G(I), & (3.1)\\ \dfrac{\partial c_f}{\partial t} = \nabla\cdot(D_c\nabla c_f) + F(I,c_f,c_b), & (3.2)\\ \dfrac{\partial c_b}{\partial t} = S(I,c_f,c_b), & (3.3) \end{cases}$$

for $x \in \Omega, t \in (0,T]$. In (3.1)-(3.3), D_I, D_c are diagonal matrices, depending on $I(t)$ and $c_f(t)$, respectively, with nonnegative diagonal entries $D_{I,ii}, i = 1,2, D_{c,ii}, i = 1,2$.

To close the system (3.1)-(3.3) we assume the initial conditions

$$I(x,0) = 0, \quad c_f(x,0) = 0, \quad c_b(x,0) = c_{b,0}(x), \quad x \in \Omega, \tag{3.4}$$

and the boundary conditions

$$I(x,t) = I_l(t), \quad x \in \Gamma_l, t \in (0,T], \tag{3.5}$$

$$\nabla I(x,t) \cdot \eta = 0, \quad x \in \partial\Omega - \overline{\Gamma}_l - \mathscr{C}_I, t \in (0,T], \tag{3.6}$$

$$\nabla c_f(x,t) \cdot \eta = 0, \quad x \in \partial\Omega - \overline{\Gamma}_r - \mathscr{C}_f, t \in (0,T], \tag{3.7}$$

$$c_f(x,t) = 0, \quad x \in \Gamma_r, t \in (0,T], \tag{3.8}$$

where $\mathscr{C}_I = \{(1,0),(1,1)\}$, $\mathscr{C}_f = \{(0,0),(0,1)\}$ and η denotes the unitary exterior normal.

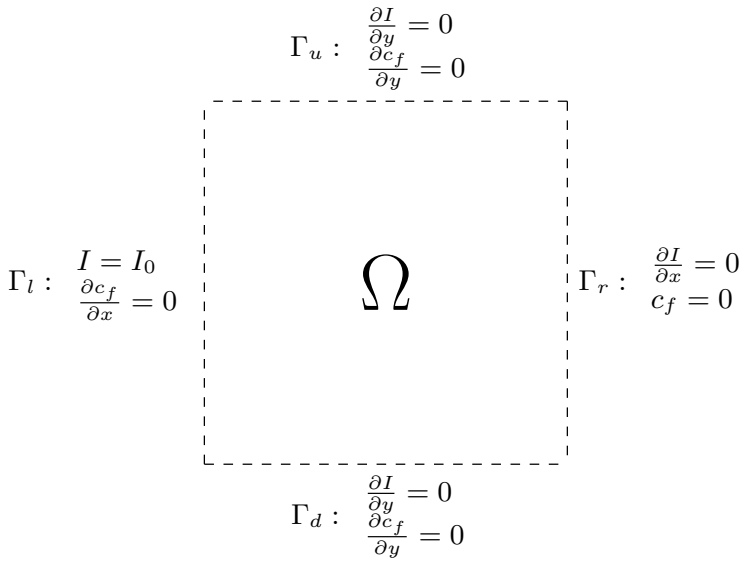

Fig. 3.1 The domain Ω and the boundary conditions for light intensity I and free drug c_f.

Our aim is to introduce a semi-discrete approximation as well as a fully discrete in space and in time finite difference method for the IBVP (3.1)-(3.8). Similarly as in Chapter 2, by choosing appropriate integration rules, the proposed method can also be written as piecewise linear finite element method. In addition, we provide the stability and convergence analysis.

One of the challenges related with the construction of such numerical methods is to obtain a spatial discretization of equations (3.1)-(3.3) and boundary conditions (3.6)-(3.6) such that the discretization satisfies an analogous of the equations (3.9)-(3.10).

$$(\nabla \cdot (D_I \nabla I), \phi)_{L^2(\Omega)} = (D_I \nabla I \cdot \eta, \phi)_{L^2(\partial\Omega - \bar{\Gamma}_l)} - (D_I \nabla I, \nabla\phi)_{[L^2(\Omega)]^2}, \forall \phi \in H^1_{0,l}(\Omega), \tag{3.9}$$

$$(\nabla \cdot (D_c \nabla c_f), \psi)_{L^2(\Omega)} = (D_c \nabla c_f \cdot \eta, \psi)_{L^2(\partial\Omega - \bar{\Gamma}_r)} - (D_c \nabla c_f, \nabla\psi)_{[L^2(\Omega)]^2}, \forall \psi \in H^1_{0,r}(\Omega), \tag{3.10}$$

where $H^1_{0,l}(\Omega) = \{v \in H^1(\Omega) : v = 0 \text{ on } \Gamma_l\}$, $(\cdot,\cdot)_{L^2(\Omega)}$, $(\cdot,\cdot)_{[L^2(\Omega)]^2}$ and $(\cdot,\cdot)_{L^2(\partial\Omega - \bar{\Gamma}_l)}$ denote the usual inner products in $L^2(\Omega)$, $L^2(\Omega) \times L^2(\Omega)$ and $L^2(\partial\Omega - \bar{\Gamma}_l)$, respectively. In (3.10) $H^1_{0,r}(\Omega)$ and $(\cdot,\cdot)_{L^2(\partial\Omega - \bar{\Gamma}_r)}$ are defined analogously.

To establish the desired discrete version of (3.9)-(3.10), as for the problem studied in Chapter 2, we need to define discrete versions of the inner products $(\cdot,\cdot)_{L^2(\Omega)}$, $(\cdot,\cdot)_{[L^2(\Omega)]^2}$ and $(\cdot,\cdot)_{L^2(\partial\Omega - \bar{\Gamma}_l)}$ and $(\cdot,\cdot)_{L^2(\partial\Omega - \bar{\Gamma}_r)}$. Moreover, if a discrete version of (3.9)-(3.10) hold, the discretization of the boundary

conditions lead to errors defined on sets of grid points on parts of the boundary. To establish a relation between the norm of a grid function defined on boundary points and the a discrete version of the H^1-norm, a discrete version of the trace inequality $\|u\|_{L^2(\partial\Omega)} \leq C\|u\|_{H^1}$, for $u \in H^1(\Omega)$, ([62]) needs to be constructed.

Section 3.3 is focused in the stability and convergence properties of the semi-discrete approximation defined by (3.26)-(3.32). Proposition 3.3.2 establishes the stability of the semi-discrete scheme in a fixed solution provided that the fixed solution is uniformly bounded in a certain sense. As in the one-dimensional case, such boundedness property for the fixed solution is consequence of Theorem 3.3.1, where we establish an error estimate for the semi-discrete approximation $I_H(t)$ for the light intensity $I(t)$, and Theorem 3.3.2 that establishes an error estimate for the semi-discrete approximations $c_{f,H}(t)$ and $c_{b,H}(t)$ for the concentration of free and bound drugs. We notice that the upper bound depends on the error of the semi-discrete approximation for the light intensity as well as on the semi-discrete approximation for the free and bound drug concentrations. Theorem 3.3.1 and Theorem 3.3.2 are use later in Section 3.3.3 to conclude the stability of system (3.26)-(3.32).

In Section 3.4 we develop the stability and convergence support for the fully discrete approximation (3.49)-(3.55) and we obtain similar results to those mentioned in Section 3.3 for this fully discrete approximation. Of course, some additional smoothness conditions in time are required.

The error estimates are established assuming that the solution of the IBVP (3.1)-(3.8) is smooth enough. Moreover, the stability and convergence analysis of the methods introduced in this chapter are established by assuming some smoothness conditions. For the reaction terms G, F, and S, there exists positive constants $C_G, C_F, C_S, C_{G_s}, C_{F_s}$, and C_{S_s}, such that

$$|G(x)| \leq C_G|x|, \tag{AG}$$

$$|F(x,y,z)| \leq C_F|x|(|y|+|z|), \tag{AF}$$

$$|S(x,y,z)| \leq C_S|x|(|y|+|z|), \tag{AS}$$

$$|G(x)-G(\tilde{x})| \leq C_{G_s}|x-\tilde{x}|, \tag{AG$_\ell$}$$

$$|F(x,y,z)-F(\tilde{x},\tilde{y},\tilde{z})| \leq C_{F_s}\Big(|\tilde{x}||z-\tilde{z}|+|z||x-\tilde{x}|\Big), \tag{AF$_\ell$}$$

$$|S(x,y,z)-S(\tilde{x},\tilde{y},\tilde{z})| \leq C_{S_s}\Big(|\tilde{x}||z-\tilde{z}|+|z||x-\tilde{x}|\Big), \tag{AS$_\ell$}$$

for $x, \tilde{x}, y, \tilde{y}, z$ and $\tilde{z}$ in $\mathbb{R}$.

Additionally, for the diffusion coefficients $D_{I,ii}$ and $D_{c,ii}$, $i = 1,2$, there exist positive constants $D_{I,0}, D_{c,0}$ and L such that

$$D_{I,ii} \geq D_{I,0} > 0 \text{ and } |D_{I,ii}(x)-D_{I,ii}(\tilde{x})| \leq L|x-\tilde{x}|, \quad x,\tilde{x} \in \mathbb{R}, i = 1,2 \tag{AD$_I$}$$

$$D_{c,ii} \geq D_{c,0} > 0 \text{ and } |D_{c,ii}(x)-D_{c,ii}(\tilde{x})| \leq L|x-\tilde{x}|, \quad x,\tilde{x} \in \mathbb{R}, i = 1,2 \tag{AD$_c$}$$

3.2 Definitions, notation and basic results

In what follows, we introduce the definitions and notations that we need to construct the numerical schemes that allow us to obtain numerical approximations for the solution of the IBVP (3.1)-(3.8) and to develop their theoretical support of stability and convergence.

In $\overline{\Omega}$ we introduce a nonuniform partition $\overline{\Omega}_H$ as follows. Let Λ be a sequence of vectors $H=(h,k)$ with $h=(h_1,\ldots,h_{N_1})$, $k=(k_1,\ldots,k_{N_2})$ with positive entries such that

$$\sum_{i=1}^{N_1} h_i = \sum_{j=1}^{N_2} k_j = 1,$$

with $H_{max}=\max\{h_{max},k_{max}\}\to 0$, where $h_{max}=\max\limits_{i=1,\ldots,N_1} h_i$ and $k_{max}=\max\limits_{j=1,\ldots,N_2} k_j$. In what follows we also use the notation $H_{min}=\min\{h_{min},k_{min}\}$, with $h_{min}=\min\limits_{i=1,\ldots,N_1} h_i$ and $k_{min}=\min\limits_{j=1,\ldots,N_2} k_j$. Let $\overline{\Omega}_H$ be the nonuniform grid

$$\overline{\Omega}_H=\{(x_i,y_j): x_i=x_{i-1}+h_i, y_j=y_{j-1}+k_j, i=1,\ldots,N_1, j=1,\ldots,N_2\}, \tag{3.11}$$

with $x_0=y_0=0$, $x_{N_1}=y_{N_2}=1$. Let $\Omega_H=\overline{\Omega}_H\cap\Omega$, $\partial\Omega_H=\overline{\Omega}_H\cap\partial\Omega$, and $\Gamma_{i,H}=\Gamma_i\cap\partial\Omega_H, i=l,u,r,d$.

By $W(\overline{\Omega}_H)$ we represent the space of grid functions defined in $\overline{\Omega}_H$, $W_{0,l}(\overline{\Omega}_H)$ and $W_{0,r}(\overline{\Omega}_H)$ denote the spaces of grid functions in $W(\overline{\Omega}_H)$ that are null on $\overline{\Gamma}_{l,H}$ and $\overline{\Gamma}_{r,H}$, respectively. We also need to consider the space $W_b(\overline{\Omega}_H-\overline{\Gamma}_{r,H})$ of grid functions defined in $\overline{\Omega}_H-\overline{\Gamma}_{r,H}$.

We introduce now the following finite difference operators:

$$D_{-x}u_H(x_i,y_j)=\frac{u_H(x_i,y_j)-u_H(x_{i-1},y_j)}{h_i},$$
$$D_x^*u_H(x_i,y_j)=\frac{u_H(x_{i+1},y_j)-u_H(x_i,y_j)}{h_{i+\frac{1}{2}}},$$

$$D_{c,x}u_H(x_i,y_j)=\frac{u_H(x_{i+1},y_j)-u_H(x_{i-1},y_j)}{h_i+h_{i+1}},$$

and

$$\nabla_H u_H=(D_{-x}u_H,D_{-y}u_H),\qquad \nabla_H^* u_H=(D_x^*u_H,D_y^*u_H),$$
$$\nabla_{c,H}u_H=(D_{c,x}u_H,D_{c,y}u_H),$$

where $D_{-y},D_{c,y}$ and D_y^* are the finite difference operators defined analogously to $D_{-x},D_{c,x}$ and D_x^*, respectively.

We define the points:

$$x_{-1/2}=x_0,\ \ x_{N_1+1/2}=x_{N_1},$$
$$y_{-1/2}=y_0,\ \ y_{N_2+1/2}=y_{N_2},$$

then, in $W(\overline{\Omega}_H)$ we define the inner product

$$(u_H,v_H)_H=\sum_{(x_i,y_j)\in\overline{\Omega}_H}|\square_{ij}|u_H(x_i,y_j)v_H(x_i,y_j),$$

where $\square_{ij} = [x_{i-\frac{1}{2}}, x_{i+\frac{1}{2}}] \times [y_{j-\frac{1}{2}}, y_{j+\frac{1}{2}}] \cap \overline{\Omega}$, and $u_H, v_H \in W(\overline{\Omega}_H)$. The norm induced by this inner product is denoted by $\|\cdot\|_H$. We also use the following notations

$$(u_H, v_H)_{x,+} = \sum_{(x_i,y_j)\in\overline{\Omega}_H - \overline{\Gamma}_{l,H}} |\square_{x,ij}| u_H(x_i,y_j) v_H(x_i,y_j),$$

$$\|u_H\|_{x,+} = \sqrt{(u_H,u_H)_{x,+}},$$

where $\square_{x,ij} = [x_{i-1}, x_i] \times [y_{j-\frac{1}{2}}, y_{j+\frac{1}{2}}] \cap \overline{\Omega}$, and $u_H, v_H \in W(\overline{\Omega}_H - \overline{\Gamma}_{l,H})$,

$$(u_H, v_H)_{y,+} = \sum_{(x_i,y_j)\in\overline{\Omega}_H - \overline{\Gamma}_{d,H}} |\square_{y,ij}| u_H(x_i,y_j) v_H(x_i,y_h),$$

$$\|u_H\|_{y,+} = \sqrt{(u_H,u_H)_{y,+}},$$

where $\square_{y,ij} = [x_{i-\frac{1}{2}}, x_{i+\frac{1}{2}}] \times [y_{j-1}, y_j] \cap \overline{\Omega}$, and $u_H, v_H \in W(\overline{\Omega}_H - \overline{\Gamma}_{d,H})$.

For $u_H = (u_{H,1}, u_{H,2}), v_H = (v_{H,1}, v_{H,2})$, where $u_{H,1}, v_{H,1} \in W(\overline{\Omega}_H - \overline{\Gamma}_{l,H})$, $u_{H,2}, v_{H,2} \in W(\overline{\Omega}_H - \overline{\Gamma}_{d,H})$, we take

$$(u_H, v_H)_{H,+} = (u_{H,1}, v_{H,1})_{x,+} + (u_{H,2}, v_{H,2})_{y,+} \quad \text{and} \quad \|u_H\|_+ = \sqrt{(u_H,u_H)_{H,+}}.$$

We introduce the average operators

$$M_h u_H(x_i,y_j) = \frac{1}{2}\big(u_H(x_i,y_j) + u_H(x_{i-1},y_j)\big),$$

being M_k defined analogously. By $D_I(M_H u_H)$ we denote the diagonal matrix with diagonal entries $D_{I,11}(M_h u_H)$ and $D_{I,22}(M_k u_H)$. The diagonal matrix $D_c(M_H u_H)$ is defined analogously.

Finally, by $R_H : C(\overline{\Omega}) \to W(\overline{\Omega}_H)$ denotes the restriction operator $R_h u(x_i,y_j) = u(x_i,y_j)$, for $(x_i,y_j) \in \overline{\Omega}_H$ and $u \in C(\overline{\Omega})$.

To discretize equation (3.1) and the boundary conditions (3.5)-(3.6) we need to consider the auxiliary point $x_{N_1+1} = x_{N_1} + h_{N_1}$, $y_{N_2+1} = y_{N_2} + k_{N_2}$ and $y_{-1} = -y_1$ and the fictitious points $\Gamma^{(I)}_{i,H}$, for $i = d,u,r$, defined by equations (3.12)-(3.14).

$$\Gamma^{(I)}_{d,H} = \{(x_i, y_{-1}), i = 1,\ldots,N_1\}, \tag{3.12}$$

$$\Gamma^{(I)}_{u,H} = \{(x_i, y_{N_2+1}), i = 1,\ldots,N_1\}, \tag{3.13}$$

$$\Gamma^{(I)}_{r,H} = \{(x_{N_1+1}, y_j), j = 0,\ldots,N_2\}. \tag{3.14}$$

Similarly, to discretize the free drug concentration equation (3.2) and the boundary condition (3.7)-(3.8) we need to introduce the auxiliary point $x_{-1} = -x_1$ and the fictitious points $\Gamma^{(c)}_{i,H}$, for $i = l,d,u$, defied by equations (3.15)-(3.17). Figure 3.2 illustrates the introduced sets of grid points.

$$\Gamma^{(c)}_{l,H} = \{(x_{-1}, y_j), j = 0,\ldots,N_2\}, \tag{3.15}$$

$$\Gamma^{(c)}_{d,H} = \{(x_i, y_{-1}), i = 0,\ldots,N_1 - 1\}, \tag{3.16}$$

$$\Gamma_{u,H}^{(c)} = \{(x_i, y_{N_2+1}), i = 0, \ldots, N_1 - 1\}. \tag{3.17}$$

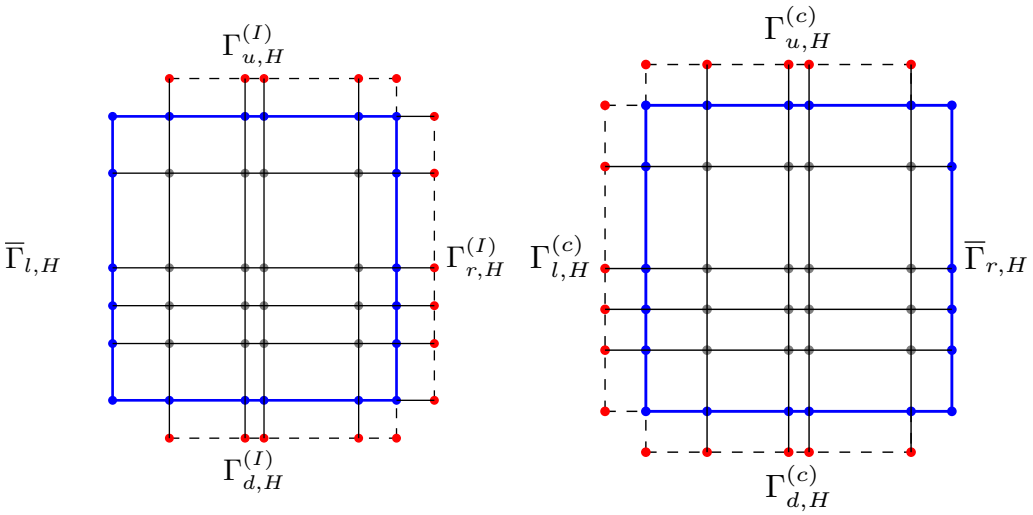

Fig. 3.2 Illustration of the sets of the fictitious grid points $\Gamma_{i,H}^{(I)}$, for $i = d,u,r$ (left) and $\Gamma_{i,H}^{(c)}$, for $i = l,d,u$ (right).

Let $W_{I,H}^*$ and $W_{c,H}^*$ be the space of grid functions defined in $\overline{\Omega}_H \cup (\cup_{i=d,r,u}\Gamma_{i,H}^{(I)})$ and $\overline{\Omega}_H \cup (\cup_{i=l,d,u}\Gamma_{i,H}^{(c)})$, respectively.

In the corner points we assume that we have two unitary normal vectors that are the unitary normal vectors to the sides of Ω. We also need to introduce the boundary operators:

$$D_{\eta_x}^{(I)}(u_H)(x_i,y_j) = \begin{cases} \frac{1}{2}\big(D_{I,11}(M_h u_H(x_{i+1},y_j))D_{-x}u_H(x_{i+1},y_j) \\ \qquad + D_{I,11}(M_h u_H(x_i,y_j))D_{-x}u_H(x_i,y_j)\big), (x_i,y_j) \in \overline{\Gamma}_{r,H}, \\ 0, \quad (x_i,y_j) \in \partial\Omega_H - \overline{\Gamma}_{r,H}, \end{cases}$$

$$D_{\eta_y}^{(I)}(u_H)(x_i,y_j) = \begin{cases} \frac{1}{2}\big(D_{I,22}(M_k u_H(x_i,y_{j+1}))D_{-y}u_H(x_i,y_{j+1}) \\ \qquad + D_{I,22}(M_k u_H(x_i,y_j))D_{-y}u_H(x_i,y_j)\big), (x_i,y_j) \in \Gamma_{I,y}, \\ 0, \quad (x_i,y_j) \in \overline{\Gamma}_{l,H} \cup \Gamma_{r,H}. \end{cases}$$

where $\Gamma_{I,y} = \Gamma_{u,H} \cup \Gamma_{d,H} \cup \{(1,0),(1,1)\}$.

The boundary operators $D_{\eta_x}^{(c)}(u_H)$ and $D_{\eta_y}^{(c)}(u_H)$ are defined analogously. Let $\nabla_{H,\eta}^{(j)}(u_H)$ be defined by $\nabla_{H,\eta}^{(j)}(u_H) = (D_{\eta_x}^{(j)}(u_H), D_{\eta_y}^{(j)}(u_H))$, for $j = I,c$.

Let $\partial\Omega'$ be a subset of $\partial\Omega$ and let $\partial\Omega'_H = \partial\Omega_H \cap \partial\Omega'$. By $W(\partial\Omega'_H)$ we represent the space of grid functions defined on $\partial\Omega'_H$. In this space we introduce the inner product

$$(u_H, v_H)_{\partial\Omega'_H} = \sum_{(x_i,y_j)\in\partial\Omega'_H} |\square'_{ij}| u_H(x_i,y_j) v_H(x_i,y_j),$$

where $\square'_{ij} = \square_{ij} \cap \partial\Omega'$, and the corresponding norm

$$\|u_H\|_{\partial\Omega'_H} = \sqrt{(u_H, u_H)_{\partial\Omega'_H}}.$$

We establish now a proposition relating the spatial discretization in (3.26) and (3.27) with the boundary operators $\nabla^{(j)}_{H,\eta}$, for $j = I, c$, which can be seen as a discrete versions of (3.9) and (3.10), respectively.

Proposition 3.2.1. *Let $u_H \in W^*_{q,H}$ and $w_H \in W_{0,p}(\overline{\Omega}_H)$. Then, for the choice of indexes $q = I, p = l$ or $q = c, p = r$, the next equality holds*

$$\begin{aligned}(\nabla^*_H \cdot (D_q(M_H u_H))\nabla_H u_H), w_H)_H = &-(D_q(M_H u_H)\nabla_H u_H, \nabla_H w_H)_{H,+} \\ &+ (\nabla^{(q)}_{H,\eta}(u_H)\cdot\eta, w_H)_{\partial\Omega_H - \overline{\Gamma}_{p,H}},\end{aligned} \tag{3.18}$$

Proof: We consider only the case $q = I, p = l$. For the term $(D^*_x(D_{I,11}(M_h u_H))D_{-x}u_H), w_H)_H$ we have successively

$$\begin{aligned}&(D^*_x(D_{I,11}(M_h u_H))D_{-x}u_H), w_H)_H \\ &\quad= \sum_{(x_i,y_j)\in\Omega_H\cup\Gamma_{d,H}\cup\Gamma_{u,H}} |\square_{ij}| D^*_x(D_{I,11}(M_h u_H))D_{-x}u_H)(x_i,y_j) w_H(x_i,y_j) \\ &\quad+ \sum_{(x_i,y_j)\in\overline{\Gamma}_{r,H}} |\square_{ij}| D^*_x(D_{I,11}(M_h u_H))D_{-x}u_H)(x_i,y_j) w_H(x_i,y_j) \\ &\quad= -\sum_{(x_i,y_j)\in\overline{\Omega}_H - \overline{\Gamma}_{l,H}} |\square_{x,ij}| D_{I,11}(M_h u_H(x_i,y_j))D_{-x}u_H)(x_i,y_j) D_{-x}w_H(x_i,y_j) \\ &\quad+ \sum_{(x_i,y_j)\in\overline{\Gamma}_{r,H}} |\square'_{ij}| D_{I,11}(M_h u_H(x_i,y_j))D_{-x}u_H(x_i,y_j) w_H(x_i,y_j) \\ &\quad+ \sum_{(x_i,y_j)\in\overline{\Gamma}_{r,H}} |\square'_{ij}| \Big(D_{I,11}(M_h u_H(x_{i+1},y_j))D_{-x}u_H(x_{i+1},y_j) \\ &\qquad\qquad - D_{I,11}(M_h u_H(x_i,y_j))D_{-x}u_H(x_i,y_j)\Big) w_H(x_i,y_j) \\ &\quad= -(D_{I,11}(M_h u_H)D_{-x}u_H, D_{-x}w_H)_{x,+} + (D^{(I)}_{\eta_x}(u_H)\eta_x, w_H)_{\partial\Omega_H - \overline{\Gamma}_{l,H}}.\end{aligned}$$

■

We shall now establish a set of inequalities that are discrete versions of the corresponding continuous ones. In particular, equation (3.20) is a discrete version of the Trace Inequality, and equation (3.21) is a discrete version of the Poincaré inequality.

Proposition 3.2.2. *There exist a positive constants C and C_T, both independent of H, such that*

$$\|u_H\|^2_\infty \le C\frac{1}{H^2_{min}}\|u_H\|^2_H, \tag{3.19}$$

$$\|u_H\|^2_{\partial\Omega_H} \le C_T\Big(\|u_H\|^2_H + \|\nabla_H u_H\|^2_+\Big), \tag{3.20}$$

for all $u_H \in W_H(\overline{\Omega})$. Moreover, there exist positive constants C_P and C_T, both independent of H, such that for all $u_H \in W(\partial\Omega_H)$ with $u_H = 0$ at least on one of the sets $\overline{\Gamma}_{j,H}$, for $j = l,u,r,d$, we have

$$\|u_H\|_H^2 \leq C_P \|\nabla_H u_H\|_+^2, \tag{3.21}$$

$$\|u_H\|_\infty^2 \leq C_P \frac{1}{H_{min}^2} \|\nabla_H u_H\|_+^2. \tag{3.22}$$

Proof: The inequality (3.19) follows immediately from the definitions.

To prove (3.20) we consider $u_H \in W(\overline{\Omega}_H)$. For $(x_0, y_j) \in \partial\overline{\Gamma}_{l,H}$ we have

$$u_H(x_0, y_j) = -\sum_{m=1}^{i} h_m D_{-x} u_H(x_m, y_j) + u_H(x_i, y_j). \tag{3.23}$$

Consequently,

$$u_H(x_0, y_j)^2 \leq 2 \sum_{m=1}^{i} h_m (D_{-x} u_H(x_m, y_j))^2 + 2u_H(x_i, y_j)^2,$$

and

$$\sum_{(x_0,y_j)\in\overline{\Gamma}_{l,H}} |\square'_{0j}| u_H(x_0, y_j)^2 \leq 2\|D_{-x}u_H\|_{x,+}^2 + 2 \sum_{(x_0,y_j)\in\overline{\Gamma}_{l,H}} |\square'_{0j}| u_H(x_i, y_j)^2,$$

that leads to

$$\sum_{(x_0,y_j)\in\overline{\Gamma}_{l,H}} |\square'_{0j}| u_H(x_0, y_j)^2 \leq C\Big(\|D_{-x}u_H\|_{x,+}^2 + \|u_H\|_H^2\Big). \tag{3.24}$$

As for $(x_i, y_j) \in \overline{\Gamma}_{m,H}$, for $m = u,r,d$, holds a representation analogous to (3.23) that leads to a similar inequality to (3.24), we conclude the proof of (3.20).

To prove (3.21), we assume without loss of generality that $u_H \in W(\overline{\Omega}_H)$ and $u_H = 0$ on $\overline{\Gamma}_{l,H}$. As

$$u_H(x_i, y_j) = \sum_{m=1}^{i} h_m D_{-x} u_H(x_m, y_j),$$

we obtain

$$|u_H(x_i, y_j)|^2 \leq \sum_{m=1}^{N_1} h_m (D_{-x} u_H(x_m, y_j)^2, \tag{3.25}$$

that leads to (3.21).

To prove (3.22), we observe that from (3.25) we obtain

$$|u_H(x_i, y_j)|^2 \leq \frac{1}{H_{min}^2} \sum_{(x_i,y_j)\in\overline{\Omega}_H} |\square_{x,ij}| (D_{-x} u_H(x_m, y_j))^2.$$

■

Semi-discrete FDM

The semi-discrete approximation $I_H(t) \in W_{I,H}^*$, $c_{f,H}(t) \in W_{c,H}^*$, $c_{b,H}(t) \in W_b(\overline{\Omega}_H - \overline{\Gamma}_{r,H})$ for the solution of the IBVP (3.1)-(3.8), $I(t), c_f(t)$, and $c_b(t)$, respectively, that we study in this chapter is solution

of the following ordinary-differential system

$$\begin{cases} \frac{1}{\beta} I'_H(t) = \nabla^*_H \cdot (D_I(M_H I_H(t)) \nabla_H I_H(t)) + G_H(t) & \text{in } (\overline{\Omega}_H - \overline{\Gamma}_{l,H}) \times (0,T], \quad (3.26) \\ c'_{f,H}(t) = \nabla^*_H \cdot (D_c(M_H c_{f,H}(t)) \nabla_H c_{f,h}(t)) + F_H(t) & \text{in } (\overline{\Omega}_H - \overline{\Gamma}_{r,H}) \times (0,T], \quad (3.27) \\ c'_{b,H}(t) = S_H(t) & \text{in } (\overline{\Omega}_H - \overline{\Gamma}_{r,H}) \times (0,T], \quad (3.28) \end{cases}$$

with initial conditions

$$I_H(0) = \hat{I}_H(0) \text{ in } \overline{\Omega}_H \quad (3.29)$$

$$c_{f,H}(0) = \hat{c}_{f,H}(0) \text{ in } \overline{\Omega}_H, \quad c_{b,H}(0) = \hat{c}_{b,H}(0) \text{ in } \overline{\Omega}_H - \overline{\Gamma}_{r,H}, \quad (3.30)$$

and boundary conditions

$$I_H(t) = R_H I_i(t) \text{ on } \overline{\Gamma}_{i,H},\ \nabla^{(I)}_H(I_H(t)) \cdot \eta = 0 \text{ on } (\partial\Omega_H - \overline{\Gamma}_{l,H}) \times (0,T], \quad (3.31)$$

$$c_{f,H}(t) = 0 \text{ on } \overline{\Gamma}_{r,H} \times (0,T],\ \nabla^{(c)}_H(c_{f,H}(t)) \cdot \eta = 0 \text{ on } (\partial\Omega_H - \overline{\Gamma}_{r,H}) \times (0,T]. \quad (3.32)$$

In (3.26)-(3.28), the terms $G_H(t)$,$F_H(t)$, and $S_H(t)$ are defined by $G_H(t) = G(I_H(t))$, $F_H(t) = F(I_H(t), c_{f,H}(t), c_{b,H}(t))$ and $S_H(t) = S(I_H(t), c_{f,H}(t), c_{b,H}(t))$. Furthermore, in equations (3.29) and (3.30), the expressions $\hat{I}_H(0)$, $\hat{c}_{f,H}(0)$ and $\hat{c}_{b,H}(0)$ denote the numerical approximations for the initial values $I(0)$, $c_f(0)$ and $c_b(0)$, respectively.

Henceforward, to simplify the analysis we take $\beta = 1$. Proposition 3.2.1 allow us to conclude that the semi-discrete problem (3.26)-(3.32) can be rewritten in the following form:

$$(I'_H(t), v_H)_H = -(D_I(M_H I_H(t)) \nabla_H I_H(t), \nabla_H v_H)_{H,+} + (G_H(t), v_H)_H, \quad (3.33)$$

$$(c'_{f,H}(t), w_H)_H = -(D_c(M_H c_{f,H}(t)) \nabla_H c_{f,H}(t), \nabla_H w_H)_{H,+} + (F_H(t), w_H)_H, \quad (3.34)$$

$$(c'_{b,H}(t), p_H)_H = (S_H(t), p_H)_H, \quad (3.35)$$

for $t \in (0,T]$, and for all $v_H \in W_{0,l}(\overline{\Omega}_H)$, $w_H \in W_{0,r}(\overline{\Omega}_H)$, and $p_H \in W_b(\overline{\Omega}_H - \Gamma_{r,H})$, with $I_H(t) = R_H I_i(t)$ on $\overline{\Omega}_{l,H} \times (0,T]$, and with initial conditions given by

$$(I_H(0), v_H)_H = (\hat{I}_H(0), v_H)_H, \quad \forall v_H \in W(\overline{\Omega}_H), \quad (3.36)$$

$$(c_{f,H}(0), w_H)_H = (\hat{c}_{f,H}(0), w_H)_H, \quad \forall w_H \in W(\overline{\Omega}_H), \quad (3.37)$$

$$(c_{b,H}(0), p_H)_H = (\hat{c}_{b,H}(0), p_H)_H, \quad \forall p_H \in W_b(\overline{\Omega}_H - \overline{\Gamma}_{r,H}). \quad (3.38)$$

To give sense to the inner product $(\cdot,\cdot)_H$ in (3.38), we consider that $(\cdot,\cdot)_H$ do not include the sum over the grid points on $\overline{\Gamma}_{r,H}$.

Remark 3.2.1. *We observe that the last problem can be obtained considering the finite element approach in space and using convenient quadrature rules.*

The variational problem is stated as follows: find $I(t) \in H^1(\Omega)$, $c_f(t) \in H^1_{0,r}(\Omega)$ and $c_b(t)$ in $L^2(\Omega)$, such that $I(t) = I_i(t)$ on Γ_l and

$$(I'(t), v)_{L^2(\Omega)} + (D_l(I(t)) \nabla I(t), \nabla v)_{[L^2(\Omega)]^2} = (G(t), v)_{L^2(\Omega)}, \quad \forall v \in H^1_{0,l}(\Omega), \quad (3.39)$$

$$(c_f'(t),w)_{L^2(\Omega)} + (D_c(c_f(t))\nabla c_f(t),\nabla w)_{[L^2(\Omega)]^2} = (F(t),w)_{L^2(\Omega)}, \quad \forall w \in H^1_{0,r}(\Omega), \tag{3.40}$$

$$(c_b'(t),p)_{L^2(\Omega)} = (S(t),p)_{L^2(\Omega)}, \quad \forall p \in L^2(\Omega), \tag{3.41}$$

with initial conditions

$$I(0) = 0 \quad \text{in } L^2(\Omega), \tag{3.42}$$

$$c_f(0) = 0, \quad c_b(0) = c_{b,0} \text{ in } L^2(\Omega). \tag{3.43}$$

The piecewise linear approximations for $I(t), c_f(t)$ and the piecewise constant approximation $c_b(t)$ are now introduced. For $H \in \Lambda$, let $\mathscr{T}_H$ be a triangulation of Ω induced by the rectangular partition $\overline{\Omega}_H$. Let P_H be the piecewise linear interpolation operator associated with $\mathscr{T}_H$ and let Q_H the piecewise constant interpolator defined by $Q_H u_H(x,y) = u_H(x_\Delta, y_\Delta), (x,y) \in \Delta, \Delta \in \mathscr{T}_H$, where (x_Δ, y_Δ) is the vertex of the right angle of Δ. We consider $\hat{u}_H = P_H u_H$ and $\bar{u}_H = Q_H u_H$. To simplify the presentation we use the following notation $\hat{G}_H(t) = G(\hat{I}_H(t))$, $\hat{F}_H(t) = F(\hat{I}_H(t)), \hat{c}_{f,H}(t), \bar{c}_{b,H}(t))$ and $\hat{S}_H(t) = S(\hat{I}_H(t)), \hat{c}_{f,H}(t), \bar{c}_{b,H}(t))$.

Then, the finite element approximation for the IBVP (3.1)-(3.8) *is defined as follows: for $t \in (0,T]$, find $I_H(t) \in W(\overline{\Omega}_H)$, $c_{f,H}(t) \in W_{0,r}(\overline{\Omega}_H)$ and $c_{b,H}(t) \in W_b(\overline{\Omega}_H - \overline{\Gamma}_r)$ such that $\hat{I}_H(t) = \hat{R_H} I_i(t)$ on Γ_l and*

$$(\hat{I}_H'(t),\hat{v}_H)_{L^2(\Omega)} + (D_l(\hat{I}_H(t))\nabla \hat{I}_H(t),\nabla \hat{v}_H)_{[L^2(\Omega)]^2} = (\hat{G}_H(t),\hat{v}_H)_{L^2(\Omega)}, \tag{3.44}$$

$$(\hat{c}_{f,H}'(t),\hat{w}_H)_{L^2(\Omega)} + (D_c(\hat{c}_{f,H}(t))\nabla \hat{c}_{f,H}(t),\nabla \hat{w}_H)_{[L^2(\Omega)]^2} = (\hat{F}_H(t),\hat{w}_H)_{L^2(\Omega)}, \tag{3.45}$$

$$(\bar{c}_{b,H}'(t),\bar{p}_H)_{L^2(\Omega)} = ((\hat{S}_H(t),\bar{p}_H)_{L^2(\Omega)}, \tag{3.46}$$

for all $v_H \in W_{0,l}(\overline{\Omega}_H)$, $w_H \in W_{0,r}(\overline{\Omega}_H)$, and $p_H \in W_b(\overline{\Omega}_H - \overline{\Gamma}_{r,H})$, and with initial conditions given by

$$I_H(0) = 0 \text{ in } \overline{\Omega}_H, \tag{3.47}$$

$$c_{f,H}(0) = 0 \text{ in } \overline{\Omega}_H, \quad c_{b,H}(0) = R_H c_{b,0} \text{ in } \overline{\Omega}_H - \overline{\Gamma}_{r,H}. \tag{3.48}$$

To compute a fully discrete in space finite element approximations for the light intensity and for the free and bound drug concentrations, we need to construct a discrete version of the last problem (3.44)-(3.48). To do that, we introduce in what follows quadrature rules used to discretize the last IBVP.

Let Δ be a triangle in $\mathscr{T}_H$ and let $(x_i,y_j), (x_{i+1},y_j)$ and (x_i,y_{j+1}) be the vertices of Δ where (x_i,y_j) is the vertex of the right angle of Δ. To approximate the integral terms involving spatial derivatives, we consider

$$\begin{aligned}
\int_\Delta a(\hat{u}_H)\frac{\partial \hat{u}_H}{\partial x}\frac{\partial \hat{w}_H}{\partial x}dxdy &\approx a(\hat{u}_H(x_{i+\frac{1}{2}},y_j))\int_\Delta \frac{\partial \hat{u}_H}{\partial x}\frac{\partial \hat{w}_H}{\partial x}dxdy \\
&\approx a(M_h u_H(x_{i+1},y_j))\Delta\frac{\partial \hat{u}_H}{\partial x}\frac{\partial \hat{w}_H}{\partial x}dxdy \\
&\approx a(M_h u_H(x_{i+1},y_j))\frac{1}{2}h_{i+1}k_{j+1}D_{-x}u_H(x_{i+1},y_j)D_{-x}w_H(x_{i+1},y_j).
\end{aligned}$$

The quadrature rule involving y-derivatives is defined analogously. To approximate the integral terms without derivatives, we take

$$\int_{\Delta} g(x,y)dxdy \approx \frac{1}{2}h_{i+1}k_{j+1}g(x_i,y_j).$$

By applying the last quadrature rules in (3.44)-(3.46) *we obtain* (3.33)-(3.35)*, respectively.*

Fully-discrete FDM

In the time domain $[0,T]$ we define the uniform grid $\{t_m, m=0,\cdots,M\}$, with $t_0=0$, $t_M=1$ and $t_{m+1}=t_m+\Delta t$, for $m=0,\cdots,M-1$.

For the functions $u_H \in W^*_{j,H}$, $j=I,f,b$, and any nonlinear function Φ with time dependent arguments u,v,w, we consider the notations

$$u_H^{m+1/2} = \frac{1}{2}(u_H(t_{m+1})+u_H(t_m)),$$
$$\Phi^{m+1/2} = \Phi(u^{m+1/2}, v^{m+1/2}, w^{m+1/2}).$$

If the arguments of the nonlinear function Φ are $u_H, v_H, w_H \in W^*_{j,H}$, for $j=I,f,b$, then, we shall use the subscript H on Φ to emphasize the dependence, i.e, $\Phi_H^{m+1/2} = \Phi(u_H^{m+1/2}, v_H^{m+1/2}, w_H^{m+1/2})$. In the case that the nonlinear function Φ depends only on one argument the definition of $\Phi^{m+1/2}$ is analogous.

The fully discrete approximations for $I(x_i,y_j,t_m), c_f(x_i,y_j,t_m), c_b(x_i,y_j,t_m)$, respectively, $I_H^m(x_i,y_j), c_{f,H}^m(x_i,y_j)$ and $c_{b,H}^m(x_i,y_j)$, with $I_H^m \in W^*_{I,H}$, $c_{f,H}^m \in W^*_{c,H}$, $c_{b,H}^m \in W_b(\overline{\Omega}_H - \overline{\Gamma}_{r,H})$, are defined by

$$\begin{cases} D_{-t}I_H^{m+1} = \nabla_H^* \cdot ((D_I(M_H I_H^{m+1/2})\nabla_H I_H^{m+1/2}) + G_H^{m+1/2} & \text{in } \overline{\Omega}_H - \overline{\Gamma}_{H,l}, \quad (3.49) \\ D_{-t}c_{f,H}^{m+1} = \nabla_H^* \cdot ((D_c(M_H c_{f,H}^{m+1/2})\nabla_H c_{f,H}^{m+1/2}) + F_H^{m+1/2} & \text{in } \overline{\Omega}_H - \overline{\Gamma}_{H,r}, \quad (3.50) \\ D_{-t}c_{b,H}^{m+1} = S_H^{m+1/2} & \text{in } \overline{\Omega}_H - \overline{\Gamma}_{H,r}, \quad (3.51) \end{cases}$$

for $m=0,\ldots,M-1$, with

$$I_H^0 = \hat{I}_H(0), \text{ in } \overline{\Omega}_H, \quad (3.52)$$

$$\begin{aligned} c_{f,H}^0 &= \hat{c}_{f,H}(0), \text{ in } \overline{\Omega}_H, \\ c_{b,H}^0 &= \hat{c}_{b,H}(0), \text{ in in } \overline{\Omega}_H - \overline{\Gamma}_{r,H}, \end{aligned} \quad (3.53)$$

and

$$I_H^m = R_H I_i(t_m) \text{ on } \overline{\Gamma}_{l,H}, m=1,\ldots,M, \nabla_H^{(I)}(I_H^{m+1/2})\cdot\eta = 0 \text{ on } (\partial\Omega_H - \overline{\Gamma}_{l,H}), \quad (3.54)$$

$$c_{f,H}^m = 0 \text{ on } \overline{\Gamma}_{r,H}, m=1,\ldots,M, \nabla_H^{(c)}(c_{f,H}^{m+1/2})\cdot\eta = 0 \text{ on } (\partial\Omega_H - \overline{\Gamma}_{r,H}). \quad (3.55)$$

We remark that system (3.49)-(3.55) can also be written in the form

$$(D_{-t}I_H^{m+1}, u_H)_H = -(D_I(M_H I_H^{m+1/2})\nabla_H I_H^{m+1/2}, \nabla_H u_H)_{H,+} + (G_H^{m+1/2}, u_H)_H \quad (3.56)$$

$$(D_{-t}c_{f,H}^{m+1}, v_H)_H = -(D_c(M_H c_{f,H}^{m+1/2})\nabla_H c_{f,h}^{m+1/2}, \nabla_H v_H)_{H,+} + (F_H^{m+1/2}, v_H)_H \quad (3.57)$$

$$(D_{-t}c_{b,H}^{m+1}, w_H)_H = (S_H^{m+1/2}, w_H)_H, \tag{3.58}$$

for all $u_H \in W_{l,0}(\overline{\Omega}_H), v_H \in W_{r,0}(\overline{\Omega}_H)$, and $w_H \in W_{b,H}^*(\overline{\Omega}_H - \overline{\Gamma}_{r,H})$ and with initial conditions

$$\begin{aligned}
&(I_H^0, u_H)_H = (\hat{I}_H(0), u_H)_H, \quad \forall u_H \in W(\overline{\Omega}_H),\\
&(c_{f,H}^0, v_H)_H = (\hat{c}_{f,H}(0), v_H)_H, \quad \forall v_H \in W(\overline{\Omega}_H),\\
&(c_{b,H}^0, w_H)_H = (\hat{c}_{b,H}(0), w_H)_H, \quad \forall w_H \in W_b(\overline{\Omega}_H - \overline{\Gamma}_{r,H}).
\end{aligned} \tag{3.59}$$

3.3 The semi-discrete FDM

In this section, we analyze the semi-discrete in space FDM (3.26)-(3.32). Similarly to the previous chapter, we first study the stability in a fixed semi-discrete solution. We observe that the stability upper bound depends on the fixed solution. To conclude the desired local stability, the fixed solution should be uniformly bounded in a sense that we precise in what follows. To get such boundedness we establish convergence upper bounds that allow us to characterize the fixed solutions where we obtain stability.

3.3.1 Stability

To study the local stability of the semi-discrete scheme (3.26)-(3.32), we fixe a solution $I_H(t) \in W_{I,H}^*, c_{f,H}(t) \in W_{c,H}^*, c_{b,H}(t) \in W_b(\overline{\Omega}_H - \overline{\Gamma}_{r,H})$ with the initial conditions $I_H(0), c_{f,H}(0)$ and $c_{b,H}(0)$, respectively. Let $\tilde{I}_H(t) \in W_{I,H}^*, \tilde{c}_{f,H}(t) \in W_{c,H}^*, \tilde{c}_{b,H}(t) \in W_b(\overline{\Omega}_H - \overline{\Gamma}_{r,H})$ be another solution defined by (3.26)-(3.32) but with the initial conditions $\tilde{I}_H(0), \tilde{c}_{f,H}(0)$ and $\tilde{c}_{b,H}(0)$. Let $\omega_{j,H}(t), j = I, f, b$ be given by

$$\begin{aligned}
\omega_{I,H}(t) &= I_H(t) - \tilde{I}_H(t),\\
\omega_{f,H}(t) &= c_{f,H}(t) - \tilde{c}_{f,H}(t),\\
\omega_{b,H}(t) &= c_{b,H}(t) - \tilde{c}_{b,H}(t).
\end{aligned}$$

Let $\rho_\varepsilon > 0$. We would like to fix $\rho_j > 0, j = I, f, c$, such that, if $\tilde{I}_H(0) \in B_{\rho_I}(I_H(0))$, $\tilde{c}_{f,H}(0) \in B_{\rho_f}(c_{f,H}(0))$, and $\tilde{c}_{b,H}(0) \in B_{\rho_b}(c_{b,H}(0))$, then

$$\|\omega_{j,H}(t)\|_H \leq \rho_\varepsilon, \;\; t \in [0,T].$$

To conclude the stability in the fixed solution, it is sufficient to establish the existence of a constant C, independent of H and t, such that

$$\|\omega_{j,H}(t)\|_H \leq C\|\omega_{j,H}(0)\|_H, \quad t \in [0,T], H \in \Lambda, j = I, f, b. \tag{3.60}$$

We start by establishing upper bounds for the solution of (3.26)-(3.32).

Proposition 3.3.1. *Let $I_H(t) \in W_{I,H}^*, c_{f,H}(t) \in W_{c,H}^*$ and $c_{b,H}(t) \in W_b(\overline{\Omega}_H - \overline{\Gamma}_{r,H})$ be solution of the IBVP* (3.26)-(3.32) *with the initial conditions $I_H(0), c_{f,H}(0)$ and $c_{b,H}(0)$ and boundary light incidence function $I_i(t) = 0$. Under conditions (AG)-(AS), and diffusion coefficients D_I and D_c such that*

$D_{I,ii} \geq D_{I,0} > 0, D_{c,ii} \geq D_{c,0} > 0$, *for* $i = 1,2$. *Then*

$$\|I_H(t)\|_H^2 + 2D_{I,0}\int_0^t e^{C_G(t-s)}\|\nabla_H I_H(s)\|_+^2 ds \leq e^{C_G t}\|I_H(0)\|_H^2, \text{ for } t \geq 0, \tag{3.61}$$

and

$$\begin{aligned}\|c_{f,H}(t)\|_H^2 + \|c_{b,H}(t)\|_H^2 + 2D_{c,0}\int_0^t e^{2(C_F+C_S)\int_s^t \|I_H(\mu)\|_\infty^2 d\mu}\|\nabla_H c_{f,H}(s)\|_+^2 ds \\ \leq e^{2(C_F+C_S)\int_0^t \|I_H(s)\|_\infty^2 ds}\Big(\|c_{f,H}(0)\|_H^2 + \|c_{b,H}(0)\|_H^2\Big), \text{ for } t \geq 0.\end{aligned} \tag{3.62}$$

Proof: To prove (3.61) is if sufficient to take $v_H = I_H(t)$ in (3.33) and to use the assumption (AG). Let us consider in (3.34) and (3.35), $w_H = c_{f,H}(t)$ and $p_H = c_{b,H}(t)$, respectively. We obtain

$$\begin{aligned}\frac{1}{2}\frac{d}{dt}\Big(\|c_{f,H}(t)\|_H^2 + \|c_{b,H}(t)\|_H^2\Big) + D_{c,0}\|\nabla_H c_{f,H}(t)\|_+^2 \\ \leq \|I_H(t)\|_\infty (C_F + C_S)\Big(\|c_{f,H}(t)\|_H^2 + \|c_{b,H}(t)\|_H^2\Big), \text{ for } t > 0,\end{aligned}$$

from where we can conclude inequality (3.62).

■

Stability bounds are established in the next result. In order to prove it, we impose the following conditions (AG_ℓ),(AF_ℓ) and (AS_ℓ) on functions G, F, and S, respectively, and the conditions (AD_I) and (AD_c) for the diffusion coefficients D_I and D_c.

Proposition 3.3.2. *Let* $\omega_{I,H}(t) = I_H(t) - \tilde{I}_H(t), \omega_{f,H}(t) = c_{f,H}(t) - \tilde{c}_{f,H}(t)$ *and* $\omega_{b,H}(t) = c_{b,H}(t) - \tilde{c}_{b,H}(t)$, *where* $I_H(t), \tilde{I}_H(t) \in W_{I,H}^*, c_{f,H}(t), \tilde{c}_{f,H}(t) \in W_{c,H}^*, c_{b,H}(t), \tilde{c}_{b,H}(t) \in W_b(\overline{\Omega}_H - \overline{\Gamma}_{r,H})$ *be solutions of the IBVP (3.26)-(3.32) with the initial conditions* $I_H(0), \tilde{I}_H(0), c_{f,H}(0), \tilde{c}_{f,H}(0)$ *and* $c_{b,H}(0), \tilde{c}_{b,H}(0)$, *respectively.*

Under the conditions (AD_I)-(AD_c) *and* (AG_ℓ)-(AS_ℓ), *we have*

$$\begin{aligned}\|\omega_{I,H}(t)\|_H^2 + 2(D_{I,0} - \varepsilon^2)\int_0^t e^{\int_\tau^t \frac{L^2}{\varepsilon^2}\|\nabla_H I_H(\mu)\|_\infty^2 d\mu}\|\nabla_H \omega_{I,H}(\tau)\|_+^2 d\tau \\ \leq e^{\int_0^t \frac{L^2}{\varepsilon^2}\|\nabla_H I_H(\mu)\|_\infty^2 d\mu}\|\omega_{I,H}(0)\|_H^2, \text{ for } t \geq 0,\end{aligned} \tag{3.63}$$

and

$$\begin{aligned}\|\omega_{f,H}(t)\|_H^2 + \|\omega_{b,H}(t)\|_H^2 + 2(D_{c,0} - \eta^2)\int_0^t e^{\int_s^t \theta(\tilde{I}_H(\mu), c_{b,H}(\mu), c_{f,H}(\mu))\, d\mu}\|\nabla_H \omega_{f,H}(s)\|_+^2 ds \\ \leq e^{\int_0^t \theta(\tilde{I}_H(s), c_{b,H}(s), c_{f,H}(s))\, ds}\big(\|\omega_{f,H}(0)\|_H^2 + \|\omega_{b,H}(0)\|_H^2\big) \\ +2\int_0^t e^{\int_s^t \theta(\tilde{I}_H(\mu), c_{b,H}(\mu), c_{f,H}(\mu))\, d\mu}\|\omega_{I,H}(s)\|_H^2 ds,\end{aligned} \tag{3.64}$$

for $t \in [0,T]$ and $\varepsilon, \eta \neq 0$ arbitrary constants.

In inequality (3.64)*, θ is given by*

$$\theta(\tilde{I}_H(t), c_{b,H}(t), c_{f,H}(t)) = \max\left\{ L^2 \frac{1}{2\eta^2} \|\nabla_H c_{f,H}(t)\|_\infty^2 + \frac{C_{F_s}}{2}\left(\|\tilde{I}_H(t)\|_\infty + C_{F_s}\|c_{b,H}(t)\|_\infty^2\right), \right. \\ \left. \left(C_{S_s} + \frac{C_{F_s}}{2}\right)\|\tilde{I}_H(t)\|_\infty + \frac{C_{S_s}^2}{2}\|c_{b,H}(t)\|_\infty^2 \right\}. \tag{3.65}$$

Proof: To prove (3.63) we take (3.33) for $\omega_{I,H}(t)$ and $v_H = \omega_{I,H}(t)$ and considering the assumption (AG_ℓ), we obtain

$$\frac{1}{2}\|\omega_{I,H}(t)\|_H^2 \leq -((D_I(M_H I_H(t)) - D_I(M_H \tilde{I}_H(t)))\nabla_H I_H(t), \nabla_H \omega_{I,H}(t))_+ \\ - (D_I(M_H \tilde{I}_H(t))\nabla_H \omega_{I,H}(t), \nabla_H \omega_{I,H}(t))_+ + C_{G_s}\|\omega_{I,H}(t)\|_H^2. \tag{3.66}$$

As

$$-((D_I(M_H I_H(t)) - D_I(M_H \tilde{I}_H(t)))\nabla_H I_H(t), \nabla_H \omega_{I,H}(t))_+ \\ \leq L^2 \frac{1}{2\varepsilon^2}\|\omega_{I,H}(t)\|_H^2 \|\nabla_H I_H(t)\|_\infty^2 + \varepsilon^2 \|\nabla_H \omega_{I,H}(t)\|_+^2$$

from (3.66) we conclude (3.63).

Following the proof of inequality (3.63) it can be easily shown that

$$\frac{1}{2}\frac{d}{dt}\|\omega_{f,H}(t)\|_H^2 + (D_{c,0} - \eta^2)\|\nabla_H \omega_{f,H}(t)\|_+^2 \leq L^2 \frac{1}{2\eta^2}\|\omega_{f,H}(t)\|_H^2 \|\nabla_H c_{f,H}(t)\|_\infty^2 \\ + (F_H(t) - \tilde{F}_H(t), \omega_{f,H}(t))_H, \tag{3.67}$$

where $\eta \neq 0$ is an arbitrary constant and $F_H(t) = F(I_H(t), c_{f,H}(t), c_{b,H}(t))$
and $\tilde{F}_H(t) = F(\tilde{I}_H(t), \tilde{c}_{f,H}(t), \tilde{c}_{b,H}(t))$.

Considering the assumption (AF_ℓ) we obtain

$$(F_H(t) - \tilde{F}_H(t), \omega_{f,H}(t))_H \leq \frac{C_{F_s}}{2}\left(\|\tilde{I}_H(t)\|_\infty + C_{F_s}\|c_{b,H}(t)\|_\infty^2\right)\|\omega_{f,H}(t)\|_H^2 \\ + \frac{C_{F_s}}{2}\|\tilde{I}_H(t)\|_\infty \|\omega_{b,H}(t)\|_H^2 + \frac{1}{2}\|\omega_{I,H}(t)\|_H^2, \tag{3.68}$$

that inserted in equation (3.67) leads to

$$\frac{1}{2}\frac{d}{dt}\|\omega_{f,H}(t)\|_H^2 + (D_{c,0} - \eta^2)\|\nabla_H \omega_{f,H}(t)\|_+^2 \\ \leq \left(L^2 \frac{1}{2\eta^2}\|\nabla_H c_{f,H}(t)\|_\infty^2 + \frac{C_{F_s}}{2}\left(\|\tilde{I}_H(t)\|_\infty + C_{F_s}\|c_{b,H}(t)\|_\infty^2\right)\right)\|\omega_{f,H}(t)\|_H^2 \\ + \frac{C_{F_s}}{2}\|\tilde{I}_H(t)\|_\infty \|\omega_{b,H}(t)\|_H^2 + \frac{1}{2}\|\|\omega_{I,H}(t)\|_H^2. \tag{3.69}$$

Considering now the assumption (*AS*) we obtain

$$\frac{1}{2}\frac{d}{dt}\|\omega_{b,H}(t)\|_H^2 \leq \left(C_{S_s}\|\tilde{I}_H(t)\|_\infty + \frac{C_{S_s}}{2}\|c_{b,H}(t)\|_\infty^2\right)\|\omega_{b,H}(t)\|_H^2 + \frac{1}{2}\|\omega_{I,H}(t)\|_H^2. \tag{3.70}$$

From (3.69) and (3.70) we deduce

$$\begin{aligned}\frac{1}{2}\frac{d}{dt}\left(\|\omega_{f,H}(t)\|_H^2 + \|\omega_{b,H}(t)\|_H^2\right) + (D_{c,0} - \eta^2)\|\nabla_H \omega_{f,H}(t)\|_H^2 \\ \leq \theta(\tilde{I}_H(t), c_{b,H}(t), c_{f,H}(t))\left(\|\omega_{f,H}(t)\|_H^2 + \|\omega_{b,H}(t)\|_H^2\right) \\ + \|\omega_{I,H}(t)\|_H^2,\end{aligned} \tag{3.71}$$

where $\theta(\tilde{I}_H(t), c_{b,H}(t), c_{f,H}(t))$ is given by (3.65). Finally, we observe that from (3.71) we easily obtain (3.64).

■

From inequalities (3.63) and (3.64), to conclude the stability we need to prove that $\|\nabla_H I_H(\mu)\|_\infty$ and $\theta(\tilde{I}_H(t), c_{b,H}(t), c_{f,H}(t))$ are uniformly bounded for $t \in [0,T]$ and $H \in \Lambda$. As in the previous chapter, we first prove a convergence result that will allow us to conclude stability in following sections.

3.3.2 Convergence

Two convergence results are stated in this section, the first guarantees the convergence of the approximation I_H, the second, the convergence of the approximations $c_{f,H}$ and $c_{b,H}$. The discrete Trace Inequality (3.20) and the discrete Poincaré inequality (3.21) have an important role in the construction of these error estimates.

Let $(I(t), c_f(t), c_b(t))$ be the solution of the IBVP (3.2)-(3.8) and let $I_H(t) \in W_{I,H}^*, c_{f,H}(t) \in W_{c,H}^*, c_{b,H}(t) \in W_b(\overline{\Omega}_H - \overline{\Gamma}_{r,H})$ be solutions of the IBVP (3.26)-(3.32). We define the errors

$$\begin{aligned}E_{I,H}(t) &= R_H I(t) - I_H(t),\\ E_{f,H}(t) &= R_H c_f(t) - c_{f,H}(t),\\ E_{b,H}(t) &= R_H c_b(t) - c_{b,H}(t).\end{aligned}$$

In this section we assume that $I(t) \in C^4(\overline{\Omega}_{I,\Lambda})$ and $c_f(t) \in C^4(\overline{\Omega}_{c_f,\Lambda})$ for $H_{\max}$ small enough, where

$$\begin{aligned}\overline{\Omega}_{I,\Lambda} &= \bigcup_{H\in\Lambda}[x_0, x_{N+1}] \times [y_{-1}, y_{M+1}],\\ \overline{\Omega}_{c_f,\Lambda} &= \bigcup_{H\in\Lambda}[x_{-1}, x_N] \times [y_{-1}, y_{M+1}].\end{aligned}$$

The assumption $I(t) \in C^4(\overline{\Omega}_{I,\Lambda})$ means that the solution of the IBVP (3.1),(3.5), (3.6), with null initial condition, admits an extension to the set $\overline{\Omega}_{I,\Lambda} \times [0,T]$, for H_{max} small enough. Moreover, such extension also belongs to $C^4(\overline{\Omega}_{I,\Lambda})$. A similar conclusion can be obtain from the assumption $c_f(t) \in C^4(\overline{\Omega}_{c_f,\Lambda})$. We remark that there exists an extensive set of results on the extension operators

defined in $W^{m,p}(\Omega)$ for smooth domains (see ([62]). In the near future we would like to define the conditions that allow us to conclude the validity of this assumption.

We recall that for the classical diffusion equation in $\mathbb{R}^+ \times \mathbb{R}^+$ and with a homogeneous boundary condition at $x = 0$, the construction of the solution uses the extension of the initial condition (even extension) to $\mathbb{R}$ and the correspondent solution $\mathbb{R} \times \mathbb{R}^+$ that depends on the Green function.

Error estimate for $E_{I,H}$

The spatial discretization error $E_{I,H}(t)$ is solution of the following IBVP

$$\begin{aligned} E'_{I,H}(t) = \nabla^*_H \cdot (D_I(M_H R_H I(t))\nabla_H R_H I(t)) - \nabla^*_H \cdot (D_I(M_H I_H(t))\nabla_H I_H(t)) \\ + G(R_H I(t)) - G(I_H(t)) + T_I(t), \end{aligned} \tag{3.72}$$

in $(\overline{\Omega}_H - \overline{\Gamma}_{l,H}) \times (0,T]$, with initial and boundary conditions:

$$E_{I,H}(0) = R_H I(0) - \hat{I}_H(0) \qquad \text{in } \overline{\Omega}_H, \tag{3.73}$$

$$E_{I,H}(t) = 0 \qquad \text{on } \overline{\Gamma}_{l,H}, \tag{3.74}$$

$$(\nabla^{(I)}_{H,\eta}(R_H I(t)) - \nabla^{(I)}_{H,\eta}(I_H(t))) \cdot \eta = T_{I,b}(t) \qquad \text{on } (\partial\Omega_H - \overline{\Gamma}_{l,H}) \times (0,T]. \tag{3.75}$$

In equation (3.72), T_I is given by

$$T_I(x_i, y_j, t) = T_{I,x}(t) + T_{I,y}(t) + T_{I,r}(x_i, y_j, t), \;\; (x_i, y_j) \in \overline{\Omega}_H - \overline{\Gamma}_{l,H},$$

where

$$T_{I,x}(x_i, y_j, t) = (h_{i+1} - h_i) s_I(x_i, y_j, t), \;\text{ and }\; T_{I,y}(x_i, y_j, t) = (k_{j+1} - k_j)\sigma_I(x_i, y_j, t),$$

with s_I and σ_I depending on the spatial derivatives with respect to x and y, respectively, of order less or equal to three and

$$|T_{I,r}(t)| \leq C \|J_{1,I}(t)\|_{C(\overline{\Omega}_{I,\Lambda})} H^2_{max}, \tag{3.76}$$

where $J_{1,I}(t)$ is a smooth function depending on the partial derivatives of I of order less than or equal to four.
In equation (3.75), $T_{I,b}(t)$ satisfies

$$|T_{I,b}(t)| \leq C \|J_{2,I}(t)\|_{C(\overline{\Omega}_{I,\Lambda})} H^2_{max}, \tag{3.77}$$

where $J_{2,I}(t)$ is a smooth function depending on the partial derivatives of I of order less or equal to three. In the estimates (3.76) and (3.77) we assume that $I(t) \in C^4(\overline{\Omega}_{I,\Lambda})$, for H_{max} small enough.

Theorem 3.3.1. *Let $I(t) \in C^4(\overline{\Omega}_{I,\Lambda})$, $t \in (0,T]$, be the solution of equation* (3.5)-(3.6)*, with null initial condition. Let $I_H(t) \in W^*_{I,H}, t \in [0,T]$, be solution of the IBVP* (3.26)*,* (3.31) *with the initial condition*

$I_H(0)$. *Under the assumption* (AD_I) *and* (AG_ℓ), *for* $E_{I,H}(t) = R_H I(t) - I_H(t)$ *holds the following*

$$\begin{aligned} &\|E_{I,H}(t)\|_H^2 + 2(D_{I,0} - 2\varepsilon^2)\int_0^t e^{\int_\tau^t \frac{L^2}{\varepsilon^2}\|\nabla_H R_H I(\mu)\|_\infty^2 d\mu} \|\nabla_H E_{I,H}(\tau)\|_+^2 d\tau \\ &\leq e^{\int_0^t \frac{L^2}{\varepsilon^2}\|\nabla_H R_H I(\mu)\|_\infty^2 d\mu} \|E_{I,H}(0)\|_H^2 + \int_0^t e^{\int_\tau^t \frac{L^2}{\varepsilon^2}\|\nabla_H R_H I(\mu)\|_\infty^2 d\mu} T_{I,H}(\tau) d\tau, \end{aligned} \tag{3.78}$$

for $t \in [0,T]$. *In (3.78),* $\varepsilon \neq 0$ *is an arbitrary constant and*

$$T_{I,H}(\tau) = C\frac{1}{2\varepsilon^2} H_{max}^4 \|J_I(t)\|_{C(\overline{\Omega}_{I,\Lambda})}^2, \tag{3.79}$$

where $J_I(t)$ *is a smooth function depending on the spatial derivatives of* I *of order less than or equal to four and* C *is a positive constant independent of* H *and* t.

Proof: Taking into account Proposition 3.2.1, from (3.72) we establish

$$\begin{aligned} (E'_{I,H}(t), E_{I,H}(t))_H =& -(D_I(M_H R_H I(t))\nabla_H R_H I(t) - D_I(M_H I_H(t))\nabla_H I_H(t), \nabla_H E_{I,H}(t))_+ \\ &+ (\nabla_{H,\eta}^{(I)} R_H I(t) - \nabla_{H,\eta}^{(I)} I_H(t)\cdot\eta, E_{I,H}(t))_{\partial\Omega_H - \overline{\Gamma}_{l,H}} \\ &+ (G(R_H I(t)) - G(I_H(t)), E_{I,H}(t))_H + (T_I(t), E_{I,H}(t)_H. \end{aligned} \tag{3.80}$$

Taking into account the boundary conditions (3.74)-(3.75) into equation (3.80) we get

$$\begin{aligned} (E'_{I,H}(t), E_{I,H}(t))_H =& -(D_I(M_H R_H I(t))\nabla_H R_H I(t) - D_I(M_H I_H(t))\nabla_H I_H(t), \nabla_H E_{I,H}(t))_+ \\ &+ (T_{I,b}(t), E_{I,H}(t))_{\partial\Omega_H - \overline{\Gamma}_{l,H}} \\ &+ (G(R_H I(t)) - G(I_H(t)), E_{I,H}(t))_H + (T_I(t), E_{I,H}(t))_H. \end{aligned} \tag{3.81}$$

To estimate $(T_I(t), E_{I,H}(t))_H$ we observe that

$$\begin{aligned} (T_{I,x}(t), E_{I,H}(t))_H =& \sum_{(x_i,y_j)\in\Omega_H} |\square_{ij}| T_{I,x}(x_i,y_j,t) E_{I,H}(x_i,y_j,t) \\ &+ \sum_{(x_i,y_j)\in\partial\Omega_H - \Gamma_{l,H}} |\square_{ij}| T_{I,x}(x_i,y_j,t) E_{I,H}(x_i,y_j,t) \\ &:= E_{r,1}(t) + E_{r,2}(t). \end{aligned} \tag{3.82}$$

To get an estimate for $E_{r,1}(t)$ we observe that

$$\begin{aligned} E_{r,1}(t) =& \sum_{i=1}^{N}\sum_{j=1}^{M-1} k_{j+1/2} h_i^2 \big(s_I(x_{i-1},y_j,t)E(x_{i-1},y_j,t) - s_I(x_i,y_j,t)E(x_i,y_j,t)\big) \\ &+ \sum_{j=1}^{M-1} k_{j+1/2} h_N^2 s_I(x_N,y_j,t)E(x_N,y_j,t) \\ &= E_{r,1}^{(1)}(t) + E_{r,1}^{(2)}(t). \end{aligned}$$

For $E_{r,1}^{(1)}(t)$ holds the representation

$$E_{r,1}^{(1)}(t) = -\sum_{i=1}^{N}\sum_{j=1}^{M-1} k_{j+1/2}h_i^3 s_I(x_{i-1},y_j,t)D_{-x}E(x_i,y_j,t) \\ -\sum_{i=1}^{N}\sum_{j=1}^{M-1} k_{j+1/2}h_i^2 \int_{x_{i-1}}^{x_i} \frac{\partial s_I}{\partial x}(x,y_j,t)dxE(x_i,y_j,t),$$

that leads to

$$|E_{r,1}^{(1)}(t)| \leq CH_{max}^2 \|s_I(t)\|_{C^1(\overline{\Omega})}\big(\|\nabla_H E_H(t)\|_+ + \|E_H(t)\|_H\big), \tag{3.83}$$

where C is a positive constant independent of H and t.

For $E_{r,1}^{(2)}(t)$ we have

$$|E_{r,1}^{(2)}(t)| \leq CH_{max}^2 \|s_I(t)\|_{C(\overline{\Omega})}\|E_H(t)\|_{\partial\Omega},$$

and considering the discrete trace inequality (3.20) we obtain

$$|E_{r,1}^{(2)}(t)| \leq CH_{max}^2 \|s_I(t)\|_{C(\overline{\Omega})}\big(\|E_H(t)\|_H^2 + \|\nabla_H E_H(t)\|_+^2\big)^{1/2}, \tag{3.84}$$

where C is a positive constant independent of H and t.

From equations (3.83) and (3.84) we conclude that there exists a positive constant C independent of H and t, such that

$$|E_{r,1}(t)| \leq CH_{max}^2 \|s_I(t)\|_{C^1(\overline{\Omega})}\big(\|E_H(t)\|_H + \|\nabla_H E_H(t)\|_+\big). \tag{3.85}$$

As for $E_{r,2}(t)$ we have an estimate analogous to (3.85) we conclude that there exists a positive constant C independent of H and T, such that

$$(T_{I,x}(t),E_{I,H}(t))_H \leq CH_{max}^2 \|s_I(t)\|_{C^1(\overline{\Omega})}\big(\|E_H(t)\|_H^2 + \|\nabla_H E_H(t)\|_+^2\big)^{1/2}. \tag{3.86}$$

Analogously, for $(T_{I,y}(t),E_{I,H}(t))_H$ it can be shown an estimate analogous to (3.86). Moreover, we also have

$$(T_{I,r}(t),E_H(t))_H \leq CH_{max}^2 \|J_{1,I}(t))\|_{C(\overline{\Omega}_{I,\Lambda})}\|E_H(t)\|_H.$$

Consequently, we obtain

$$(T_I(t),E_{I,H}(t))_H \leq CH_{max}^2\big(\|s_I(t)\|_{C^1(\overline{\Omega}_{I,\Lambda})} + \|\sigma_I(t)\|_{C^1(\overline{\Omega}_{I,\Lambda})} + \|J_{1,I}(t)\|_{C(\overline{\Omega}_{I,\Lambda})}\big)\big(\|E_H(t)\|_H + \|\nabla_H E_H(t)\|_+\big). \tag{3.87}$$

where C denotes a positive constant independent of H and t.

An estimate for $(T_{I,b}(t),E_{I,H}(t))_{\partial\Omega_H-\overline{\Gamma}_{l,H}}$ is now established using Cauchy-Schwartz inequality and the discrete trace inequality (3.20)

$$(T_{I,b}(t),E_{I,H}(t))_{\partial\Omega_H-\overline{\Gamma}_{l,H}} \leq CH_{max}^2 \|J_{2,I}(t)\|_{C(\overline{\Omega}_{I,\Lambda})}\big(\|E_H(t)\|_H + \|\nabla_H E_H(t)\|_+\big). \tag{3.88}$$

Taking into account the discrete Poincaré inequality (3.21) in (3.87) and in (3.88) we finally conclude

$$(T_I(t),E_{I,H}(t))_H+(T_{I,b}(t),E_{I,H}(t))_{\partial\Omega_H-\overline{\Gamma}_{l,H}}\leq C\frac{1}{4\varepsilon^2}H_{max}^4\|J_I(t)\|^2_{C(\overline{\Omega}_{I,\Lambda})}+\varepsilon^2\|\nabla_H E_H(t)\|^2_+, \quad (3.89)$$

where $\varepsilon\neq 0$ is an arbitrary constant.

Following now the proof of inequality (3.63) we conclude the proof of (3.78). ■

Error estimate for $E_{f,H}$ and $E_{b,H}$

In what follows we establish, for the errors associated with the approximations $c_{f,H}(t)$ and $c_{b,H}(t)$, a result analogous to Theorem 3.3.1. As for the light intensity solution $I(t)$, we assume that the free drug concentration $c_f(t)$ belongs to $C^4(\overline{\Omega}_{c_f,\Lambda})$ for H_{max} small enough.

The spatial errors $E_{f,H}(t)$ and $E_{b,H}(t)$, for $t\in[0,T]$, satisfy the following

$$\begin{aligned}E'_{f,H}(t)&=\nabla^*_H\cdot(D_c(M_HR_Hc_f(t))\nabla_HR_Hc_f(t))-\nabla^*_H\cdot(D_c(M_Hc_{f,H}(t))\nabla_Hc_{f,H}(t))\\&\quad+F_H(t)-F(t)+T_{c_f}(t), \quad (3.90)\\E'_{b,H}(t)&=S_H(t)-S(t), \quad (3.91)\end{aligned}$$

in $(\overline{\Omega}_H-\overline{\Gamma}_{r,H})\times(0,T]$, with initial and boundary conditions:

$$\begin{aligned}E_{f,H}(0)&=R_Hc_f(0)-c_{f,H}(0) && \text{in } \overline{\Omega}_H, && (3.92)\\E_{b,H}(0)&=R_Hc_b(0)-c_{b,H}(0) && \text{in } \overline{\Omega}_H-\overline{\Gamma}_{r,H}, && (3.93)\\E_{f,H}(t)&=0 && \text{on } \overline{\Gamma}_{r,H}, && (3.94)\\\nabla^{(c)}_{H,\eta}(R_Hc_f(t))-\nabla^{(c)}_{H,\eta}(c_{f,H}(t))\cdot\eta&=T_{c_f,b}(t) && \text{on } (\partial\Omega_H-\overline{\Gamma}_{r,H})\times(0,T]. && (3.95)\end{aligned}$$

We remark that in equations (3.90)-(3.91) we have $F(t)=F(I(t),c_f(t),c_b(t))$ and $F_H(t)=F(I_H(t),c_{f,H}(t),c_{b,H}(t))$. Analogously for the terms $S(t)$ and $S_H(t)$. In addition T_{c_f} is given by

$$T_{c_f}(x_i,y_j,t)=T_{c_f,x}(t)+T_{c_f,y}(t)+T_{c_f,r}(x_i,y_j,t),\ \ (x_i,y_j)\in\overline{\Omega}_H-\overline{\Gamma}_{r,H},$$

where

$$T_{c_f,x}(x_i,y_j,t)=(h_{i+1}-h_i)s_f(x_i,y_j,t),\ \text{ and }\ T_{c_f,y}(x_i,y_j,t)=(k_{j+1}-k_j)\sigma_f(x_i,y_j,t),$$

with s_f and σ_f depending on the spatial derivatives of c_f with respect to x and y, respectively, of order less or equal to three and

$$|T_{c_f,r}(t)|\leq C\|J_{1,c_f}(t)\|_{C(\overline{\Omega}_{c_f,\Lambda})}H^2_{max}, \quad (3.96)$$

where $J_{1,c_f}(t)$ is a smooth function depending on the spatial derivatives of c_f of order less than or equal to four. In (3.94)-(3.95), $T_{c_f,b}(t)$ satisfies

$$|T_{c_f,b}(t)|\leq C\|J_{2,c_f}(t)\|_{C(\overline{\Omega}_{c_f,\Lambda})}H^2_{max}, \quad (3.97)$$

where $J_{2,c_f}(t)$ is a smooth function depending on the spatial derivatives of c_f of order less than or equal to three.

In Theorem 3.3.2 we establish an upper bound for $\|E_{f,H}(t)\|_H^2+\|E_{b,H}(t)\|_H^2$ without the proof. We remark that the proof of such result follows the proof of Proposition 3.3.2 with $I_H(t)$ and $\tilde{I}_H(t)$ replaced by $R_HI(t)$ and $I_H(t)$, respectively, $c_{f,H}(t),\tilde{c}_{f,H}(t)$ replaced by $R_Hc_f(t)$ and $c_{f,H}(t)$, respectively, and $c_{b,H}(t),\tilde{c}_{b,H}(t)$ replaced by $R_Hc_b(t)$ and $c_{b,H}(t)$. In the error equation involving $(E'_{f,H}(t),E_{f,H}(t))_H+(E'_{b,H}(t),E_{b,H}(t))_H$, that corresponds to the error equation (3.81) for $E_{I,H}(t)$, the term

$$(T_{c_f}(t),E_{f,H}(t))_H+(T_{c_f,b}(t),E_{f,H}(t))_{\partial\Omega_H-\overline{\Gamma}_{r,H}} \tag{3.98}$$

needs to be considered. The construction of an upper bound for the this term follows the construction of the upper bound in Theorem 3.3.1 for the correspondent term considered in the equation for the light intensity error $E_{I,H}(t)$.

Theorem 3.3.2. *Let $I(t),c_f(t),c_b(t)$ be the solution of the IBVP* (3.2)-(3.8) *with initial conditions $I(0),c_f(0),c_b(0)$, where $c_f(t)\in C^4(\overline{\Omega}_{c_f,\Lambda})$, $t\in(0,T]$. Let $I_H(t)\in W^*_{I,H},c_{f,H}(t)\in W^*_{c,H},c_{b,H}(t)\in W_b(\overline{\Omega}_H-\overline{\Gamma}_{r,H})$ be solutions of the IBVP* (3.26)-(3.32) *with the initial conditions $I_H(0),c_{f,H}(0)$ and $c_{b,H}(0)$, respectively. Under the condition (AD_c) and (AF_ℓ)-(AS_ℓ), for $E_{f,H}(t)$ and $E_{b,H}(t)$ we have*

$$\begin{aligned}\|E_{f,H}(t)\|_H^2+\|E_{b,H}(t)\|_H^2+2(D_{c,0}-2\eta^2)\int_0^t e^{\int_\tau^t\theta(I_H(\mu),R_Hc_b(\mu),R_Hc_f(\mu))d\mu}\|\nabla_HE_{f,H}(\tau)\|_+^2d\tau\\ \leq e^{\int_0^t\theta(I_H(\mu),R_Hc_b(\mu),R_Hc_f(\mu))d\mu}\left(\|E_{f,H}(0)\|_H^2+\|E_{b,H}(0)\|_H^2\right)\\ +\int_0^t e^{\int_\tau^t\theta(I_H(\mu),R_Hc_b(\mu),R_Hc_f(\mu))d\mu}T_{c,H}(\tau)d\tau\\ +2\int_0^t e^{\int_\tau^t\theta(I_H(\mu),R_Hc_b(\mu),R_Hc_f(\mu))d\mu}\|E_{I,H}(\tau)\|_H^2d\tau,\end{aligned} \tag{3.99}$$

for $t\in[0,T]$ and $H\in\Lambda$ with H_{max} small enough.

In inequality (3.99), we have $E_{I,H}(t)=R_HI(t)-I_H(t)$ and

$$T_{c,H}(t)=C\frac{1}{2\varepsilon^2}H_{max}^4\|J_{c_f}(t)\|^2_{C(\overline{\Omega}_{c,\Lambda})},$$

where $J_{c_f}(t)$ is a smooth function depending on the spatial derivatives of c_f of order less than or equal to four, where C is a positive constant independent of H and t. Moreover, $\theta(I_H(\mu),R_Hc_b(\mu),R_Hc_f(\mu))$ is defined in equation (3.65)*, and $\eta\neq0$ is an arbitrary constant.*

From Theorem 3.3.2, if we fix η conveniently, we observe that the upper bound (3.99) for

$$\|E_{f,H}(t)\|_H^2+\|E_{b,H}(t)\|_H^2+\int_0^t\|\nabla_HE_{f,H}(\tau)\|_+^2d\tau,$$

depends on $\int_0^t \|I_H(s)\|_\infty ds$. To get an estimate with a controlled upper bound we should establish condition that allow us to guarantee that $\int_0^t \|I_H(s)\|_\infty ds$ is uniformly bounded for $t \in [0,T], H \in \Lambda$.

From Theorem 3.3.1, for ε conveniently fixed, we conclude that there exists a positive integer p_I such that

$$\|J_I(t)\|_{C(\overline{\Omega}_{I,\Lambda})} \leq C\|I\|^{p_I}_{C^4(\overline{\Omega}_{I,\Lambda})}, \tag{3.100}$$

where C is independent of I, moreover, we obtain

$$\|E_{I,H}(t)\|^2_H + \int_0^t \|\nabla_H E_{I,H}(\tau)\|^2_+ d\tau \leq C\Big(\|E_{I,H}(0)\|^2_H + H^4_{max}\int_0^t \|I(s)\|^{2p_I}_{C^4(\overline{\Omega}_{I,\Lambda})} ds\Big), \tag{3.101}$$

for $t \in [0,T], H \in \Lambda$.

Considering that we have

$$\int_0^t \|I_H(s)\|_\infty ds \leq \int_0^t \|E_{I,H}(s)\|_\infty ds + \int_0^t \|R_H I(s)\|_\infty ds,$$

where, from inequalities (3.22) and (3.101),

$$\begin{aligned}\int_0^t \|E_{I,H}(s)\|_\infty ds &\leq \frac{1}{\sqrt{H_{min}}}\int_0^t \|\nabla_H E_{I,H}(s)\|_+ ds \\ &\leq \sqrt{\frac{T}{H_{min}}}\Big(\int_0^t \|\nabla_H E_{I,H}(s)\|^2_+ ds\Big)^{1/2} \\ &\leq C\sqrt{\frac{T}{H_{min}}}\Big(\|E_{I,H}(0)\|_H + H^2_{max}\Big(\int_0^t \|I(s)\|^{2p_I}_{C^4(\overline{\Omega}_{I,\Lambda})} ds\Big)^{1/2}\Big),\end{aligned} \tag{3.102}$$

we deduce

$$\begin{aligned}\int_0^t \|I_H(s)\|_\infty ds \leq C\sqrt{\frac{T}{H_{min}}}\Big(\sqrt{H_{max}} + H^2_{max}\Big(\int_0^t \|I(s)\|^{2p_I}_{C^4(\overline{\Omega}_{I,\Lambda})} ds\Big)^{1/2}\Big) \\ + \int_0^t \|R_H I(s)\|_\infty ds,\end{aligned} \tag{3.103}$$

provided that $I_H(0)$ is such that

$$\|I_H(0) - R_H I(0)\|_H \leq C\sqrt{H_{max}}, H \in \Lambda. \tag{3.104}$$

Finally, if the sequence of grids $\overline{\Omega}_H, H \in \Lambda$, satisfies the following condition

$$\frac{H_{max}}{H_{min}} \leq C_G, H \in \Lambda, \tag{3.105}$$

we conclude that $\int_0^t \|I_H(s)\|_\infty ds \leq C, t \in [0,T], H \in \Lambda$, where C is independent of H and t.

For the free concentration, we remark that there exists a positive integer p_c such that

$$|J_{c_f}(t)|_{C(\overline{\Omega}_{c,\Lambda})} \leq C\|c_f(t)\|^{p_c}_{C(\overline{\Omega}_{c,\Lambda})}.$$

From Theorems 3.3.1 and 3.3.2 we obtain the following result.

Corollary 3.3.1. *Under the assumptions of Theorems 3.3.1 and 3.3.2, if the sequence of grids* $\overline{\Omega}_H, H \in \Lambda$, *satisfies (3.105) and* $I_H(0) \in B_{\rho_H}(R_H I(0))$, *with* $\rho_H \leq CH_{max}^p, H \in \Lambda, p \geq \frac{1}{2}$, *the there exists positive constants* C_1 *and* C_2, *both independent of* H *and* t, *such that*

$$\|E_{I,H}(t)\|_H^2 + \int_0^t \|\nabla_H E_{H,I}(s)\|_+^2 ds \leq C_1 H_{max}^{2p}\Big(1 + H_{max}^{4-2p}\int_0^t \|I(s)\|_{C^4(\overline{\Omega}_{I,\Lambda})}^{2p_I} ds\Big), \tag{3.106}$$

and

$$\begin{aligned}\|E_{f,H}(t)\|_H^2 + \|E_{b,H}(t)\|_H^2 + \int_0^t \|\nabla_H E_{c,I}(s)\|_+^2 ds &\leq C_1 H_{max}^{2p}\Big(1 + H_{max}^{4-2p}\int_0^t \|I(s)\|_{C^4(\overline{\Omega}_{I,\Lambda})}^{2p_I} ds\Big) \\ &+ C_2\left(\|E_{f,H}(0)\|_H^2 + \|E_{b,H}(0)\|_H^2 + H_{max}^4 \int_0^t \left(\|c_f(s)\|_{C^4(\overline{\Omega}_{c_f,\Lambda})}^{p_c}\right)^2 ds\right),\end{aligned} \tag{3.107}$$

for $t \in [0,T]$ *and* $H \in \Lambda$, *with* H_{max} *small enough.*

If $I_H(0) = R_H I(0)$ *then inequality* (3.106) *holds with* $p = 2$.

3.3.3 Concluding stability

We return now to the stability analysis. From Proposition 3.3.2, to conclude the stability of the IBVP (3.26)-(3.32) in $I_H(t), c_{f,H}(t), c_{b,H}(t)$, $H \in \Lambda, t \in [0,T]$, we need to prove that following four statements hold.

1. There exists $\rho_I > 0$ and $C > 0$ such that, for all $I_H(0) \in B_{\rho_I}(R_H I(0))$, we have

$$\int_0^t \|\nabla_H I_H(s)\|_\infty^2 ds \leq C, \qquad t \in [0,T], H \in \Lambda, \tag{3.108}$$

Proof: From Corollary 3.3.1, we have inequality (3.106) provided that $I_H(0) \in B_{\rho_H}(R_H I(0))$, with $\rho_{I,H} \leq CH_{max}^p, H \in \Lambda, p \geq \frac{1}{2}$. Then, we have

$$\begin{aligned}\int_0^t \|\nabla_H I_H(s)\|_\infty^2 ds &\leq 2\int_0^t \|\nabla_H E_{I,H}(s)\|_\infty^2 ds + 2\int_0^t \|\nabla_H R_H I(s)\|_\infty^2 ds \\ &\leq \frac{2}{H_{min}^2}\int_0^t \|\nabla_H E_{I,H}(s)\|_+^2 ds + 2\int_0^t \|\nabla_H R_H I(s)\|_\infty^2 ds \\ &\leq CT\left(\frac{H_{max}}{H_{min}}\right)^2 H_{max}^{2p-2}\left(1 + H_{max}^{4-2p}\int_0^t \|I(s)\|_{C^4(\overline{\Omega}_{I,\Lambda})}^{2p_I} ds\right) + 2\int_0^t \|\nabla_H R_H I(s)\|_\infty^2 ds \\ &\leq C + 2\int_0^t \|\nabla_H R_H I(s)\|_\infty^2 ds,\end{aligned}$$

where the last inequality is established taking $p \geq 1$ and considering that the sequence of grids $\overline{\Omega}_H, H \in \Lambda$, satisfies (3.105). Consequently, inequality (3.108) holds.

2. There exists $\rho_{\tilde{I}} > 0$ and $C > 0$ such that, for all $\tilde{I}_H(0) \in B_{\rho_{\tilde{I}}}(R_H I(0))$, we have

$$\int_0^t \|\tilde{I}_H(s)\|_\infty ds \leq C, \qquad t \in [0,T], H \in \Lambda, \tag{3.109}$$

Proof:

We deduce successively

$$\begin{aligned}\int_0^t \|\tilde{I}_H(s)\|_\infty ds &\leq \int_0^t \|\omega_{I,H}(s)\|_\infty ds + \int_0^t \|I_H(s)\|_\infty ds \\ &\leq \frac{1}{H_{min}} \int_0^t \|\nabla_H \omega_{I,H}(s)\|_+ ds + \int_0^t \|I_H(s)\|_\infty ds \\ &\leq \frac{1}{H_{min}} \Big(\int_0^t \|\nabla_H \omega_{I,H}(s)\|_+^2 ds \Big)^{1/2} + \int_0^t \|I_H(s)\|_\infty ds.\end{aligned} \tag{3.110}$$

By Proposition 3.63, inequality (3.63), with ε conveniently fixed and considering that inequality (3.108) holds for $I_H(0) \in B_{\rho_{I,H}}(R_H I(0))$, with $\rho_{\tilde{I},H} \leq C H_{max}^p, H \in \Lambda, p \geq 1$, and $\overline{\Omega}_H, H \in \Lambda$, satisfies (3.105), we have

$$\frac{1}{H_{min}} \Big(\int_0^t \|\nabla_H \omega_{I,H}(s)\|_+^2 ds \Big)^{1/2} \leq C \frac{1}{H_{min}} \|\omega_{I,H}(0)\|_H.$$

Then

$$\frac{1}{H_{min}} \Big(\int_0^t \|\nabla_H \omega_{I,H}(s)\|_+^2 ds \Big)^{1/2} \leq C, \;\; t \in [0,T], H \in \Lambda, \tag{3.111}$$

where C is independent of H and t, provided that $\tilde{I}_H(0) \in B_{\rho_{\tilde{I},H}}(I_H(0)), H \in \Lambda$, with $\rho_{\tilde{I},H} \leq C_{\tilde{I}} H_{max}^p$, with $p \geq 1$, and $\overline{\Omega}_H, H \in \Lambda$, satisfies (3.105). Finally, as $\int_0^t \|I_H(s)\|_\infty ds \leq C, t \in [0,T], H \in \Lambda$, where C is independent of H and t, combining (3.111) with (3.110), we conclude (3.109).

3. There exists $\rho_f > 0$ and $C > 0$ such that, for all $c_{f,H}(0) \in B_{\rho_f}(R_H c_f(0))$,

$$\int_0^t \|\nabla_H c_{f,H}(s)\|_\infty^2 ds \leq C, \qquad t \in [0,T], H \in \Lambda, \tag{3.112}$$

Proof: To establish the conditions that lead to (3.112), we remark that following the proof of inequality (3.108), it is enough to assume that $I_H(0) \in B_{\rho_{I,H}}(R_H I(0)), \rho_{I,H} \leq C_I H_{max}^p, c_{f,H}(0) \in B_{\rho_{c_{f,H}}}(R_H c_f(0)), \rho_{c_f,H} \leq C_f H_{max}^q, c_{b,H}(0) \in B_{\rho_{c_{b,H}}}(R_H c_b(0)), \rho_{c_b,H} \leq C_b H_{max}^r$, where $p, q, r \geq 1$ and $C_i, i = b, I, f$, are independent of H.

4. There exists $\rho_b > 0$ and $C > 0$ such that, for all $c_{b,H}(0) \in B_{\rho_b}(R_H c_b(0))$,

$$\int_0^t \|c_{b,H}(s)\|_\infty^2 ds \leq C, \qquad t \in [0,T], H \in \Lambda. \tag{3.113}$$

Proof: We observe that

$$\|c_{b,H}(t)\|_\infty \leq \frac{1}{H_{min}^2} \|E_{b,H}\|_H + \|R_H c_b(t)\|_\infty,$$

and considering the error estimate (3.107), we conclude that (3.113) holds provided that $c_{f,H}(0) \in B_{\rho_{c_f,H}}(R_H c_f(0)), \rho_{c_f,H} \leq C_f H_{max}^q c_{b,H}(0) \in B_{\rho_{c_b,H}}(R_H c_b(0)), \rho_{c_b,H} \leq C_b H_{max}^r$, where $q, r \geq 2$ and $C_i, i = b, f$, are independent of H.

In the next corollary we characterize the set of semi-discrete solution $I_H(t) \in W_{I,H}^*, c_{f,H}(t) \in W_{c,H}^*, c_{b,H}(t) \in W_b(\overline{\Omega}_H - \overline{\Gamma}_{r,H})$ defined by the IBVP (3.26)-(3.32) with the initial conditions $I_H(0), c_{f,H}(0)$ and $c_{b,H}(0)$, where we have stability.

Corollary 3.3.2. *Under the assumptions of Proposition 3.3.2 and Theorem 3.3.1, 3.3.2 where $I_H(0) \in B_{\rho_{I,H}}(R_H I(0)), \rho_{I,H} \leq C_I H_{max}^p, c_{f,H}(0) \in B_{\rho_{c_f,H}}(R_H c_f(0)), \rho_{c_f,H} \leq C_f H_{max}^q, c_{b,H}(0) \in B_{\rho_{c_b,H}}(R_H c_b(0)), \rho_{c_b,H} \leq C_b H_{max}^r$, where $p \geq 1$, $q, r \geq 2$ and $C_i, i = b, I, f$, are independent of H. If the sequence of spatial grids $\overline{\Omega}_H, H \in \Lambda$, satisfies (3.105), then there exists a positive constant C, independent of H and t, such that*

$$\|\omega_{I,H}(s)\|_H^2 + \int_0^t \|\nabla_H \omega_{I,H}(s)\|_+^2 ds \leq C\|\omega_{I,H}(0)\|_H^2,$$
$$\|\omega_{b,H}(t)\|_H^2 + \|\omega_{f,H}(t)\|_H^2 + \int_0^t \|\nabla_H \omega_{f,H}(s)\|_+^2 ds \leq C\big(\|\omega_{b,H}(0)\|_H^2 + \|\omega_{f,H}(0)\|_H^2 + \|\omega_{I,H}(0)\|_H^2\big),$$

for $t \in [0,T], H \in \Lambda$, H_{max} small enough, and provided that $\tilde{I}_H(0) \in B_{\rho_{\tilde{I},H}}(I_H(0))$, where $\rho_{\tilde{I},H} \leq C_{\tilde{I}} H_{max}^p$, $p \geq 1$.

■

3.4 A Crank-Nicolson fully-discrete FDM

This section is dedicated to the stability and convergence analysis of the fully discrete (space and time) method (3.49)-(3.55).

3.4.1 Stability

Let $I_H^m \in W_{I,H}^*$, $c_{f,H}^m \in W_{c,H}^*$, and $c_{b,H}^m \in W_b(\overline{\Omega}_H - \overline{\Gamma}_{r,H})$ be a solution of the IBVP (3.49)-(3.55) with the initial conditions I_H^0, $c_{f,H}^0$ and $c_{b,H}^0$, respectively. Let $\tilde{I}_H^m \in W_{I,H}^*$, $\tilde{c}_{f,H}^m \in W_{c,H}^*$, $\tilde{c}_{b,H}^m \in W_b(\overline{\Omega}_H - \overline{\Gamma}_{r,H})$ be another solution with initial conditions $\tilde{I}_H^0$, $\tilde{c}_{f,H}^0$ and $\tilde{c}_{b,H}^0$. For $m = 0, \cdots, M$, we define

$$\omega_{I,H}^m = I_H^m - \tilde{I}_H^m,$$
$$\omega_{f,H}^m = c_{f,H}^m - \tilde{c}_{f,H}^m,$$
$$\omega_{b,H}^m = c_{b,H}^m - \tilde{c}_{b,H}^m.$$

We recall that the solution $(I_H^m, c_{f,H}^m, c_{b,H}^m)$ is stable, for $m = 0, \ldots, M$, if for all $\varepsilon > 0$, there exists $\rho_\varepsilon > 0$ such that, for any other solution $(\tilde{I}_H^m, \tilde{c}_{f,H}^m, \tilde{c}_{b,H}^m)$, if

$$\|\omega_{j,H}^0\| \leq \rho_\varepsilon, \text{ for } j = l, b, f, \tag{3.114}$$

then

$$\|\omega_{j,H}^m\| \leq \varepsilon, \text{ for } m = 1, \ldots, M, j = l, b, f, \tag{3.115}$$

for $\Delta t \in (0, \Delta t_0]$, $H \in \Lambda$, with H_{max} small enough. As in the stability analysis presented in previous sections, we will consider that ρ_ε depends on $H \in \Lambda$.

To obtain the stability of the solution $I_H^m \in W_{l,H}^*$, $c_{f,H}^m \in W_{c,H}^*$, $c_{b,H}^m \in W_b(\overline{\Omega}_H - \overline{\Gamma}_{r,H})$, $m = 0, \ldots, M$, we first develop in the present Section some estimates for $\omega_{I,H}^m$, $\omega_{f,H}^m$, and $\omega_{b,H}^m$. Then, in Section 3.4.2 we establish the error analysis which is also necessary to conclude stability in Section 3.4.3.

We shall prove the following estimate for $\omega_{I,H}^m$.

Proposition 3.4.1. *Let $I_H^m, \tilde{I}_H^m \in W_{l,H}^*$, for $m = 0, \ldots, M$, defined by (3.49), (3.52) and (3.54) where the reaction term G and the diffusion entries $D_{I,ii}, i = 1, 2$, satisfy (AG_ℓ) and (AD_I), respectively. Then for $\omega_{I,H}^m = I_H^m - \tilde{I}_H^m$, we have*

$$\|\omega_{I,H}^{m+1}\|_H^2 + \Delta t D_{I,0} \sum_{j=0}^{m} \|\nabla_H \omega_{I,H}^{j+1/2}\|_+^2 \leq \prod_{\ell=0}^{m} (1 + \Delta t \sigma_I(\ell)) \|\omega_{I,H}^0\|_H^2, \tag{3.116}$$

where

$$\sigma_I(m) = \frac{2\left(\frac{L^2}{D_{I,0}} \|\nabla_H I_H^{m+1/2}\|_\infty^2 + C_{G_s}\right)}{\left(1 - \Delta t_0 (\frac{L^2}{D_{I,0}} \|\nabla_H I_H^{m+1/2}\|_\infty^2 + C_{G_s})\right)}, \tag{3.117}$$

and $\Delta t \in (0, \Delta t_{I,0}]$, with

$$1 - \Delta t_{I,0} \left(\frac{L^2}{D_{I,0}} \|\nabla_H I_H^{m+1/2}\|_\infty^2 + C_{G_s} \right) > 0, \quad m = 0, \ldots, M-1. \tag{3.118}$$

Proof: From equation (3.56), by considering the assumptions (AG_ℓ) and (AD_I), we get successively

$$\begin{aligned}
(D_{-t}\omega_{I,H}^{m+1}, \omega_{I,H}^{m+1/2})_H &= -(D_I(M_H I_H^{m+1/2}) \nabla_H I_H^{m+1/2} - D_I(M_H \tilde{I}_H^{m+1/2}) \nabla_H \tilde{I}_H^{m+1/2}, \nabla_H \omega_{I,H}^{m+1/2})_{H,+} \\
&\quad + (G_H^{m+1/2} - \tilde{G}_H^{m+1/2}, \omega_{I,H}^{m+1/2})_H \\
&\leq -D_{I,0} \|\nabla_H \omega_{I,H}^{m+1/2}\|_+^2 - \left(\left(D_I(M_H I_H^{m+1/2}) - D_I(M_H \tilde{I}_H^{m+1/2}) \right) \nabla_H I_H^{m+1/2}, \nabla_H \omega_{I,H}^{m+1/2} \right)_{H,+} \\
&\quad + \frac{1}{2} C_{G_s} \left(\|\omega_{I,H}^{m+1}\|_H^2 + \|\omega_{I,H}^m\|_H^2 \right) \\
&\leq -D_{I,0} \|\nabla_H \omega_{I,H}^{m+1/2}\|_+^2 + \frac{L^2}{4\varepsilon_1^2} (\|\omega_{I,H}^{m+1}\|_H^2 + \|\omega_{I,H}^m\|_H^2) \|\nabla_H I_H^{m+1/2}\|_\infty^2 + \varepsilon_1^2 \|\nabla_H \omega_{I,H}^{m+1/2}\|_+^2 \\
&\quad + \frac{1}{2} C_{G_s} \left(\|\omega_{I,H}^{m+1}\|_H^2 + \|\omega_{I,H}^m\|_H^2 \right),
\end{aligned}$$

where $\varepsilon_1 \neq 0$. Consequently, we obtain

$$\begin{aligned}
&\left(1 - \Delta t \left(\frac{L^2}{2\varepsilon_1^2} \|\nabla_H I_H^{m+1/2}\|_\infty^2 + C_{G_s} \right) \right) \|\omega_{I,H}^{m+1}\|_H^2 + 2\Delta t (D_{I,0} - \varepsilon_1^2) \|\nabla_H \omega_{I,H}^{m+1/2}\|_+^2 \\
&\qquad \leq \left(1 + \Delta t \left(\frac{L^2}{2\varepsilon_1^2} \|\nabla_H I_H^{m+1/2}\|_\infty^2 + C_{G_s} \right) \right) \|\omega_{I,H}^m\|_H^2.
\end{aligned} \tag{3.119}$$

Taking $\varepsilon_1^2 = \dfrac{D_{I,0}}{2}$ in equation (3.119) and considering $\Delta t \in (0, \Delta t_{I,0}]$ with Δt_0 satisfying (3.118), we establish

$$\|\omega_{I,H}^{m+1}\|_H^2 + \Delta t D_{I,0} \|\nabla_H \omega_{I,H}^{m+1/2}\|_+^2 \leq (1 + \Delta t \sigma_I(m)) \|\omega_{I,H}^m\|_H^2, \tag{3.120}$$

for $m = 0, \ldots, M-1$, where $\sigma_I(m)$ is defined by equation (3.117).
From equation (3.120) we deduce

$$\|\omega_{I,H}^{m+1}\|_H^2 + \Delta t D_{I,0}\Big(\|\nabla_H \omega_{I,H}^{m+1/2}\|_+^2 + \sum_{j=1}^{m}\prod_{\ell=j}^{m}(1+\sigma_I(\ell))\|\nabla_H \omega_{I,H}^{j+1/2}\|_+^2\Big) \leq \prod_{\ell=0}^{m}(1+\Delta t\,\sigma_I(\ell))\|\omega_{I,H}^0\|_H^2, \tag{3.121}$$

for $m = 0, \ldots, M-1$, and this last equation leads to (3.116). ■

Corollary 3.4.1. *Under the conditions of Proposition 3.4.1, we have*

$$\|\omega_{I,H}^{m+1}\|_H^2 + \Delta t D_{I,0}\sum_{j=0}^{m}\|\nabla_H \omega_{I,H}^{j+1/2}\|_+^2\Big) \leq \exp\Big(2(m+1)\Delta t\,\sigma_I\Big)\|\omega_{I,H}^0\|_H^2, \tag{3.122}$$

for $m = 0, \ldots, M-1$, and $\Delta t \in (0, \Delta t_{I,0}]$, with

$$\sigma_I = \frac{\dfrac{L^2}{D_{I,0}}\max\limits_{j=0,\ldots,M-1}\|\nabla_H I_H^{j+1/2}\|_\infty^2 + C_{G_s}}{1-\Delta t_0\left(\dfrac{L^2}{D_{I,0}}\max\limits_{j=0,\ldots,M-1}\|\nabla_H I_H^{j+1/2}\|_\infty^2 + C_{G_s}\right)}, \tag{3.123}$$

$$1-\Delta t_{I,0}\left(\frac{L^2}{D_{I,0}}\max_{j=0,\ldots,M-1}\|\nabla_H I_H^{j+1/2}\|_\infty^2 + C_{G_s}\right) > 0. \tag{3.124}$$

and $H \in \Lambda$.

Looking to the condition (3.124) we realise that the restriction on the time step size depends on the solution where we would like to conclude stability. If it is possible, we would like to establish conditions that do not depend on I_H^m, for $m = 1, \ldots, M$, and imply (3.124).

Proposition 3.4.2. *Let $I_H^m, \tilde{I}_H^m \in W_{I,H}^*$, $c_{f,H}^m, \tilde{c}_{f,H}^m \in W_{c,H}^*$, $c_{b,H}^m, \tilde{c}_{b,H}^m \in W_b(\overline{\Omega}_H - \overline{\Gamma}_{r,H})$, $m = 0, \ldots, M$, be solutions of the IBVP* (3.49)-(3.55)*. If the reaction terms F and S satisfy the assumptions (AF_ℓ), (AS_ℓ), respectively, and the condition (AD_c) holds for the entries of D_c, then, for $m = 0, \ldots, M-1$, we have*

$$\begin{aligned}\|\omega_{f,H}^{m+1}\|_H^2 + \|\omega_{b,H}^{m+1}\|_H^2 + \Delta t D_{c,0}\sum_{j=0}^{m}\|\nabla_H \omega_{f,H}^{j+1/2}\|_+^2 &\leq \prod_{\ell=0}^{m}(1+\Delta t\,\sigma_{f,b}(\ell))\big(\|\omega_{f,H}^0\|_H^2 + \|\omega_{b,H}^0\|_H^2\big)\\ &+\Delta t\sum_{j=1}^{m}\prod_{\ell=j}^{m}(1+\Delta t\,\sigma_{f,b}(\ell))\frac{(C_F+C_s)\max_{i=j,j+1}\|c_{b,H}^i\|_\infty^2}{2(1-\Delta t_0\theta_{\max})}\big(\|\omega_{I,H}^{j+1}\|_H^2 + \|\omega_{I,H}^j\|_H^2\big)\\ &+\Delta t\frac{C_F+C_s}{2}\max_{i=m,m+1}\|c_{b,H}^i\|_\infty^2\big(\|\omega_{I,H}^{m+1}\|_H^2 + \|\omega_{I,H}^m\|_H^2\big),\end{aligned} \tag{3.125}$$

where $\theta(m) = \left(\frac{L^2}{D_{c,0}}\|\nabla_H c_{f,H}^{m+1/2}\|_\infty^2 + \frac{C_F+2C_S}{2}\left(\max_{j=m,m+1}\|\tilde{I}_H^j\|_\infty + 1\right)\right)$ and

$$\sigma_{f,b}(m) = \frac{2\left(\dfrac{L^2}{D_{c,0}}\|\nabla_H c_{f,H}^{m+1/2}\|_\infty^2 + \dfrac{C_F+2C_S}{2}\left(\max\limits_{j=m,m+1}\|\tilde{I}_H^j\|_\infty + 1\right)\right)}{(1-\Delta t_0\theta(m))}, \tag{3.126}$$

and $\Delta t \in (0, \Delta t_{c,0}]$ *with*

$$1 - \Delta t_{c,0}\left(\frac{L^2}{D_{c,0}}\|\nabla_H c_{f,H}^{m+1/2}\|_\infty^2 + \frac{C_F + 2C_S}{2}\left(\max_{j=m,m+1}\|\tilde{I}_H^j\|_\infty + 1\right)\right) > 0, \;\; m = 0, \ldots, M-1, \quad (3.127)$$

Proof: From equation (3.57) and (3.58) we obtain

$$\begin{aligned}(D_{\cdot t}\omega_{f,H}^{m+1}, \omega_{f,H}^{m+1/2})_H = &-(D_c(M_H c_{f,H}^{m+1/2})\nabla_H c_{f,H}^{m+1/2} - D_c(M_H \tilde{c}_{f,H}^{m+1/2})\nabla_H \tilde{c}_{f,h}^{m+1/2}, \nabla_H \omega_{f,H}^{m+1/2})_{H,+} \\ &+ (F_H^{m+1/2} - \tilde{F}_H^{m+1/2}, \omega_{f,H}^{m+1/2})_H, \quad (3.128)\\ (D_{\cdot t}\omega_{b,H}^{m+1}, \omega_{b,H}^{m+1/1})_H = &(S_H^{m+1/2} - \tilde{S}_H^{m+1/2}, w_H)_H, \quad (3.129)\end{aligned}$$

where $\tilde{F}_H^{m+1/2}$ and $\tilde{S}_H^{m+1/2}$ are defined as $F_H^{m+1/2}$ and $S_H^{m+1/2}$, respectively, with $I_H^j, c_{f,H}^j, c_{b,H}^j, j = m, m+1$ replaced by $\tilde{I}_H^j, \tilde{c}_{f,H}^j, \tilde{c}_{b,H}^j, j = m, m+1$, respectively.

From equation (3.128) we get

$$\begin{aligned}(D_{\cdot t}\omega_{f,H}^{m+1}, \omega_{f,H}^{m+1/2})_H = &-(D_c(M_H c_{f,H}^{m+1/2})\nabla_H \omega_{f,H}^{m+1/2}, \nabla_H \omega_{f,H}^{m+1/2})_+ \\ &- ((D_c(M_H c_{f,H}^{m+1/2}) - D_c(M_H \tilde{c}_{f,H}^{m+1/2}))\nabla_H c_{f,H}^{m+1/2}, \nabla_H \omega_{f,H}^{m+1/2})_+ \\ &+ (F_H^{m+1/2} - \tilde{F}_H^{m+1/2}, \omega_{f,H}^{m+1/2})_H.\end{aligned}$$

Considering the assumption (AD_c) for the entries of D_c, from equation (3.128) we get

$$\begin{aligned}(D_{\cdot t}\omega_{f,H}^{m+1}, \omega_{f,H}^{m+1/2})_H \le -D_{c,0}\|\nabla_H \omega_{f,H}^{m+1/2}\|_+^2 + \frac{L^2}{4\varepsilon_1^2}\|\nabla_H c_{f,H}^{m+1/2}\|_\infty^2\left(\|\omega_{f,H}^{m+1}\|_H^2 + \|\omega_{f,H}^m\|_H^2\right) \\ + (F_H^{m+1/2} - \tilde{F}_H^{m+1/2}, \omega_{f,H}^{m+1/2})_H,\end{aligned} \quad (3.130)$$

where $\varepsilon_1 \neq 0$.

As

$$\begin{aligned}(F_H^{m+1/2} - \tilde{F}_H^{m+1/2}, \omega_{f,H}^{m+1/2})_H \le &\frac{C_F}{4}\max_{j=m,m+1}\|\tilde{I}_H^j\|_\infty\left(\|\omega_{b,H}^{m+1}\|_H^2 + \omega_{b,H}^m\|_H^2\right) \\ &+ \frac{C_F}{4}\left(\max_{j=m,m+1}\|\tilde{I}_H^j\|_\infty + 1\right)\left(\|\omega_{f,H}^{m+1}\|_H^2 + \omega_{f,H}^m\|_H^2\right) \\ &+ \frac{C_F}{4}\max_{j=m,m+1}\|c_{b,H}^j\|_\infty^2\left(\|\omega_{I,H}^{m+1}\|_H^2 + \omega_{I,H}^m\|_H^2\right),\end{aligned}$$

and

$$\begin{aligned}(S_H^{m+1/2} - \tilde{S}_H^{m+1/2}, \omega_{b,H}^{m+1/2})_H \le &\frac{C_S}{4}\left(2\max_{j=m,m+1}\|\tilde{I}_H^j\|_\infty + 1\right)\left(\|\omega_{b,H}^{m+1}\|_H^2 + \omega_{b,H}^m\|_H^2\right) \\ &+ \frac{C_S}{4}\max_{j=m,m+1}\|c_{b,H}^j\|_\infty^2\left(\|\omega_{I,H}^{m+1}\|_H^2 + \omega_{I,H}^m\|_H^2\right),\end{aligned}$$

from equation (3.130) and considering equation (3.129), we deduce

$$\begin{aligned}(1 - \Delta t\,\theta_f(m))\|\omega_{f,H}^{m+1}\|_H^2 + (1 - \Delta t\,\theta_b(m))\|\omega_{b,H}^{m+1}\|_H^2 + 2\Delta t(D_{c,0} - \varepsilon_1^2)\|\nabla_H \omega_{f,H}^{m+1/2}\|_+^2 \\ \le (1 + \Delta t\,\theta_f(m))\|\omega_{f,H}^m\|_H^2 + (1 + \Delta t\,\theta_b(m))\|\omega_{b,H}^m\|_H^2 + \Delta t\,\theta_I(m),\end{aligned} \quad (3.131)$$

where

$$\theta_f(m) = \frac{L^2}{2\varepsilon_1^2}\|\nabla_H c_{f,H}^{m+1/2}\|_\infty^2 + \frac{C_F}{2}\big(\max_{j=m,m+1}\|\tilde{I}_H^j\|_\infty + 1\big),$$
$$\theta_b(m) = \frac{C_F + 2C_s}{2}\max_{j=m,m+1}\|\tilde{I}_H^j\|_\infty,$$
$$\theta_I(m) = \frac{C_F + C_S}{2}\max_{j=m,m+1}\|c_{b,H}^j\|_\infty^2\big(\|\omega_{I,H}^{m+1}\|_H^2 + \omega_{I,H}^m\|_H^2\big)$$

Fixing $\varepsilon_1 = \frac{D_{c,0}}{2}$, from equation (3.131) we establish

$$\begin{aligned}\|\omega_{f,H}^{m+1}\|_H^2 + \|\omega_{b,H}^{m+1}\|_H^2 + \Delta t D_{c,0}\|\nabla_H \omega_{f,H}^{m+1/2}\|_+^2 \\ \leq (1+\Delta t\,\sigma_{f,b}(m))\big(\|\omega_{f,H}^m\|_H^2 + \|\omega_{b,H}^m\|_H^2\big) + \frac{\Delta t}{1-\Delta t\,\theta(m)}\theta_I(m),\end{aligned} \tag{3.132}$$

where $\sigma_{f,b}(m)$ defined by equation (3.126) with $\Delta t_{c,0}$ fixed by (3.127) and $\theta(m) = \max\{\theta_f(m), \theta_b(m)\}$. Finally, inequality (3.132) leads to (3.125). ■

Corollary 3.4.2. *Under the conditions of Proposition 3.4.2, we have for $m = 0, \ldots, M-1$,*

$$\begin{aligned}&\|\omega_{f,H}^{m+1}\|_H^2 + \|\omega_{b,H}^{m+1}\|_H^2 + \Delta t D_{c,0}\sum_{j=0}^m \|\nabla_H \omega_{f,H}^{j+1/2}\|_+^2 \\ &\leq e^{(m+1)\Delta t\sigma_{f,b}}\left(\big(\|\omega_{f,H}^0\|_H^2 + \|\omega_{b,H}^0\|_H^2\big) + \Delta t\frac{(C_F+C_s)\max_{m=0,\ldots,M}\|c_{b,H}^m\|_\infty^2}{2(1-\Delta t_0\theta_{\max})}\sum_{j=1}^{m+1}\big(\|\omega_{I,H}^{j+1}\|_H^2 + \|\omega_{I,H}^j\|_H^2\big)\right)\end{aligned} \tag{3.133}$$

where $\theta_{\max} = \left(\frac{L^2}{D_{c,0}}\max_{m=0,\ldots,M-1}\|\nabla_H c_{f,H}^{m+1/2}\|_\infty^2 + \frac{C_F+2C_S}{2}\left(\max_{m=0,\ldots,M}\|\tilde{I}_H^m\|_\infty + 1\right)\right)$ *and*

$$\sigma_{f,b} = \frac{2\left(\frac{L^2}{D_{c,0}}\max_{m=0,\ldots,M-1}\|\nabla_H c_{f,H}^{m+1/2}\|_\infty^2 + \frac{C_F+2C_S}{2}\left(\max_{m=0,\ldots,M}\|\tilde{I}_H^j\|_\infty + 1\right)\right)}{1-\Delta t_0\theta_{\max}}, \tag{3.134}$$

and $\Delta t \in (0, \Delta t_{c,0}]$ *with*

$$1 - \Delta t_{c,0}\left(\frac{L^2}{D_{c,0}}\max_{m=0,\ldots,M-1}\|\nabla_H c_{f,H}^{m+1/2}\|_\infty^2 + \frac{C_F+2C_S}{2}\left(\max_{m=0,\ldots,M}\|\tilde{I}_H^m\|_\infty + 1\right)\right) > 0. \tag{3.135}$$

From Propositions 3.4.1 and 3.4.2 we establish the next result:

Corollary 3.4.3. *Under the conditions of Proposition 3.4.1 and 3.4.2 we have for $m = 0, \ldots, M-1$,*

$$\|\omega_{I,H}^{m+1}\|_H^2 + \Delta t D_{I,0}\sum_{j=0}^m \|\nabla_H \omega_{I,H}^{j+1/2}\|_+^2 \leq e^{2T\sigma_I}\|\omega_{I,H}^0\|_H^2, \tag{3.136}$$

and

$$\|\omega_{f,H}^{m+1}\|_H^2+\|\omega_{b,H}^{m+1}\|_H^2+\Delta t D_{c,0}\sum_{j=0}^{m}\|\nabla_H\omega_{f,H}^{j+1/2}\|_+^2\leq e^{(m+1)\Delta t\sigma_{f,b}}\Big(\big(\|\omega_{f,H}^0\|_H^2+\|\omega_{b,H}^0\|_H^2\big)\\ +(C_F+C_s)\max_{m=0,\dots,M}\|c_{b,H}^m\|_\infty^2 Te^{2T\sigma_I}\|\omega_{I,H}^0\|_H^2\Big), \tag{3.137}$$

where σ_I *and* $\sigma_{f,b}$ *are defined by* (3.123) *and* (3.134)*, respectively, with* $\Delta t\in(0,\Delta t_0]$ *given by* $\Delta t_0=\min\{\Delta t_{I,0},\Delta t_{c,0}\}$ *where* $\Delta t_{I,0},\Delta t_{c,0}$ *defined by (3.124) and (3.135), respectively.*

To conclude the stability from Propositions 3.4.1 and 3.4.2, we need to prove that $\|\nabla_H I_H^m(\mu)\|_\infty$ and $\sigma_{f,b}(m)$ are uniformly bounded for $m=1,\dots,M$ and $H\in\Lambda$. Similarly to the previous section, we first prove a convergence result that will allow us to conclude stability in section 3.4.3.

3.4.2 Convergence

Let (I,c_f,c_b) be the solution of the IBVP (3.2)-(3.8) and let $I_H^m\in W_{I,H}^*, c_{f,H}^m(t)\in W_{c,H}^*, c_{b,H}^m(t)\in W_b(\overline{\Omega}_H-\overline{\Gamma}_{r,H})$ be solutions of the IBVP (3.49)-(3.55). For $m=0,\cdots,M$, we define the errors

$$\begin{aligned}E_{I,H}^m&=R_HI(t_m)-I_H^m,\\ E_{f,H}^m&=R_Hc_f(t_m)-c_{f,H}^m,\\ E_{b,H}^m&=R_Hc_b(t_m)-c_{b,H}^m.\end{aligned}$$

We shall now establish error estimates for each of the errors $E_{I,H}^m$, $E_{f,H}^m$, and $E_{b,H}^m$. Because we consider now the fully discrete case, to use the Taylor representation of the truncation error, we require some smoothness conditions over the solution (I,c_f,c_b) in the space domain $\overline{\Omega}$, and the time domain $[0,T]$.

Let k_1 and k_2 be nonnegative integers and $U\subset\mathbb{R}^2$ closed. We denote $\mathrm{C}^{k_1,k_2}(U\times[0,T])$ the space of functions $u:U\times[0,T]\to\mathbb{R}$ such that, u is k_1-times continuously differentiable in U and k_2-times continuously differentiable in $[0,T]$. In addition, we use the norm

$$\|u\|_{\mathrm{C}^{k_1,k_2}(U\times[0,T])}=\max_{\substack{\alpha_1+\alpha_2\leq k_1\\ \beta\leq k_2}}\max_{U\times[0,T]}\left\{\left|\frac{\partial^\beta u}{\partial t^\beta}(x,y,t)\right|,\left|\frac{\partial^{\alpha_1+\alpha_2}u}{\partial x^{\alpha_1}\partial y^{\alpha_2}}(x,y,t)\right|\right\}$$

For ease of notation, we shall use C^{k_1,k_2} we we refer to $\mathrm{C}^{k_1,k_2}(\overline{\Omega}\times[0,T])$.

Error estimate for $E_{I,H}^m$

We remark that $E_{I,H}^m, m=0,\dots,M$, is solution of the following discrete IBVP

$$D_{-t}E_{I,H}^{m+1}=\nabla_H^*\cdot\Big(D_I(M_HR_HI^{m+1/2})\nabla_HR_HI^{m+1/2}\Big)-\nabla_H^*\cdot\Big(D_I(M_HI_H^{m+1/2})\nabla_HI_H^{m+1/2}\Big)\\ +G^{m+1/2}-G_H^{m+1/2}+T_I^{m+1}\ \text{ in }\ (\overline{\Omega}_H-\overline{\Gamma}_{l,H})\times(0,T], \tag{3.138}$$

with initial and boundary conditions

$$E_{I,H}^m=R_HI(0)-I_H^0\qquad\text{in }\overline{\Omega}_H, \tag{3.139}$$

$$E_{I,H}^{j} = 0 \qquad \text{on } \overline{\Gamma}_{l,H}, j = 0,\ldots,M, \tag{3.140}$$

$$(\nabla_{H,\eta}^{(I)}(R_H I^{m+1/2}) - \nabla_{H,\eta}^{(I)}(I_H^{m+1/2}))\cdot\eta = T_{I,b}^{m+1} \qquad \text{on } (\partial\Omega_H - \overline{\Gamma}_{l,H}),\ \ m = 0,\ldots,M-1. \tag{3.141}$$

In equation (3.138), T_I^m is given by $T_I^m = T_{I,t}^m + T_{I,s}^m$, where

$$|T_{I,t}^m(x_i,y_j)| \le C\Delta t^2 \left(\left\| \frac{\partial^3 I}{\partial t^3} \right\|_{\mathrm{C}^{0,0}} + \| \frac{\partial^2 I}{\partial t^2} \|_{\mathrm{C}^{2,0}} \left(\|I\|_{\mathrm{C}^{2,0}}^2 + 2\|I\|_{\mathrm{C}^{2,0}} + 1 \right) + \left\| \frac{\partial I}{\partial t} \right\|_{\mathrm{C}^{1,0}} \right),$$

with C independent of H and Δt, and $T_{I,s}^m$ is defined as $T_I(t)$ in (3.72) with $I(t)$ replaced by $I^{m+1/2}$, and

$$T_{I,b}^m = T_{I,b,H}^m + T_{I,b,t}^m,$$

$T_{I,b,H}^m$ is defined as $T_{I,b}(t)$ in equation (3.75) with $I(t)$ replaced by $I^{m+1/2}$, and

$$|T_{I,b,t}^{m+1}(x_i,y_j)| \le C\Delta t^2 \left(\left\| \frac{\partial^2 I}{\partial t^2} \right\|_{\mathrm{C}^{0,0}} \|I\|_{\mathrm{C}^{1,0}} + \left\| \frac{\partial^2 I}{\partial t^2} \right\|_{\mathrm{C}^{1,0}} \right), \tag{3.142}$$

for H_{max} small enough.
Following the proof of Theorem 3.3.1, it can be shown that

$$\begin{aligned} \left(1 - \Delta t \left(\frac{L^2}{2\varepsilon_1^2} \|\nabla_H R_H I^{m+1/2}\|_\infty^2 + C_{G_s} \right) \right) \|E_{I,H}^{m+1}\|_H^2 + 2\Delta t (D_{I,0} - \varepsilon_1^2) \|\nabla_H E_{I,H}^{m+1/2}\|_+^2 \\ \le \left(1 + \Delta t \left(\frac{L^2}{2\varepsilon_1^2} \|\nabla_H R_H I^{m+1/2}\|_\infty^2 + C_{G_s} \right) \right) \|E_{I,H}^m\|_H^2 \\ + \Delta t (T_I^{m+1}, E_{I,H}^{m+1/2})_H + \Delta t (T_{I,b}^{m+1}, E_{I,H}^{m+1/2})_{\partial\Omega_H - \overline{\Gamma}_{l,H}}. \end{aligned} \tag{3.143}$$

To bound the term $(T_I^{m+1}, E_{I,H}^{m+1/2})_H$ we follow the steps in the proof of Theorem 3.3.1, and we can obtain similar inequalities to (3.87)-(3.88). Thereafter, by using the discrete Poincaré inequality (3.21), we have

$$\begin{aligned} (T_I^{m+1}, E_{I,H}^{m+1/2})_H &\le A(I) \left(\|E_{I,H}^{m+1/2}\|_H + \|\nabla_H E_{I,H}^{m+1/2}\|_+ \right) \\ &\le (C_P + 1) A(I) \|\nabla_H E_{I,H}^{m+1/2}\|_+ \\ &\le \frac{C}{4\varepsilon_2^2} A(I)^2 + \varepsilon_2^2 \|\nabla_H E_{I,H}^{m+1/2}\|_+^2, \end{aligned}$$

where $\varepsilon_2 \neq 0$ and $A(I)$ is given by

$$\begin{aligned} A(I) = C \Bigg(H_{max}^2 \|I\|_{C^{4,0}(\overline{\Omega}_{I,\Lambda}\times[0,T])}^{p_I} + \ \Delta t^2 \Bigg(\left\| \frac{\partial^3 I}{\partial t^3} \right\|_{\mathrm{C}^{0,0}} \\ + \| \frac{\partial^2 I}{\partial t^2} \|_{\mathrm{C}^{2,0}} \left(\|I\|_{\mathrm{C}^{2,0}}^2 + 2\|I\|_{\mathrm{C}^{2,0}} + 1 \right) \Bigg) \Bigg), \end{aligned}$$

Moreover, in equation (3.143), by first using the trace inequality (3.20) and then, the discrete Poincaré inequality (3.21), we have

$$\begin{aligned}(T_{I,b}^{m+1}, E_{I,H}^{m+1/2})_{\partial\Omega_H-\overline{\Gamma}_{l,H}} &\leq C_T B(I)\big(\|E_{I,H}^{m+1/2}\|_H + \|\nabla_H E_{I,H}^{m+1/2}\|_+\big)\\ &\leq CB(I)\|\nabla_H E_H(t)\|_+\\ &\leq \frac{C}{4\varepsilon_3^2}B(I)^2 + \varepsilon_3^2\|\nabla_H E_{I,H}^{m+1/2}\|_+^2,\end{aligned}$$

where $\varepsilon_3 \neq 0$ and

$$B(I) = C\left(H_{max}^2\|I\|_{\mathrm{C}^{3,0}}^{p_I} + \Delta t^2\left(\|\frac{\partial^2 I}{\partial t^2}\|_{\mathrm{C}^{0,0}}\|I\|_{\mathrm{C}^{1,0}} + \|\frac{\partial^2 I}{\partial t^2}\|_{\mathrm{C}^{1,0}}\right)\right),$$

where C is a positive constant independent of H and Δt.
Combining the two last upper bounds and taking $\varepsilon_1 = \varepsilon_2 = \varepsilon_3$, for the last term of (3.143) we obtain

$$(T_I^{m+1}, E_{I,H}^{m+1/2})_H + (T_{I,b}^{m+1}, E_{I,H}^{m+1/2})_{\partial\Omega_H-\overline{\Gamma}_{l,H}} \leq C\frac{1}{4\varepsilon_1^2}(A(I)^2 + B(I)^2) + 2\varepsilon_1^2\|\nabla_H E_{I,H}^{m+1/2}\|_+^2. \quad (3.144)$$

By substituting equation (3.144) into equation (3.143) we deduce

$$\begin{aligned}\left(1 - \Delta t\left(\frac{L^2}{2\varepsilon_1^2}\|\nabla_H R_H I^{m+1/2}\|_\infty^2 + C_{G_s}\right)\right)\|E_{I,H}^{m+1}\|_H^2 + 2\Delta t(D_{I,0} - 3\varepsilon_1^2)\|\nabla_H E_{I,H}^{m+1/2}\|_+^2\\ \leq \left(1 + \Delta t\left(\frac{L^2}{2\varepsilon_1^2}\|\nabla_H R_H I^{m+1/2}\|_\infty^2 + C_{G_s}\right)\right)\|E_{I,H}^m\|_H^2 + \Delta t\frac{1}{\varepsilon_1^2}\gamma_I,\end{aligned} \quad (3.145)$$

with

$$\begin{aligned}\gamma_I = C\Bigg(H_{max}^4\|I\|_{\mathrm{C}^{4,0}}^{2p_I} + \Delta t^4\Bigg(&\left\|\frac{\partial^3 I}{\partial t^3}\right\|_{\mathrm{C}^{0,0}}^2\\ &+\|\frac{\partial^2 I}{\partial t^2}\|_{C^{2,0}}^2\left(\|I\|_{\mathrm{C}^{2,0}}^4 + \|I\|_{\mathrm{C}^{2,0}}^2 + 1\right) + \left\|\frac{\partial I}{\partial t}\right\|_{\mathrm{C}^{1,0}}\Bigg)\Bigg).\end{aligned}$$

Taking $\varepsilon_1^2 = \frac{D_{I,0}}{6}$ in inequality (3.145), we conclude the following result:

Theorem 3.4.1. *Let $I_H^m \in W_{l,H}^*, m = 0,\ldots,M$, defined by equations* (3.49)*,* (3.52) *and* (3.54) *where the reaction term G and the diffusion entries $D_{I,ii}, i = 1,2$, satisfy (AG_ℓ) and (AD_I), respectively. Let $I \in C^{4,0}(\overline{\Omega}_{I,\Lambda}\times[0,T]) \cap C^{0,3}(\overline{\Omega}\times[0,T]) \cap \{u : \overline{\Omega}\times[0,T] \to \mathbb{R}, \exists\frac{\partial^2 u}{\partial t^2} \in C^{2,0}(\overline{\Omega}\times[0,T])\}$ be the solution of the IBVP (3.5), (3.6) with initial condition $I(0)$. Then, there exists a positive constant C independent of I, H, and Δt, such that, for $m = 0,\ldots,M$ holds the following*

$$\|E_{I,H}^{m+1}\|_H^2 + \Delta t D_{I,0}\sum_{j=0}^{m}\|\nabla_H E_{I,H}^{j+1/2}\|_+^2 \leq e^{(m+1)\Delta t\sigma_I}\|E_{I,H}^0\|_H^2 + \frac{e^{(m+1)\Delta t\sigma_I}}{1-\Delta t_0\theta_I}\gamma_I, \quad (3.146)$$

where γ_I, σ_I, and θ_I are such that

$$\gamma_I \leq C\left(H_{max}^4\|I\|^{2p_I}_{C^{4,0}(\overline{\Omega}_{I,\Lambda}\times[0,T])} + \Delta t^4\left(\|I\|^2_{\mathrm{C}^{0,3}} + \|\frac{\partial^2 I}{\partial t^2}\|^2_{\mathrm{C}^{2,0}}\left(\|I\|^4_{\mathrm{C}^{2,0}} + \|I\|^2_{\mathrm{C}^{2,0}} + 1\right)\right)\right),$$

$$\sigma_I = \frac{\theta_I}{1-\Delta t_0\theta_I}, \qquad \theta_I = 2\frac{L^2}{D_{I,0}}\|\nabla I\|^2_{(C(\overline{\Omega}\times[0,T]))^2} + C_{G_s},$$

and $\Delta t \in (0, \Delta t_{I,0}]$ with

$$1 - \Delta t_{I,0}\theta_I > 0. \tag{3.147}$$

Error estimate for $E^m_{f,H}$ and $E^m_{b,H}$

We consider now the errors for the concentrations: free drug $E^m_{f,H}$ and bound drug $E^m_{b,H}$, for $m = 0,\ldots,M$, that are defined by the following equations

$$\begin{aligned} D_{-t}E^{m+1}_{f,H} &= \nabla^*_H\cdot(D_c(M_H R_H c_f^{m+1/2})\nabla_H R_H c_f^{m+1/2} - \nabla^*_H\cdot(D_c(M_H c^{m+1/2}_{f,H})\nabla_H c^{m+1/2}_{f,H}) \\ &\quad + F^{m+1/2} - F_H^{m+1/2} + T^{m+1}_{c_f}, \end{aligned} \tag{3.148}$$

$$D_{-t}E^{m+1/2}_{b,H} = S_H^{m+1/2} - S^{m+1/2} + T^{m+1}_{c_b} \qquad \text{in } \overline{\Omega}_H - \overline{\Gamma}_{r,H}, \text{ for } m = 0,\ldots,M-1, \tag{3.149}$$

with initial and boundary conditions

$$E^0_{f,H} = R_H c_f(t_0) - c^0_{f,H} \qquad \text{in } \overline{\Omega}_H, \tag{3.150}$$

$$E^0_{b,H} = R_H c_b(0) - c^0_{b,H} \qquad \text{in } \overline{\Omega}_H - \overline{\Gamma}_{r,H}, \tag{3.151}$$

$$E^j_{f,H} = 0 \qquad \text{on } \overline{\Gamma}_{r,H}, j = 0,\ldots,M, \tag{3.152}$$

$$(\nabla^{(c)}_{H,\eta}(R_H c_f^{j+1/2}) - \nabla^{(c)}_{H,\eta}(c^{j+1/2}_{f,H}))\cdot\eta = T^{j+1}_{c_f,b} \qquad \text{on } (\partial\Omega_H - \overline{\Gamma}_{r,H}), j = 0,\ldots,M-1. \tag{3.153}$$

In equations (3.148)-(3.149), $T^{m+1}_{c_f}$ is given by $T^{m+1}_{c_f} = T^{m+1}_{c_f,t} + T^{m+1}_{c_f,s}$, where

$$|T^{m+1}_{c_f,t}(x_i,y_j)| \leq C\Delta t^2\left(\left\|\frac{\partial^3 c_f}{\partial t^3}\right\|_{\mathrm{C}^{0,0}} + \|\frac{\partial^2 I}{\partial t^2}\|_{\mathrm{C}^{2,0}}\left(\|I\|^2_{\mathrm{C}^{2,0}} + 2\|I\|_{\mathrm{C}^{2,0}} + 1\right) + \|\frac{\partial c_f}{\partial t}\|_{\mathrm{C}^{1,0}} + \|I\|_{\mathrm{C}^{0,2}}\|c_b\|_{\mathrm{C}^{0,2}}\right),$$

and $T^{m+1}_{c_f,s}$ can be bounded as $T_I(t)$ in section 3.3.2. Then, we have

$$\begin{aligned} (T^{m+1}_{c_f}, E^{m+1/2}_{f,H})_H &\leq A_f(c_f)\left(\|E^{m+1/2}_{f,H}\|_H + \|\nabla_H E^{m+1/2}_{f,H}\|_+\right) \\ &\leq (C_P+1)A_f(c_f)\|\nabla_H E^{m+1/2}_{f,H}\|_+ \\ &\leq \frac{C}{4\varepsilon_2^2}A_f(c_f)^2 + \varepsilon_2^2\|\nabla_H E^{m+1/2}_{f,H}\|^2_+, \end{aligned}$$

where $\varepsilon_2 \neq 0$ and $A(I)$ is given by

$$A_f(c_f) = C\left(H^2_{max}\|c_f\|^{p_c}_{\mathrm{C}^{4,0}(\overline{\Omega}_{c_f,\Lambda}\times[0,T])} + \Delta t^2\left[\left\|\frac{\partial^3 c_f}{\partial t^3}\right\|_{\mathrm{C}^{0,0}} + \|\frac{\partial^2 c_f}{\partial t^2}\|_{\mathrm{C}^{2,0}}\left(\|c_f\|^2_{\mathrm{C}^{2,0}} + 2\|c_f\|_{\mathrm{C}^{2,0}} + 1\right)\right.\right.$$
$$\left.\left. + \|\frac{\partial c_f}{\partial t}\|_{\mathrm{C}^{1,0}} + \|I\|_{\mathrm{C}^{0,2}}\|c_b\|_{\mathrm{C}^{0,2}}\right]\right).$$

Similarly, we have

$$\begin{aligned}(T_{c_f,b}^{m+1}, E_{f,H}^{m+1/2})_{\partial\Omega_H-\overline{\Gamma}_{r,H}} &\le C_T B_f(c_f)\big(\|E_{I,H}^{m+1/2}\|_H + \|\nabla_H E_{I,H}^{m+1/2}\|_+\big)\\ &\le C B_f(c_f)\|\nabla_H E_H(t)\|_+\\ &\le \frac{C}{4\varepsilon_3^2}B_f(c_f)^2 + \varepsilon_3^2\|\nabla_H E_{c_f,H}^{m+1/2}\|_+^2,\end{aligned}$$

where $\varepsilon_3 \neq 0$ and

$$B_f(c_f) = C\left(H_{max}^2\|c_f\|^{p_c}_{\mathrm{C}^{3,0}(\overline{\Omega}_{c_f,\Lambda}\times[0,T])} + \Delta t^2\left(\left\|\frac{\partial^2 c_f}{\partial t^2}\right\|_{\mathrm{C}^{0,0}}\left\|\frac{\partial c_f}{\partial x}\right\|_{\mathrm{C}^{0,0}} + \left\|\frac{\partial^3 c_f}{\partial t^2\partial x}\right\|_{\mathrm{C}^{0,0}}\right)\right).$$

Now, for the truncation error $T_{c_b}^{m+1}$ we have

$$|T_{c_b}^m(x_i,y_j)| \le C\Delta t^2\left(\left\|\frac{\partial^3 c_b}{\partial t^3}\right\|_{\mathrm{C}^{0,0}} + \|I\|_{\mathrm{C}^{0,0}}\left\|\frac{\partial^2 c_b}{\partial t^2}\right\|_{\mathrm{C}^{0,0}} + \|c_b\|_{\mathrm{C}^{0,0}}\left\|\frac{\partial^2 I}{\partial t^2}\right\|_{\mathrm{C}^{0,0}}\right).$$

and then

$$(T_{c_b}^{m+1}, E_{f,H}^{m+1/2})_H \le \Delta t^4\frac{C}{2}B_b^2(c_b) + \frac{1}{4}\left(\|E_{b,H}^{m+1}\|_H^2 + \|E_{b,H}^m\|_H^2\right),$$

where

$$B_b(c_b) = \left\|\frac{\partial^3 c_b}{\partial t^3}\right\|_{\mathrm{C}^{0,0}} + \|c_b\|_{\mathrm{C}^{0,0}}\left\|\frac{\partial^2 I}{\partial t^2}\right\|_{\mathrm{C}^{0,0}} + \|I\|_{\mathrm{C}^{0,0}}\left\|\frac{\partial^2 c_b}{\partial t^2}\right\|_{\mathrm{C}^{0,0}}.$$

Following the proof of Proposition 3.4.2, it can be shown the following

$$\begin{aligned}&(1-\Delta t\theta_f(m))\|E_{f,H}^{m+1}\|_H^2 + (1-\Delta t\theta_b(m))\|E_{b,H}^{m+1}\|_H^2 + 2\Delta t(D_{c,0}-\varepsilon_1^2)\|\nabla_H E_{f,H}^{m+1/2}\|_+^2\\ &\le (1+\Delta t\theta_f(m))\|E_{f,H}^m\|_H^2 + (1+\Delta t\theta_b(m))\|E_{b,H}^m\|_H^2 + \Delta t\theta_I(m)\\ &+ 2\Delta t(T_{c_f}^{m+1}, E_{f,H}^{m+1/2})_H + 2\Delta t(T_{c_f,b}^{m+1}, E_{f,H}^{m+1/2})_{\partial\Omega_H-\overline{\Gamma}_{r,H}} + 2\Delta t(T_{c_b}^{m+1}, E_{b,H}^{m+1/2})_H,\end{aligned} \tag{3.154}$$

where

$$\begin{aligned}\theta_f(m) &= \frac{L^2}{2\varepsilon_1^2}\|\nabla_H R_H c_f^{m+1/2}\|_\infty^2 + \frac{C_F}{2}\big(\max_{j=m,m+1}\|I_H^j\|_\infty + 1\big),\\ \theta_b(m) &= \frac{C_F+2C_s}{2}\max_{j=m,m+1}\|I_H^j\|_\infty,\\ \theta_I(m) &= \frac{C_F+C_S}{2}\max_{j=m,m+1}\|R_H c_b^j\|_\infty^2\big(\|E_{I,H}^{m+1}\|_H^2 + \|E_{I,H}^m\|_H^2\big).\end{aligned}$$

Consequently, from (3.154) we deduce

$$\begin{aligned}&(1-\Delta t\theta_f)\|E_{f,H}^{m+1}\|_H^2 + (1-\Delta t\theta_b)\|E_{b,H}^{m+1}\|_H^2 + 2\Delta t(D_{c,0}-\varepsilon_1^2-\varepsilon_2^2-\varepsilon_3^2)\|\nabla_H E_{f,H}^{m+1/2}\|_+^2\\ &\le (1+\Delta t\theta_f)\|E_{f,H}^m\|_H^2 + (1+\Delta t\theta_b)\|E_{b,H}^m\|_H^2 + \Delta t\theta_I(m) + \Delta t\gamma_{f,b}(m),\end{aligned} \tag{3.155}$$

where

$$\theta_f = \frac{L^2}{2\varepsilon_1^2}\|\nabla c_f\|^2_{(\mathrm{C}^{0,0})^2} + \frac{C_F}{2}\left(\max_{j=0,\dots,M}\|I_H^j\|_\infty + 1\right),$$

$$\theta_b = \frac{C_F + 2C_s}{2} \max_{j=0,\dots,M} \|I_H^j\|_\infty + 1,$$
$$\theta_I(m) = \frac{C_F + C_S}{2} \|c_b\|^2_{\mathrm{C}^{0,0}} \left(\|E_{I,H}^{m+1}\|_H^2 + E_{I,H}^m\|_H^2 \right),$$

and

$$\begin{aligned}\gamma_{f,b} = C \Bigg(& H_{max}^4 \|c_f\|^{2p_c}_{C^{4,0}(\overline{\Omega}\times[0,T])} + \Delta t^4 \left[\left\| \frac{\partial^3 c_f}{\partial t^3} \right\|^2_{\mathrm{C}^{0,0}} + \left\| \frac{\partial^3 c_b}{\partial t^3} \right\|^2_{\mathrm{C}^{0,0}} \right. \\ & \left. + \| \frac{\partial^2 c_f}{\partial t^2} \|^2_{\mathrm{C}^{2,0}} \left(\|c_f\|^2_{\mathrm{C}^{2,0}} \left(\|c_f\|^2_{\mathrm{C}^{2,0}} + 1 \right) + 1 \right) + \| \frac{\partial c_f}{\partial t} \|^2_{C^{1,0}} + \|c_b\|^2_{C^{0,2}} \|I\|^2_{C^{0,2}} \right] \Bigg).\end{aligned} \tag{3.156}$$

Fixing $\varepsilon_1^2 = \varepsilon_2^2 = \varepsilon_3^2 = \frac{D_{c,0}}{6}$, the inequality (3.155) implies that

$$\begin{aligned}&(1 - \Delta t \theta_{b,f}) \left(\|E_{f,H}^{m+1}\|_H^2 + \|E_{b,H}^{m+1}\|_H^2 \right) + \Delta t D_{c,0} \|\nabla_H E_{f,H}^{m+1/2}\|_+^2 \\ &\quad \le (1 + \Delta t \theta_{b,f}) \left(\|E_{f,H}^m\|_H^2 + \|E_{b,H}^m\|_H^2 \right) + \Delta t \alpha_{b,f} \left(\|E_{I,H}^{m+1}\|_H^2 + \|E_{I,H}^m\|_H^2 \right) + \Delta t \gamma_{b,f},\end{aligned} \tag{3.157}$$

for $m = 0, \dots, M-1$. In inequality (3.157),

$$\theta_{b,f} = \frac{2L^2}{D_{c,0}} \|\nabla c_f\|^2_{(\mathrm{C}^{0,0})^2} + \frac{C_F + 2C_S}{2} \left(\max_{j=0,\dots,M} \|I_H^j\|_\infty + 1 \right), \tag{3.158}$$

$$\alpha_{b,f} = \frac{C_F + C_S}{2} \|c_b\|^2_{\mathrm{C}^{0,0}}. \tag{3.159}$$

Let $\Delta t_{c,0}$ be such that

$$1 - \Delta t_{c,0} \theta_{b,f} > 0. \tag{3.160}$$

Then, from (3.157), for $\Delta t \in (0, \Delta t_{c,0}]$ and for $m = 0, \dots, M-1$, we have

$$\begin{aligned}\left(\|E_{f,H}^{m+1}\|_H^2 + \|E_{b,H}^{m+1}\|_H^2 \right) + \Delta t D_{c,0} \|\nabla_H E_{f,H}^{m+1/2}\|_+^2 &\le (1 + \Delta t \sigma_{b,f}) \left(\|E_{f,H}^m\|_H^2 + \|E_{b,H}^m\|_H^2 \right) \\ &+ \Delta t \frac{\alpha_{b,f}}{1 - \Delta t_{c,0} \theta_{b,f}} \left(\|E_{I,H}^{m+1}\|_H^2 + \|E_{I,H}^m\|_H^2 \right) + \Delta t \frac{1}{1 - \Delta t_{c,0} \theta_{b,f}} \gamma_{b,f},\end{aligned}$$

with

$$\sigma_{b,f} = \frac{\theta_{b,f}}{1 - \Delta t_{c,0} \theta_{bf}}. \tag{3.161}$$

We are now ready to state the convergence result for the concentration errors $E_{f,H}^m$ and $E_{b,H}^m$.

Theorem 3.4.2. *Let I, c_f, c_b be the solution of the IBVP (3.2)-(3.8) with initial conditions $I(0), c_f(0), c_b(0)$. Let $I \in C^{0,2}(\overline{\Omega} \times [0,T])$, $c_f \in C^{4,0}(\overline{\Omega}_{c_f,\Lambda} \times [0,T]) \cap C^{0,3}(\overline{\Omega} \times [0,T]) \cap \{u : \overline{\Omega} \times [0,T] \to \mathbb{R}, \exists \frac{\partial^2 u}{\partial t^2} \in C^{2,0}(\overline{\Omega} \times [0,T])\}$ and $c_b \in C^{0,3}(\overline{\Omega} \times [0,T])$. Let $I_H^m \in W_{I,H}^*, c_{f,H}^m \in W_{c,H}^*, c_{b,H}^m \in W_b(\overline{\Omega}_H - \overline{\Gamma}_{r,H})$ be solutions of the IBVP (3.49)-(3.55) with the initial conditions $I_H^0, c_{f,H}^0$ and $c_{b,H}^0$, respectively. Under the conditions (AF_ℓ), (AS_ℓ) and (AD_c), there exists a positive constant C, independent of I, c_f, c_b, H,*

and Δt, such that

$$\begin{aligned}\|E_{f,H}^{m+1}\|_H^2+\|E_{b,H}^{m+1}\|_H^2+\Delta t D_{c,0}\sum_{j=0}^{m}\|\nabla_H E_{f,H}^{j+1/2}\|_+^2 \le e^{(m+1)\Delta t\sigma_{b,f}}\left(\|E_{f,H}^0\|_H^2+\|E_{b,H}^0\|_H^2\right)\\ +\frac{C}{1-\Delta t\theta_{b,f}}e^{(m+1)\Delta t\sigma_{b,f}}\left(2\alpha_{b,f}\max_{j=0,\dots,m+1}\|E_{I,H}^j\|_H^2+\gamma_{b,f}\right),\end{aligned} \tag{3.162}$$

for $m=0,\dots,M-1$, $\Delta t\in(0,\Delta t_{c,0}]$, with $\Delta t_{c,0}$ defined by (3.160) and $H\in\Lambda$. In inequality (3.162)*, $\theta_{b,f}$, $\alpha_{b,f}$, $\sigma_{b,f}$ and $\gamma_{b,f}$ are defined by (3.158), (3.159), (3.161), (3.156), respectively.*

We remark that $\sigma_{b,f}$ depends on $\|I_H^m\|_\infty$, $m=0,\dots,M$. Considering the upper bound (3.146), we have successively

$$\begin{aligned}\|I_H^m\|_\infty^2 &\le 2\|E_{I,H}^m\|_\infty^2+2\|R_H I(t_m)\|_\infty^2\\ &\le \frac{2}{H_{min}^2}\|E_{I,H}^m\|_H^2+2\|R_H I(t_m)\|_\infty^2\\ &\le \frac{2}{H_{min}^2}C\left(\|E_{I,H}^0\|_H^2+H_{max}^4+\Delta t^4\right)+2\|R_H I(t_m)\|_\infty^2.\end{aligned}$$

Consequently, if $I_H^0\in B_{\rho_H}(R_I(0))$ with $\rho_H\le CH_{max}$, and the spatial grids $\overline{\Omega}_H$, $H\in\Lambda$, satisfy (3.105) we obtain

$$\|I_H^m\|_\infty^2\le 2CC_G\left(1+H_{max}^2+C_{G,sup}\Delta t^3\right)+\|R_H I(t_m)\|_\infty^2,$$

provided that the sequence Λ and the time stepsize Δt satisfy the following condition

$$\frac{\Delta t}{H_{max}^2}\le C_{G,sup}. \tag{3.163}$$

Corollary 3.4.4. *Under the assumptions of Theorems 3.4.1 and 3.4.2, there exists a positive constant C, independent of Δt and H, such that*

$$\|E_{I,H}^{m+1}\|_H^2+\Delta t D_{I,0}\sum_{j=0}^{m}\|\nabla_H E_{I,H}^{j+1/2}\|_+^2\le C\left(\|E_{I,H}^0\|_H^2+H_{max}^4\|I\|_{C^{4,0}(\overline{\Omega}_{I,\Lambda}\times[0,T])}^{2p_I}+\Delta t^4\gamma_T\right), \tag{3.164}$$

Moreover, if $I_H^0\in B_{\rho_H}(R_H I(0))$, with $\rho_H\le CH_{max}$, and the grids $\overline{\Omega}_H, H\in\Lambda$, satisfies the condition (3.105) and (3.163), then there exists a positive constant C such that

$$\begin{aligned}\|E_{f,H}^{m+1}\|_H^2+\|E_{b,H}^{m+1}\|_H^2+\Delta t D_{c,0}\sum_{j=0}^{m}\|\nabla_H E_{f,H}^{j+1/2}\|_+^2 \le C\Big(\|E_{f,H}^0\|_H^2+\|E_{b,H}^0\|_H^2\\ +\|E_{I,H}^0\|_H^2+H_{max}^4\|c_f\|_{C^{4,0}(\overline{\Omega}_{I,\Lambda}\times[0,T])}^{2p_c}+\Delta t^4\gamma_T\Big),\end{aligned} \tag{3.165}$$

for $m = 0,\dots,M-1$, $\Delta t \in (0,\Delta t_0]$ *with* $\Delta t_0 = \min\{\Delta t_{I,0}, \Delta t_{c,0}\}$. *In equations* (3.164)-(3.165), γ_T *is defined by*

$$\begin{aligned}\gamma_T =& C\left(H_{max}^4\left(\|I\|^{2p_I}_{C^{4,0}(\overline{\Omega}_{l,\Lambda}\times[0,T])} + \|c_f\|^{2p_c}_{C^{4,0}(\overline{\Omega}_{c,\Lambda}\times[0,T])}\right) + \Delta t^4\left[\|I\|_{\mathrm{C}^{0,3}} + \|c_f\|_{\mathrm{C}^{0,3}} + \|c_b\|_{\mathrm{C}^{0,3}}\right.\right.\\ &+\|\frac{\partial^2 c_f}{\partial t^2}\|^2_{\mathrm{C}^{2,0}}\left(\|c_f\|^2_{\mathrm{C}^{2,0}}\left(\|c_f\|^2_{\mathrm{C}^{2,0}}+1\right)+1\right) + \|\frac{\partial c_f}{\partial t}\|^2_{C^{1,0}} + \|c_b\|^2_{C^{0,2}}\|I\|^2_{C^{0,2}}\\ &\left.\left.\|\frac{\partial^2 I}{\partial t^2}\|^2_{\mathrm{C}^{2,0}}\left(\|I\|^4_{\mathrm{C}^{2,0}} + \|I\|^2_{\mathrm{C}^{2,0}}+1\right)\right]\right.\end{aligned}$$

■

We remark that the convergence rates depend on $\|E^0_{I,H}\|^2_H$ and $\|E^0_{f,H}\|^2_H + \|E^0_{b,H}\|^2_H$. To get the error estimate (3.165), we should have $\|E^0_{I,H}\|_H \le CH_{max}$. Moreover, to obtain convergence we should impose

$$\|E^0_{j,H}\|_H \le CH^2_{max}, \text{ for } j = I,f,b.$$

3.4.3 Concluding stability

To conclude the stability from Propositions 3.4.1 and 3.4.2, we need to prove that $\|\nabla_H I^m_H(\mu)\|_\infty$ and $\sigma_{f,b}(m)$ are uniformly bounded for $m = 1,\dots,M$ and $H \in \Lambda$. This boundedness follows from the next four statements:

1. There exists $\rho_{I,\varepsilon} > 0$ and $C_I > 0$ such that, for all $I^0_H \in B_{\rho_{I,\varepsilon}}(R_H I(0))$, we have

$$\|\nabla_H I^{m+1/2}_H\|^2_\infty \le C_I. \tag{3.166}$$

Proof: We have

$$\begin{aligned}\|\nabla_H I^{m+1/2}_H\|^2_\infty &\le 2\|\nabla_H E^{m+1/2}_{I,H}\|^2_\infty + 2\|\nabla_H R_H I^{m+1/2}\|^2_\infty\\ &\le \frac{2}{\Delta t H^2_{min}}\Delta t\sum_{j=0}^{m}\|\nabla_H E^{j+1/2}_{I,H}\|^2_+ + 2\|\nabla_H R_H I^{m+1/2}\|^2_\infty,\end{aligned}$$

and then, using the estimate (3.164), we deduce

$$\|\nabla_H I^{m+1/2}_H\|^2_\infty \le \frac{2}{\Delta t H^2_{min}} C\left(\|E^0_{I,H}\|^2_H + H^4_{max} + \Delta t^4\right) + 2\|\nabla_H R_H I^{m+1/2}\|^2_\infty. \tag{3.167}$$

Assuming that (3.105) and (3.163) hold and $I^0_H \in B_{\rho_{H,\Delta t}}(R_H I(0))$, with $\rho_H \le C\sqrt{\Delta t}H_{max}$, from (3.167) we obtain

$$\|\nabla_H I^{m+1/2}_H\|^2_\infty \le C\left(1 + C_G\frac{H^2_{max}}{\Delta t} + C_G C_{G,sup}\Delta t^2 + 2\|\nabla_H R_H I^{m+1/2}\|^2_\infty\right). \tag{3.168}$$

From (3.168), to conclude (3.166) we need to replace the condition (3.163) by the following new one

$$C_{G,inf} \le \frac{\Delta t}{H^2_{max}} \le C_{G,sup}, \tag{3.169}$$

where $C_{G,inf}$ and $C_{G,sup}$ are positive constants.

2. There exists $\rho_{\tilde{I},\varepsilon} > 0$ and $C_{\tilde{I}} > 0$ such that, for all $\tilde{I}_H^0 \in B_{\rho_{\tilde{I},\varepsilon}}(R_H I_H(0))$,

$$\|\tilde{I}_H^m\|_\infty \leq C_{\tilde{I}}. \tag{3.170}$$

Proof: We observe that

$$\begin{aligned}\|\tilde{I}_H^m\|_\infty^2 &\leq 2\|\omega_{I,H}^m\|_\infty^2 + 2\|I_H^m\|_\infty^2 \\ &\leq \frac{2}{H_{min}^2}\|\omega_{I,H}^m\|_H^2 + 2\|I_H^m\|_\infty^2.\end{aligned}$$

Before we proved that if $I_H^0 \in B_{\rho_H}(R_H I(0))$, with $\rho_H \leq CH_{max}$, and the spatial grids $\overline{\Omega}_H$, $H \in \Lambda$, satisfy (3.105) and (3.163), then $\|I_H^m\|_\infty^2 \leq C_I, m = 0,\ldots,M, H \in \Lambda$. Moreover, imposing that $I_H^0 \in B_{\rho_{H,\Delta t}}(R_H I(0))$, with $\rho_H \leq C\sqrt{\Delta t}H_{max}$, and (3.169) holds, we have (3.166). Then, from (3.122), we get

$$\frac{1}{H_{min}^2}\|\omega_{I,H}^m\|_\infty^2 \leq C\frac{1}{H_{min}^2}\|\omega_{I,H}^0\|_H^2.$$

Consequently, if $\tilde{I}_H^0 \in B_{\rho_H}(I_H^0)$, with $\rho_H \leq CH_{max}$, and by considering the condition (3.105) we conclude that (3.170) holds.

3. There exists $\rho_{f,\varepsilon} > 0$ and $C_f > 0$ such that, for all $c_{f,H}^0 \in B_{\rho_{f,\varepsilon}}(R_H c_f(0))$,

$$\|\nabla_H c_{f,H}^{m+1/2}\|_\infty^2 \leq C_f. \tag{3.171}$$

Proof: Following the proof of (3.166), we need to assume that $I_H^0 \in B_{\rho_{H,\Delta t}}(R_H I(0))$, $c_{f,H}^0 \in B_{\rho_{H,\Delta t}}(R_H c_f(0))$, $c_{b,H}^0 \in B_{\rho_{H,\Delta t}}(R_H c_b(0))$ with $\rho_{H,\Delta t} \leq C\sqrt{\Delta t}H_{max}$, and that (3.105), (3.169) hold.

4. There exists $\rho_{b,\varepsilon} > 0$ and $C_b > 0$ such that, for all $c_{b,H}^0 \in B_{\rho_{b,\varepsilon}}(R_H c_b(0))$,

$$\|c_{b,H}^m\|_\infty^2 \leq C_b. \tag{3.172}$$

The proof of this inequality is similar to the proof of (3.170).

The following result summarizes the previous conclusions:

Corollary 3.4.5. *Under the assumptions of Propositions 3.4.1 and 3.4.2 and Theorems 3.4.1, 3.4.2, if (3.105) and (3.169) hold, then (3.49)-(3.55) is stable in the solution* $I_H^m \in W_{I,H}^*, c_{f,H}^m \in W_{c,H}^*, c_{b,H}^m \in W_b(\overline{\Omega}_H - \overline{\Gamma}_{r,H})$ *of the IBVP* (3.49)-(3.55) *with the initial conditions* $I_H^0, c_{f,H}^0$ *and* $c_{b,H}^0$*, respectively, provided that and* $I_H^0 \in B_{\rho_{H,\Delta t}}(R_H I(0))$, $c_{f,H}^0 \in B_{\rho_{H,\Delta t}}(R_H c_f(0))$, $c_{b,H}^0 \in B_{\rho_{H,\Delta t}}(R_H c_b(0))$ *with* $\rho_{H,\Delta t} \leq C\sqrt{\Delta t}H_{max}$. ■

3.5 Numerical experiments

This section has two main objectives: to investigate the convergence properties of the scheme (3.26)-(3.32) using an IMEX method for time integration and considering the smooth and nonsmooth solutions in space, in addition, a comparison with the fully implicit and second-order Crank-Nicolson (CN) method is presented in this section.

We consider that the fully-discrete approximations $I_H^m \in W_{I,H}^*$, $c_{f,H}^m \in W_{c,H}^*$, $c_{b,H}^m \in W_b(\overline{\Omega}_H - \overline{\Gamma}_{r,H})$ are solution of the system

$$\begin{cases} \frac{1}{\beta} D_{-t} I_H^m = \nabla_H^* \cdot ((D_I(M_H I_H^m) \nabla_H I_H^{m+1})) + G(I_H^m) & \text{in } \overline{\Omega}_H - \overline{\Gamma}_{l,H}, \quad (3.173) \\ D_{-t} c_{f,H}^m = \nabla_H^* \cdot ((D_c(M_H c_{f,H}^m) \nabla_H c_{f,h}^{m+1})) + F(I_H^m, c_{f,H}^m, c_{b,H}^m) & \text{in } \overline{\Omega}_H - \overline{\Gamma}_{r,H}, \quad (3.174) \\ D_{-t} c_{b,H}^m = S(I_H^m, c_{f,H}^m, c_{b,H}^m) & \text{in } \overline{\Omega}_H - \overline{\Gamma}_{r,H}, \quad (3.175) \end{cases}$$

complemented by the following initial and boundary conditions

$$I_H^m = R_H I_i(t_m) \text{ on } \overline{\Gamma}_{H,l},\ \nabla_{c,H} I_H^m \cdot \eta = 0 \text{ on } (\partial\Omega_H - \overline{\Gamma}_{H,l}) \times (0,T], \quad (3.176)$$

$$c_{f,H}^m = 0 \text{ on } \overline{\Gamma}_{r,H} \times (0,T],\ \nabla_{c,H} c_{f,H}^m \cdot \eta = 0 \text{ on } (\partial\Omega_H - \overline{\Gamma}_{r,H}) \times (0,T]. \quad (3.177)$$

The system (3.173)-(3.177) defines an IMEX method that we use to approximate the solution of system (3.26)-(3.32).

By using the fictitious points we can state that $\nabla_H^* \cdot ((D_c(M_H c_{f,H}^m) \nabla_H c_{f,h}^{m+1}))$ is well defined in $\overline{\Omega}_H - \overline{\Gamma}_{H,l}$. Moreover, $\nabla_{c,H} I_H^m \cdot \eta$ is well defined in $\Gamma_{H,i}, i = u,r,d$ and in the corner points $(1,0)$ and $(1,1)$ where we consider two unitary normals: the vectors $e_1, -e_2$ and e_1, e_2, respectively, where $\{e_1, e_2\}$ is the canonical basis of $\mathbb{R}^2$. The same remarks hold for the discretizations of the free drug concentration.

System (3.173)-(3.177) can be established using the so-called Method of Lines approach: spatial discretization using finite difference operators, which allows us to replace the IBVP (3.1)-(3.8) by an ordinary differential problem, followed by a time integration using an IMEX approach to deal with the nonlinear terms. We discretize the nonlinear reaction terms ($G(\cdot)$, $S(\cdot)$, and $F(\cdot)$) and the nonlinear diffusion terms ($D_I(\cdot)$ and $D_c(\cdot)$) explicitly and the remaining terms implicitly. Following this approach, we can obtain the numerical approximation by solving a linear system at each time level. For instance, for the intensity light approximation I_H^{m+1}, we get the following matrix equation,

$$\frac{1}{\beta}\left(I_d - \Delta t A_H(I_H^m)\right) I_H^{m+1} = I_H^m + \Delta t (F_H(I_H^m) + G(I_H^m)), \quad (3.178)$$

where I_d is the identity matrix of order $N_1(N_2+1) \times N_1(N_2+1)$ and $A_H(I_H^m)$ is a tridiagonal block matrix.

We observe that we can fix Δt such that $\Delta t \|A_H\|_\infty < 1$. Consequently, $I_d - \Delta t A_H(I_H^m)$ is nonsingular and then, for each time level, there exists a unique solution of the linear system (3.178). Using similar arguments, we can guarantee that, for each time level, there exists a unique numerical free drug concentration.

To illustrate the convergence behaviour we introduce the following errors

$$\text{Error}_I^2 = \max_{m=1,\ldots,M} \|E_I^m\|_H^2 + \Delta t \sum_{k=1}^{m} \|\nabla_H E_I^k\|_+^2, \tag{3.179}$$

$$\text{Error}_{c_f}^2 = \max_{m=1,\ldots,M} \|E_{c_f}^m\|_H^2 + \Delta t \sum_{k=1}^{m} \|\nabla_H E_{c_f}^k\|_+^2, \tag{3.180}$$

$$\text{Error}_{c_b}^2 = \max_{m=1,\cdots,M} \|E_{c_b}^m\|_H, \tag{3.181}$$

where $E_I^m = R_H I(t_m) - I_H^m$, R_H is the restriction operator. Analogously, $E_{c_f}^m = R_H c_f(t_m) - c_{f,H}^m$ and $E_{c_b}^m = R_H c_b(t_m) - c_{b,H}^m$.

The numerical convergence rates are estimated by

$$\text{R}_{\ell,H} = \log_2\left(\frac{\text{E}_{\ell,H}}{\text{E}_{\ell,H/2}}\right),$$

for $\ell = I, c_f, c_b$. Here, $E_{\ell,H/2}$ represent the errors associated with the spatial mesh $H/2$ that we obtain from a mesh H by introducing in the intervals (x_i, x_{i+1}) and (y_j, y_{j+1}) the corresponding midpoints $x_{i+1/2}$ and $y_{j+1/2}$.

To illustrate the convergence behaviour of our method in time, we introduce $Error_{\Delta t,\ell}$, for $\ell = I, f, b$ defined by

$$\text{Error}_{\Delta t,I}^2 = \max_{m=1,\cdots,M} \|E_I^m\|_H, \tag{3.182}$$

$$\text{Error}_{\Delta t,f}^2 = \max_{m=1,\cdots,M} \|E_{c_f}^m\|_H, \tag{3.183}$$

$$\text{Error}_{\Delta t,b}^2 = \max_{m=1,\cdots,M} \|E_{c_b}^m\|_H, \tag{3.184}$$

and the corresponding convergence rates

$$\text{R}_{\ell,H}^{\Delta t} = \log_2\left(\frac{\text{E}_{\Delta t,\ell}}{\text{E}_{\Delta t/2,\ell}}\right), \tag{3.185}$$

for $\ell = I, f, b$.

Example 3.5.1. *Let us consider system* (3.1)-(3.3) *with initial-boundary conditions given by* (3.4)-(3.8)*, diffusion coefficients and reaction functions defined by* $D_{I,11} = D_{I,22} = I^2 + 0.1$*,* $D_{c,11} = D_{c,22} = 0.1c_f^2$*,* $G(I) = 2I^2 + I$*,* $S(I, c_f, c_b) = I^2 c_b^2 c_f$ *and* $F(I, c_f, c_b) = I^3 c_b c_f^2$*. Let us also add suitable source functions to the right-hand side of the equations* (3.1)-(3.3)*, such that the exact solution of this problem is*

$$
\begin{aligned}
I(x,y,z) &= 2t(2x-x^2)\frac{1}{\pi}\left(-(y-1)\cos(\pi y) + \frac{1}{\pi}\sin(\pi y)\right),\\
c_f(x,y,z) &= \exp(t)\left(\frac{1}{x^2+1} - \frac{1}{2}\right)\left(\frac{y^2}{2} + \frac{1}{\pi^2}(\pi y \sin(\pi y) + \cos(\pi y))\right),\\
c_b(x,y,z) &= 2\exp(t)\sinh(y)\frac{\cosh(10-x)}{\cosh(10)}.
\end{aligned}
$$

We solve the resulting system of differential equations using the method (3.173)-(3.177)*. We start with a random nonuniform spatial grid and define the sequence of grids by halving the step sizes. The time stepsize* Δt *is fixed,* $\Delta t \leq H_{\max}^2$*, consequently, the error induced by the time integration has a small contribution in the global error that will be dominated by the error in space. The total simulation time is* $T = 1$*. We give the errors and the estimated numerical convergence rates in Table 3.1.*

$H_{\max}$	N_1	N_2	Error_I	Rate_I	Error_{c_f}	Rate_{c_f}	Error_{c_b}	Rate_{c_b}
1.3429E-1	12	10	1.3552E-3	-	3.4017E-6	-	1.2989E-4	-
6.7143E-2	24	20	5.6034E-6	3.9590	1.1923E-7	2.4172	9.1878E-6	1.9107
3.3572E-2	48	40	3.6037E-7	1.9794	8.0611E-9	1.9433	6.2452E-7	1.9395
1.6786E-2	96	80	2.2647E-8	1.9960	5.2261E-10	1.9736	4.0505E-8	1.9733
8.3929E-3	192	160	1.4182E-9	1.9986	3.3268E-11	1.9868	2.5775E-9	1.9870
4.1965E-3	384	320	8.8726E-11	1.9993	2.0987E-12	1.9933	1.6255E-10	1.9935

Table 3.1 Space errors and convergence rates.

The results presented in Table 3.1 suggest that the spatial errors of I*,* c_f *and* c_b *have second order convergence. Note that by definition of the errors for* I *and* c_f*, equations (3.179) and (3.180), respectively, the second order accuracy holds not only for the numerical approximations* I_H^m *and* $c_{f,H}^m$*, but also for the numerical gradients* $\nabla_H I_H^m$ *and* $\nabla_H c_{f,H}^m$*. In Figure 3.3 we plot* I_H*,* $c_{f,H}$ *and* $c_{b,H}$ *at final time.*

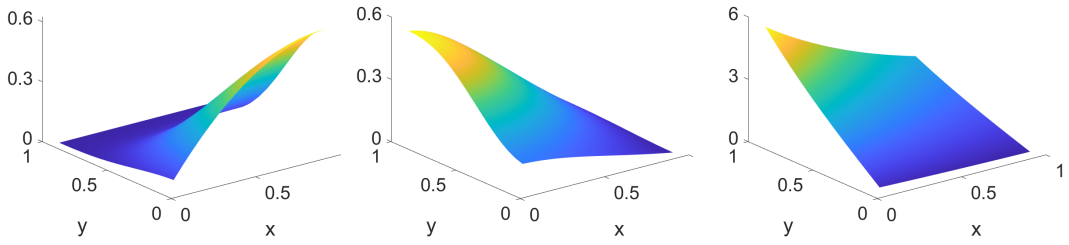

(a) I_H. (b) $c_{f,H}$. (c) $c_{b,H}$.

Fig. 3.3 Numerical solution for Example (3.5.1).

Example 3.5.2. *The goal of this example is to compare the convergence behaviour of the two methods for the differential problem* (3.1)-(3.3)*: the IMEX scheme* (3.173)-(3.177) *and the CN method, which is, theoretically, second order convergent in time.*

Let the diffusion coefficients and reaction functions defined by $D_{I,11} = D_{I,22} = 0.01I^2 + 1 \times 10^{-4}$, $D_{c,11} = D_{c,22} = c_f^4 + 1 \times 10^{-4}$, $G(I) = I^2$, $S(I, c_f, c_b) = I^2 c_b^2 c_f$ *and* $F(I, c_f, c_b) = I^3 c_f^2 c_b$*. Let us also add suitable source functions to the right hand side of the equations* (3.1)-(3.3)*, such that the exact solution of this problem is*

$$
\begin{aligned}
I(x,y,z) &= \exp(t)\left(-\frac{x^3}{3} - \frac{x^2}{2}\right)(-\cos(\pi y)),\\
c_f(x,y,z) &= \exp(t)(1-x^2)\left(-\frac{y^3}{3} + \frac{y^2}{2}\right),\\
c_b(x,y,z) &= \exp(t)x^2y^2\sin(\pi y^2)\sin(\pi x^2).
\end{aligned}
$$

We fix $N_1 = N_2 = 100$ *and successively halve the time step. To evaluate the performance in time of the mentioned methods, we use the equations* (3.182)-(3.185) *for the numerical errors and convergence rates. Table* (3.2) *and* (3.3) *illustrate the results obtained with the IMEX method and CN method, respectively. The results suggest that the IMEX method has first order convergence while the CN method has second order convergence. In Figure 3.4 we present the approximation* $I_H, c_{f,H}$ *and* $c_{b,H}$ *using the CN method.*

Δt	$\text{Error}_{\Delta t,I}$	Rate_I	$\text{Error}_{\Delta t,c_f}$	Rate_{c_f}	$\text{Error}_{\Delta t,c_b}$	Rate_{c_b}
5.0E-1	3.5967E-2	-	4.1233E-2	-	4.0470E-2	-
2.50E-1	1.8542E-2	0.95587	2.1034E-2	0.97106	2.6208E-2	0.62684
1.250E-1	9.2611E-3	1.0015	1.0487E-2	1.0042	1.4217E-2	0.88236
6.25E-2	4.6192E-3	1.0036	5.2284E-3	1.0041	7.3463E-3	0.95255

Table 3.2 Error on time for IMEX method.

Δt	$\text{Error}_{\Delta t,I}$	Rate_I	$\text{Error}_{\Delta t,c_f}$	rate_{c_f}	$\text{Error}_{\Delta t,c_b}$	Rate_{c_b}
5.0E-1	1.1326E-3	-	1.3120E-5	-	1.0118E-5	-
2.50E-1	5.5360E-5	2.1773	8.8022E-7	1.9489	6.3143E-7	2.0010
1.250E-1	3.1752E-6	2.0619	5.6698E-8	1.9782	3.9436E-8	2.0005
6.25E-2	1.6873E-7	2.1170	3.7257E-9	1.9638	2.4635E-9	2.0003

Table 3.3 Error on time for CN method.

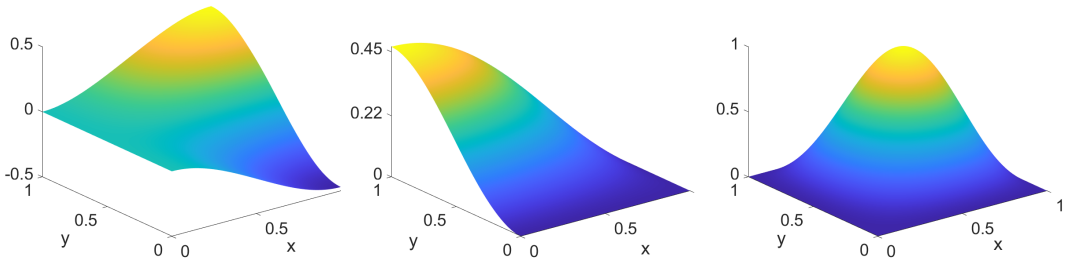

(a) I_H. (b) $c_{f,H}$. (c) $c_{b,H}$.

Fig. 3.4 Numerical solution for Example (3.5.2) using CN method.

Example 3.5.3. *In the present chapter we do not study if low regularity can affect convergence. However, one may wonder if something similar to what was studied in Chapter 2 also holds for the system* (3.1)-(3.3) *with initial-boundary conditions given by* (3.4)-(3.8). *This example is intended to give a clue to the answer to that question. Let the diffusion coefficients and reaction functions be defined by* $D_{I,11} = D_{I,22} = I+1$, $D_{c,11} = D_{c,22} = c_f^2+1$, $G(I) = I$, $S(I,c_f,c_b) = Ic_b^2c_f$ *and* $F(I,c_f,c_b) = Ic_bc_f$. *For the fixed data, we consider* (3.1)-(3.3) *with convenient source terms such that this IBVP as the following solution*

$$
\begin{aligned}
I(x,y,z) &= 2t(2x-x^2)\frac{1}{\pi}\left(-(y-1)\cos(\pi y)+\frac{1}{\pi}\sin(\pi y)\right),\\
c_f(x,y,z) &= \exp(t)(x^3-x^2)\left(\frac{y^3}{3}-\frac{y^2}{2}\right)|x-0.5|^{\alpha},\\
c_b(x,y,z) &= \exp(t)xy\sin(\pi y)\sin(\pi x),
\end{aligned}
$$

for $x \in \Omega, t \in (0,T]$. *We remark that, for* $\alpha = 2.1$, $c_f \in H^2(\Omega)$, *in contrast, for* $\alpha = 3.1$ *we have* $c_f \in H^3(\Omega)$. *Table 3.4 and 3.5 illustrate the convergence rates for each of the variables. Notice that for the case of the rate* $\text{Rate}_{c_f,H}$ *we have second order convergence rate for the value* $\alpha = 3.1$ *(Table 3.5) and only first order convergence rate for* $\alpha = 2.1$ *(Table 3.4).*

$H_{\max}$	N_1	N_2	Error_I	Rate_I	Error_{c_f}	Rate_{c_f}	Error_{c_b}	Rate_{c_b}
1.000E-1	10	10	2.8990E-5	-	5.2886E-8	-	1.4787E-6	-
5.000E-2	20	20	1.8312E-6	1.9924	1.3695E-8	0.97462	9.1431E-8	2.0077
2.500E-2	40	40	1.1192E-7	2.0161	3.7220E-9	0.93975	5.7390E-9	1.9969
1.250E-2	80	80	6.8539E-9	2.0147	9.3061E-10	0.99992	3.5845E-10	2.0005
6.250E-3	160	160	4.2312E-10	2.0089	2.1886E-10	1.0441	2.2328E-11	2.0024
3.125E-3	320	320	2.6269E-11	2.0048	4.9678E-11	1.0697	1.3861E-12	2.0049

Table 3.4 Space errors and convergence rates for the case $\alpha = 2.1$.

This example suggests that the method's convergence order (in space) can depend on the theoretical solution regularity.

$H_{\max}$	N_1	N_2	Error$_I$	Rate$_I$	Error$_{c_f}$	Rate$_{c_f}$	Error$_{c_b}$	Rate$_{c_b}$
1.000E-1	10	10	2.8990E-5	-	9.2469E-9	-	1.4794E-6	-
5.000E-2	20	20	1.8312E-6	1.9924	9.1735E-10	1.6667	9.1528E-8	2.0073
2.500E-2	40	40	1.1192E-7	2.0161	7.3440E-11	1.8214	5.7511E-9	1.9961
1.250E-2	80	80	6.8539E-9	2.0147	5.1920E-12	1.9111	3.5992E-10	1.9990
6.250E-3	160	160	4.2312E-10	2.0089	3.4588E-13	1.9540	2.2503E-11	1.9998
3.125E-3	320	320	2.6269E-11	2.0048	1.4590E-14	1.9835	1.2813E-12	1.9999

Table 3.5 Spacial errors and convergence rates for $\alpha = 3.1$.

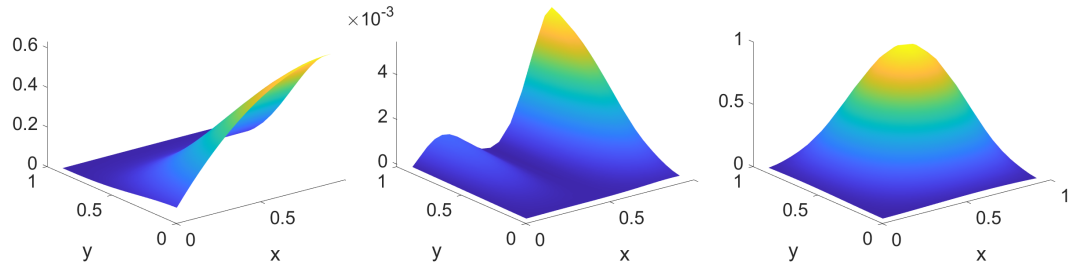

(a) I_H. (b) $c_{f,H}$. (c) $c_{b,H}$.

Fig. 3.5 Numerical solution for Example (3.5.3) for $\alpha = 2.1$.

Chapter 4

Drug delivery enhanced by light

4.1 Beer-Lambert Law

In this section, we deal with the mathematical modeling of light-triggered drug delivery, a research area with applications in cancer treatment. We focus our discussion on a near-infrared (NIR) light-triggered drug delivery from hydrogels. NIR light-responsive hydrogels are considered ideal candidates for drug delivery. On one hand, NIR light is safe and allows deep penetration into human tissues. On the other hand, hydrogels are highly biocompatible and highly tunable, i.e., drug release can be easily controlled by changing hydrogel properties and light parameters like intensity, duration, and wavelength ([21, 24–29]).

In vivo experiments involving cancer treatment using NIR light-responsive hydrogels are promising. For instance, in [26], such type of therapy led to a significant reduction of tumors in nude mice when compared to control groups. However, as stated by the authors, the translation to human clinical trials requires further investigations concerning the design of more efficient hydrogels. Mathematical modeling and simulation can make a significant contribution to this effort. A reliable mathematical simulation tool is a cheap and fast way to find the light- and hydrogel-related parameters combination that gives the desired drug release profile.

Now, we present the drug delivery mathematical model that motivated us to study a numerical scheme for the system (2.1)-(2.4). Let us consider a one-dimensional domain $\Omega = (a,b)$, containing a NIR-responsive hydrogel with bound drug particles that we denote by c_b (g/cm^3). When exposed to NIR light irradiation, the photocleavage of the hydrogel leads to the release of the bound drug c_b. The released free drug c_f (g/cm^3) diffuses by Fick's law to the surrounding medium.

Let I (W/cm^2) be the NIR light intensity and ϕ (cm^2/(Wmin)) the conversion rate of bound drug c_b to free drug c_f. The evolution of c_b is governed by

$$\frac{\partial c_b}{\partial t} = -\phi I c_b, \quad \text{in } \Omega \times (0,T]. \tag{4.1}$$

Let D (cm^2/min) be the free drug diffusion coefficient. The evolution of c_f is governed by

$$\frac{\partial c_f}{\partial t} = D\frac{\partial^2 c_f}{\partial x^2} + \phi I c_b, \quad \text{in } \Omega \times (0,T], \tag{4.2}$$

which is a classical Fick's diffusion equation with an additional right-hand-side term that takes into account the unbinding reaction described by equation (4.1). Note that system (4.1),4.2 is a particular case of the general system (2.1)-(2.4). For the mathematical description of NIR light intensity I we use the Beer-Lambert law

$$I(x) = I_0 \exp(-\beta x), \quad x \in \overline{\Omega}, \tag{4.3}$$

where I_0 (W/cm^2) is the known incident light intensity at $x = a$ and β (1/cm) is the attenuation coefficient.

In the following, we investigate if the motivational model (4.1)-(4.3) is adequate to reproduce the laboratory experiment reported in [26]. The experimental setup consists of a PBS (Phosphate-Buffered Saline) solution containing a NIR light-responsive hydrogel loaded with the chemotherapy drug doxorubicin. To simulate this experiment we consider the spatial domain $\overline{\Omega} = [0,1]$ (cm), representing the PBS solution, being the hydrogel located at $0 \leq x \leq 0.05$. In Figure 4.1, we give an illustration of our computational setup. Initially, all the drug is bound to the hydrogel then, we consider the initial

Fig. 4.1 Computational 1D domain. The blue line indicates the location of the drug-loaded hydrogel and the arrow indicates the direction of the light source.

conditions

$$c_b(x,0) = C_0, \quad 0 \leq x \leq 0.05,$$
$$c_b(x,0) = 0, \quad 0.05 < x \leq 1,$$

for the bound drug c_b, with $C_0 = 1$ the normalized initial drug concentration, and

$$c_f(x,0) = 0, \quad 0 \leq x \leq 1,$$

for the free drug. We also consider no-flux boundary conditions for c_f.

The authors of [26] irradiated the PBS solution with NIR light and measured the drug release rate from the hydrogel. To test the responsiveness of the hydrogel, this type of experiment was repeated using different configurations, like, incident light intensity, hydrogel composition, and drug concentration. Here, we focus on the experiment that analyzed the impact of changing light intensity on the drug release rate. Three different intensities were tested, $I_0 = 0.5, 1.0, 1.5$. To replicate the experiment, we proceed as follows. First, based on the literature [69, 70], we set the drug diffusion coefficient D at 3×10^{-4}, then, using the experimental data obtained with $I_0 = 0.5$, we found the best-fit values for the parameters β and ϕ. In Table 4.1, we give the parameters values. Second, to validate the model, we calculated the simulated drug release rate from the hydrogel with the incident

Symbol	Variable	Value	Units
β	Attenuation coefficient	4×10^{-3}	1/cm
ϕ	Conversion rate	3×10^{-2}	cm^2/(W min)
D	Diffusion coefficient	3×10^{-4}	cm^2/min

Table 4.1 Model parameters values used in the numerical simulations.

light intensities $I_0 = 1.0, 1.5$ and compared it against the experimental data. To solve the model (4.1)-4.3 we used the fully discrete scheme (2.24)-(2.27) with the uniform space step $h = 5 \times 10^{-4}$ and the time step $\Delta t = 1 \times 10^{-3}$.

The release rate (%) at time t is given by the amount of free drug c_f in the PBS solution at time t divided by the initial ($t = 0$) amount of bound drug c_b in the hydrogel. In Figure 4.2, we show the results of our simulation. Overall, one can say that there is a relatively good agreement between experimental (circles) and simulated data (solid line). For the case $I_0 = 1$, Figure 4.2 on the left,

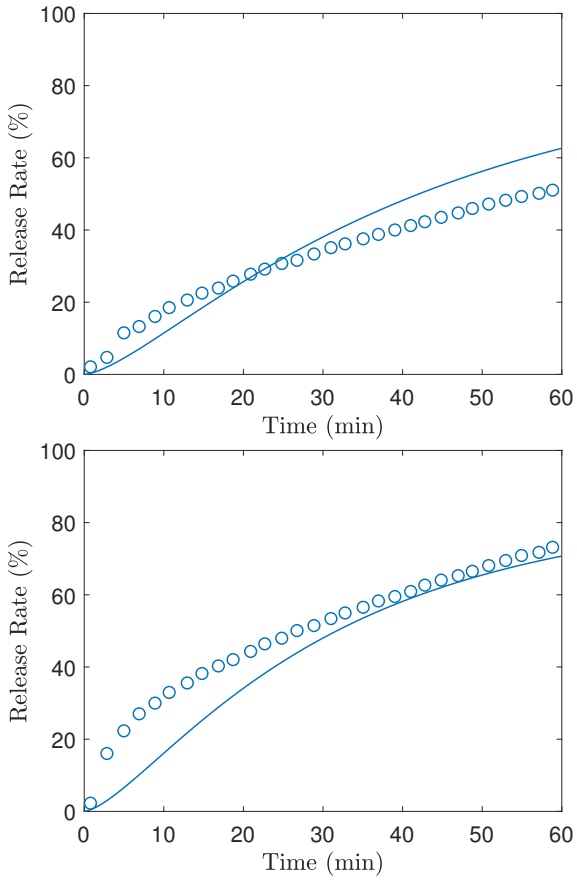

Fig. 4.2 Release rate of free drug c_f with $I_0 = 1\,(\text{W/cm}^2)$ (on the left) and with $I_0 = 1.5\,(\text{W/cm}^2)$ (on the right). The experimental data are plotted in solid circles and the simulation data in solid lines.

the simulated release rate closely follows the experimental data until the 30 (min) mark. Afterward, the simulated values being to deviate from the experimental ones, with the model over-predicting the release rate. For the case $I_0 = 1.5$, Figure 4.2 on the right, the model initially under-predicts the

release rate, but after the 30 (min) mark, the simulated release rate closely follows the experimental one.

$I_0\,(\mathrm{W/cm^2})$	Experimental $t_n = 60\,(\mathrm{min})$	Numerical $t_n = 60\,(\mathrm{min})$	Absolute Error $t_n = 60\,(\mathrm{min})$	Mean Absolute Error
1	51.04%	62.44%	11.40%	5.86%
1.5	73.17%	70.50%	2.67%	6.68%

Table 4.2 Quantitative evaluation of the numerical simulation results.

To obtain a more precise quantification of the error between the numerical and the experimental data, we present in Table 4.2 two metrics: the absolute error in the release rate at the end of the simulation and the mean absolute error, defined by,

$$\text{Mean Absolute Error} = \frac{1}{n}\sum_{i=1}^{n} |r_h(t_i) - r^*(t_i)|,$$

where n is the number of experimental observations and $r_h(t_i)$ and $r^*(t_i)$ are the numerical and the experimental release rate at time t_i, $i = 1,\ldots,n$, with $t_1 = 0$ and $t_n = 60$. The values obtained indicate that the mathematical model performs better for the case $I_0 = 1.5$ than for the case $I_0 = 1$, the absolute error at the end of the simulation is significantly lower, 2.67% versus 11.40%, and the mean absolute error is only slightly higher, 6.68% versus 5.86%. Based on the available data, it is difficult to conclude that this difference in the model performance is only due to the change in incident light intensity I_0. We would need more experimental data, maybe with varied values of I_0, to draw further conclusions.

Considering both cases ($I_0 = 1$ and $I_0 = 1.5$), we have an average absolute error of 7.04% and an average mean absolute error of 6.27%. Given the simplicity of the mathematical model (4.1)-(4.3) and the one-dimensional setting, errors of this order of magnitude are reasonable. To improve the results, we could, e.g., consider a three-dimensional domain, replace the Beer-Lambert approximation (4.3) with the more accurate parabolic diffusion approximation, and account for hydrogel erosion during NIR light irradiation.

	$\Delta t = 1\times10^{-3}$		$\Delta t = 1\times10^{-4}$	
h	Mean Absolute Error	Deviation	Mean Absolute Error	Deviation
5×10^{-4}	5.863%	-	5.863%	$< 0.001\%$
2.5×10^{-4}	5.817%	0.046%	5.818%	0.045%
1.25×10^{-4}	5.797%	0.066%	5.797%	0.066%
6.25×10^{-5}	5.787%	0.076%	5.788%	0.075%

Table 4.3 Mesh sensitivity analysis for the case $I_0 = 1(\mathrm{W/cm^2})$.

We also perform a mesh sensitivity analysis to ensure that the experimental results are independent of the space-time mesh used. For this study, we solved again the case $I_0 = 1$ over refined space-time meshes. In Table 4.3 we show the mean absolute error on the new meshes and also his deviation from the one obtained with the space-time mesh that we used in the previous numerical simulation,

$h = 5 \times 10^{-4}$ and $\Delta t = 1 \times 10^{-3}$. The values show that the experimental results are reliable since the deviation in the mean absolute error is consistently lower than 0.1%. We can obtain a similar conclusion for the case $I_0 = 1.5$.

4.2 Controlled Transdermal Drug Delivery

4.2.1 Introduction

Transdermal drug delivery is an attractive area of research due to the recognized skin potential as a viable alternative to the traditional oral or parenteral routes. The main advantages of transdermal delivery are the possibility of direct drug application close to the target site, the bypass of drug metabolic transformations that occur in the gastrointestinal tract, and a noninvasive and self-administration format that improves patient compliance. The main drawback of transdermal delivery is the low permeability of the stratum corneum, the skin's outermost layer. The lipid structure in the stratum corneum acts as a barrier that has limited transdermal delivery to drugs with moderate lipid solubility, drugs with small molecular weight, or low-dosage drugs.

However, recently developed strategies, like the application of ultrasound waves, have the power to disrupt the stratum corneum, enhancing drug absorption through the skin. In ultrasound permeation, the disruption of the stratum corneum is due to the ultrasound-induced oscillation of endogenous gas bubbles, a phenomenon known as acoustic cavitation. Other permeation strategies include iontophoresis, microneedles, and thermal ablation. The application of drug micro-carriers to enhance skin penetration is also usual, and liposomes, carbon nanotubes, and gold or polymeric nanoparticles are some of the options available. These drug carriers can even be designed to bind to specific receptors located in the target cells, promoting drug accumulation in the target site [1, 71–73].

Recent clinical trials have shown that transdermal drug delivery is a promising therapy option for some cancers, such as localized skin and breast cancers. For the particular case of breast cancer, a recent trial sought to compare the usual oral administration of the chemotherapeutic agent 4-hydroxytamoxifen (4-OHT), in the tablet form of Tamoxifen, with the transdermal administration of 4-OHT in gel form. The clinical data revealed that the concentration level of 4-OHT in cancer tissue was similar in both groups. However, the oral administration of Tamoxifen leads to the spiking of 4-OHT concentration in the blood, which can have serious systemic side effects, such as the risk of venous thromboembolic events. Therefore, this clinical trial showed that transdermal delivery was superior to the traditional oral route [74].

Immunomodulation, a technique based on manipulating immune responses to an antigen, is another fascinating research topic where transdermal delivery has a central role. The skin is particularly appealing for this purpose due to very active immune mechanisms with several tissue-resident immune cells. The skin is also easy to access and has connections with many organs. Cancer vaccines and the treatment of viral, infections, and autoimmune diseases are among the targets of transdermal immunomodulation [75]. For example, oral administration of immunosuppressive agents is the standard therapy for psoriasis, one of the most common skin inflammation disorders. Oral administration is effective, but since it does not target the psoriasis sites, it is associated with the risk of systemic side effects. In [76], the authors used a transdermal hydrogel formulation containing the

immunosuppressant agent Tacrolimus in a psoriasis-induced mouse model. The topical formulation showed no signs of toxicity, and the results indicate that the therapy can be efficient in psoriasis treatment.

So far, we have seen that localized drug delivery achieved by transdermal delivery is vital to avoid systemic side effects caused by high-toxicity drugs. Controlled release is the other crucial feature of a state-of-the-art delivery system. This ability is mandatory to keep drugs within their optimal therapeutic window, i.e., above the minimum therapeutic level and below the maximum safe concentration value. In transdermal delivery, we get controlled release using stimuli-responsive carriers that release the drug only when excited by internal or external stimuli like temperature or near-infrared (NIR) light [71–73].

One experiment concerned with controlled transdermal delivery is described in [77]. Here, the authors used a NIR light-responsive transdermal system to treat superficial mice bearing breast tumors. For this purpose, they encapsulated the chemotherapeutic anti-cancer drug Doxorubicin (DOX) in a polymeric structure containing NIR light-sensitive nanoparticles and placed it over the target site. The NIR light protocol consisted of a short laser-on period given once every three days. After 7 days, the transdermal-treated mice showed complete tumor eradication without adverse side effects. After 50 days, there was no tumor recurrence. All the untreated mice were dead within 16 days. Traditionally DOX is given intravenously or directly injected into the target site. Compared with transdermal delivery, these approaches represent a more invasive procedure with higher systemic and local toxicity since higher doses of DOX are required. These findings show that controlled transdermal delivery could be an effective treatment option for superficial cancers.

This brief overview shows how transdermal delivery can revolutionize many established therapies. Easy access, a non-invasive format, and local and controlled delivery are some of the properties that make transdermal delivery a state-of-the-art technology. The rest of this work focuses on NIR light-controlled transdermal delivery (NIRTDD). NIRTDD is a popular choice because NIR light is reasonably safe for human tissues and parameters like intensity and duration are easily adjustable. NIR-responsive drug carriers are also relatively simple to design, with a wide range of photoresponsive materials available [78]. The dynamics of NIRTDD consist of two main processes: drug release from the transdermal patch triggered by NIR light and drug diffusion through the skin until systemic absorption in the skin network capillarity.

Assume that the engineers have developed a perfect NIRTDD system loaded with a very effective drug for a specific condition. According to the pharmacologist, the drug's optimal therapeutic window is reached with an absorption rate of 0.04/h (a.u.). Everything appears to be in place for a successful treatment, but the medical team faces one question: what NIR light protocol do I need to prescribe for this goal absorption rate? What is the intensity and length of the pulse? What is the recommended number of laser-on cycles? The answer is complex and depends on several factors, including the material responsiveness to NIR light and drug diffusivity in the skin. It may be possible to discover the answer through a series of time-consuming and perhaps costly laboratory studies. We aim to solve this problem using mathematical simulation, a considerably faster and less expensive alternative.

Transdermal drug delivery is a multidisciplinary field with numerous research topics. The literature on the subject is vast, and it covers various aspects such as coated or swellable drug carriers [79, 80], electric- or nanoparticle-mediated delivery [81, 82], and accurate geometric representation of relevant

skin structures like the stratum corneum [83, 84]. These studies follow a similar pattern, with the derived mathematical models being essentially used to analyze drug release profiles under various combinations of the model's parameters.

For instance, in [79], the authors derive a diffusion model for studying drug release from coated multilayer drug carriers. The interest in such materials stems from their intriguing properties like increased stability, extended sustainable drug release, and good protection against chemical aggression. Drug release profiles for various critical parameters such as device geometry and coating resistance are computed and analyzed for discussion.

A coupled diffusion-deformation model to study transdermal drug delivery from liquid swellable drug carriers is presented in [80]. One of the interests in these materials lies in controlling the drug release rate by manipulating the swelling properties of the drug carrier. The rationale is that liquid-induced swelling allows faster movement of drug molecules, resulting in increased drug release. Analysis of drug release profiles confirms this reasoning, but the increase in release reaches a plateau when swelling doubles the drug carrier's initial weight.

Despite some intriguing findings, the practical utility of these models is limited. For example, in the context of [79], how should a drug carrier be designed to replicate a target drug release profile? In the absence of an optimization procedure, the only option is to use a trial-and-error approach covering all possible model parameter combinations. In this sense, our work goes a step further, allowing us to find the optimal NIR light protocol behind a target drug absorption profile.

The next sections are organized as follows: in the next section 4.2.2, we validate a two-dimensional mathematical model that governs the dynamics of NIRTDD, namely, light propagation, bound to free drug conversion due to NIR light irradiation, and free drug transport through the skin. Section 4.2.3, is dedicated to the NIR light protocol optimization. The proposed approach relies on an optimization problem where the goal is to minimize the mismatch between target and simulated drug absorption profiles and where the minimization variables are suitable NIR light protocol parameters.

4.2.2 A Mathematical Model for NIRTDD

As illustrated in Figure 4.3, the proposed computational domain is of multilayer type, including the polymeric drug carrier and three skin layers: viable epidermis, where we find the stratum corneum, followed by dermis and hypodermis. To model NIRTDD, we use three equations, one for each of the three main variables, NIR light intensity and bound and free drug concentration.

Let $\Omega \times [0,T]$ represent the spatial-temporal domain. We denote by c_b mg/cm^3, c_f mg/cm^3, respectively, the bound and free drug concentration, and by I W/cm^2 the light intensity, i.e., the photon fluence rate. We assume that the dissociation of the bound drug c_b from the carrier is triggered by NIR light-cleavage of chemical bonds at a rate proportional to the light intensity I. Let us also assume that Fick's law for diffusion is valid. Then, the bound drug is governed by the equation

$$\frac{\partial c_b}{\partial t} = -\phi I c_b, \quad (x,y) \in \Omega, 0 < t \leq T, \tag{4.4}$$

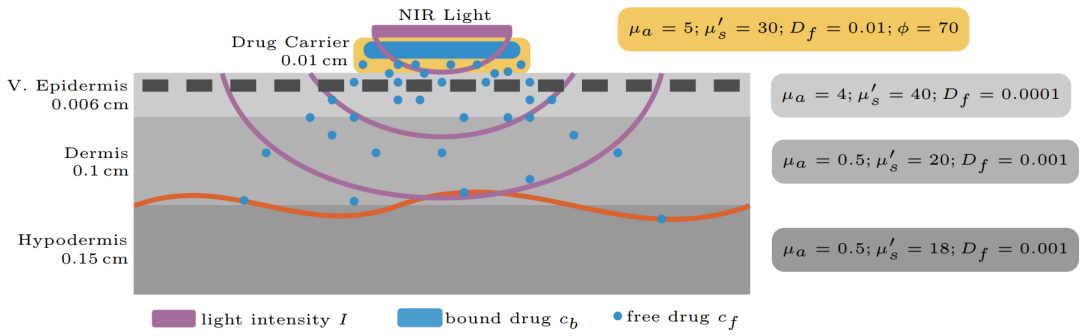

Fig. 4.3 Schematic representation, not in scale, of the computational multilayer domain and the main simulation parameters, namely: thickness cm, light attenuation μ_a cm^{-1}, light scattering $\mu_s^{'}$ cm^{-1}, free drug diffusion D_f cm^2/h, and conversion rate of bound to free drug ϕ cm^2/Wh. The values adopted for thickness, optical parameters, and drug diffusion are based on the data available in [1–5], and [1, 2, 6–8], respectively. The brick-like structure in the viable epidermis represents the stratum corneum, and the horizontal line represents the skin microvessels. By action of NIR light intensity I, the bond drug c_b in the drug carrier is converted into free drug c_f, which diffuses through the skin until systemic absorption in the skin microvessels.

where ϕ cm^2/Wh is the conversion rate of bound to free drug, and the free drug is governed by the equation

$$\frac{\partial c_f}{\partial t} = \nabla \cdot (D_f \nabla c_f) + \phi I c_b, \quad (x,y) \in \Omega, 0 < t \leq T, \tag{4.5}$$

where D_f cm^2/h is the drug diffusion coefficient.

Light propagation is governed by the elliptic equation

$$-\nabla \cdot (D_I \nabla I) + \mu_a I = 0, \quad (x,y) \in \Omega, 0 \leq t \leq T, \tag{4.6}$$

which arises from the diffusion approximation to light transport. Here, $D_I = (3(\mu_a + \mu_s'))^{-1}$ cm is the light diffusion coefficient, with μ_a 1/cm the attenuation coefficient and μ_s' 1/cm the reduced scattering coefficient.

We consider the boundary conditions from chapter 3 for light intensity and free drug. However, we extended the computational domain to ensure that the boundary conditions do not affect light propagation. At the initial time, no free drug is in the system,

$$c_f(x,y,0) = 0, \quad (x,y) \in \Omega,$$

and all the bound drug is in the drug carrier Ω_{DC} at a normalized concentration of

$$c_b(x,y,0) = 1, \quad (x,y) \in \Omega_{DC}.$$

Equations (4.4)-(4.6) are well-accepted options for describing the underlying processes, and several other authors used similar equations in various contexts [85–87]. The values of the main parameters are given in Figure 1.

To discretize the system of equations (4.4)-(4.6) in space, we apply the second-order finite difference scheme presented in Chapter 3. In time, we use the implicit BDF2 (Backwards Differentiation Formula 2) method sequentially: first, we solve (4.6), then (4.4), and finally (4.5). The BDF2 is a two-step method, and whenever required, we used the implicit Euler method for initialization.

For the following simulations, the time step and the mesh step size were fixed at $\Delta t = 0.05h$ and $h = 2.5 \times 10^{-4} cm$. We found these values using mesh sensitivity analysis, as described in the following section.

Next, we validate the NIRTDD model (4.4)-(4.6) against experimental data.

Drug Diffusion: we start the validation of our methodology with the free drug diffusion model. For now, we ignore the light intensity contribution, and we assume that the drug in the polymeric patch is free to diffuse through the skin. That is, we consider only equation (4.5) without the light intensity-related term. The goal is to verify if the free drug diffusion equation and the transdermal computational domain in Figure 4.3 can describe the drug dynamics through the skin layers. To validate our model, we compare our simulations against the laboratory results reported in [88]. In this paper, the authors performed in vitro penetration experiment of drug molecules in extraneous skin. Following the experiment protocol, we placed a probe in the dermis at a skin depth of 0.017 cm and measured the evolution of the drug concentration at this point during a 10 h period.

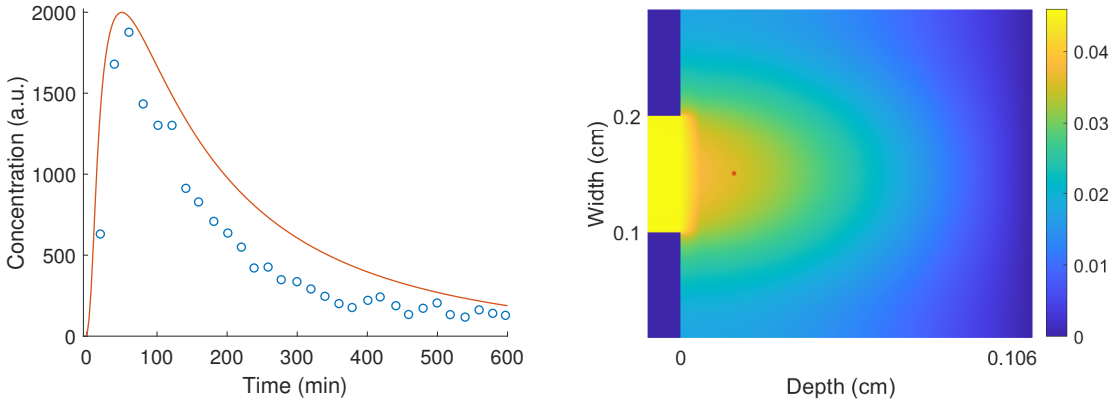

Fig. 4.4 On the left: free drug concentration-time profile at a skin depth of 0.017 cm; solid line stands for the numerical simulation results, while the dots refer to experimental data. On the right: surf plot of the normalized free drug c_f concentration at the 300 min time point. The dot marks the location of the probe in the dermis at a depth of 0.017 cm.

Figure 4.4 on the left shows the experimental data in dots. We observe a rapid rise in concentration until the peak around the 80min mark, followed by a slower decay. Due to the high diffusivity ($D_f = 0.01 cm^2/h$), the drug is quickly released from the patch, creating a concentration plume with a very sharp front and a relatively short tail. The viable epidermis's much lower diffusivity ($D_f = 0.0001 cm^2/h$) acts as a barrier, smoothing and delaying the concentration plume. The plume front becomes less sharp, and the tail lengthens, giving rise to the experimental data shape shown in Figure 4.4 on the left.

The simulation data is also displayed in Figure 4.4 on the left as a solid line. Overall, one can say that there is a good agreement between simulation and experimental data, with the simulation

capturing the main dynamics, quick rise in concentration until the 80min mark, followed by a slower decay. In particular, the model accurately captures the concentration peak and the concentration profile after the 400min mark. During the 150 to 400min time interval, a difference between numerical and experimental data is observed, with the model predicting a slightly higher concentration.

Drug Cleavage Mediated by NIR Light: the second validation step deals with the NIR light cleavage of the drug-polymer linkages with the subsequent drug release by diffusion. Here, we need to consider the full model, i.e., equation (4.6) for light intensity, equation (4.4) for bound drug, and equation (4.5) for free drug. For the validation, we consider the laboratory experiment described in [68]. The authors study the responsiveness of a drug-loaded polymeric structure that is sensitive to NIR light. They used an 808 nm laser and four on/off laser cycles, each cycle consisting of 3min of irradiation followed by an off period of 30min. They measured the amount of drug released from the polymer during the duration of the experiment. The results revealed that the drug was released step-wise, triggered by the laser-on period and with no noticeable release during the laser-off period.

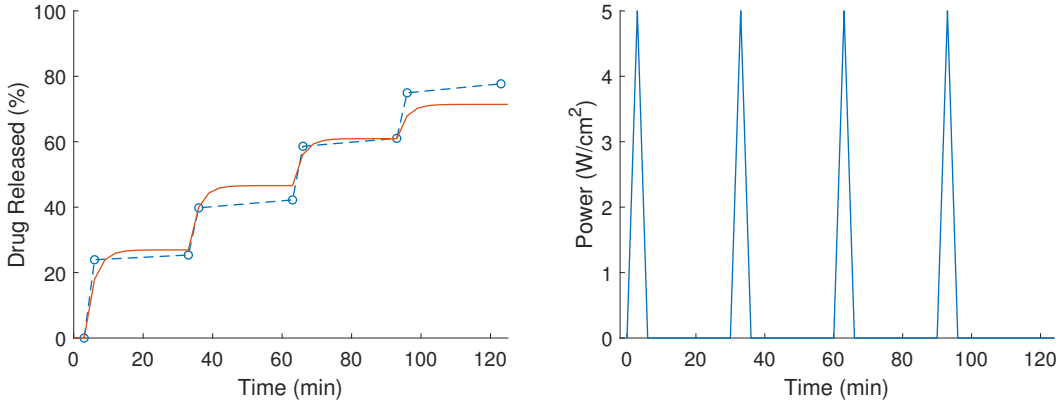

Fig. 4.5 On the left: experimental (dashed-dotted line) versus computational (solid line) cumulative drug release from the polymeric carrier. On the right: intensity-time profile of the laser source. Note the direct relationship between the jumps in the cumulative drug release and the laser-on periods.

For the simulation, and following [68], we use a light source with the time profile shown in Figure 4.5 on the right. It consists of four on/off cycles where each on cycle has 3 min of irradiation with a power of 5 W/cm^2 followed by an off period of 30 min. The light source is located at the middle top of the polymeric drug patch (see Figure 4.3) and has a uniform line shape with a width of 0.1 cm. By trial and error, we found the best fit value ϕ (the conversion rate of bound to free drug) to be 70 cm^2/W. The comparison between experimental and numerical data given in Figure 4.5 reveals a good fit by the model. The percentage of drug release during each laser irradiation period is identical to the experimental one. By the end of the simulation, the total amount of drug released was 70%, relatively close to the experimental data of 78%.

We give in Figure 4.6 the contour plot of the normalized light intensity (%) during a laser-on period. At the dermis-hypodermis interface, at a depth of 0.106 cm, the normalized light intensity is 17%, meaning that light intensity has decreased by more than 80%. The light intensity at the end of the hypodermis, at a depth of 0.256 cm, is around 1%, revealing that we have a light penetration depth of around 0.25 cm. This level of penetration in light-tissue interaction is similar to the results reported in the literature [89]. Note that the drug patch is optically similar to the viable epidermis

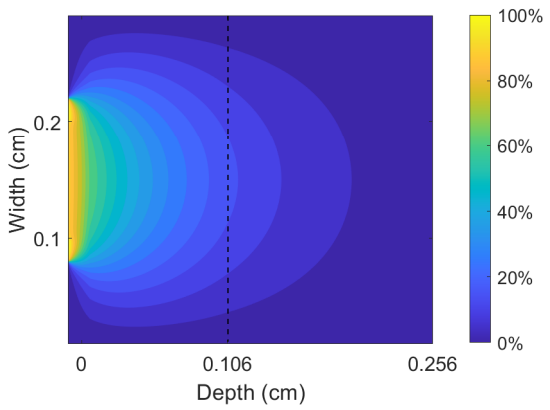

Fig. 4.6 Contour plots of incident light intensity (%) with a beam-width of 0.1 cm (on the left) and a power of 5 W/cm^2. The vertical dashed line marks the interface between dermis and hypodermis.

(see Figure 4.3), so it is reasonable that our results are close to the ones obtained in pure light-tissue interactions. In the following simulations, the light source is located at the middle top of the polymeric drug patch and has a uniform line shape with a width of 0.1 cm, as described in this section.

Remark 4.2.1. *To test the sensitivity of the numerical scheme to mesh parameters, we solved the previous experiment using a computational mesh featuring two times more spatial points. For the percentage of drug released, the maximum and mean absolute differences were 0.321% and 0.254%. These results should carry over to the following experiments, keeping our numerical solutions within an acceptable tolerance error.*

Remark 4.2.2. *Some discrepancies between experimental and simulated data observed in Figures 4.4 and 4.5 are related to model simplifications. For example, we assume free drug concentration continuity at each interface between two adjacent layers instead of a more realistic partition condition translating the observed concentration jumps [10]. Also, in the experiment in Figure 4.5, NIR light-induced drug release is accompanied by polymer melting as the temperature rises, and we neglected these phenomena in our model. On the other hand, the goal of this section was the model validation and not the model fitting to these particular experiments. For the simulation in Figure 4.4, for example, we did not adjust the dimensions of the skin layers to the experimental ones. Overall, the results of this section indicate that the model is valid and has reasonable accuracy.*

4.2.3 Optimizing the NIR Light Protocol

Which NIR light protocol should we use given a target drug absorption profile? As detailed in the section Introduction, the success of any NIRTDDD treatment is dependent on the answer to this question. Next, we propose and investigate the feasibility of a computational approach to this challenge.

To reduce complexity, we assume that a NIR light protocol consists of several identical cycles characterized by three parameters: the laser power, Lp, the laser-on period, Lo, and the laser-off period, Lf. In Figure 4.7, we give a schematic representation of this standardized protocol.

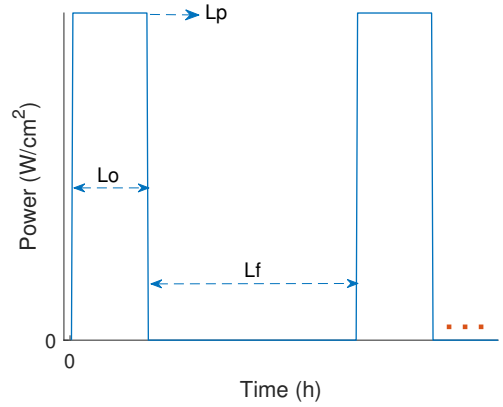

Fig. 4.7 Schematic representation of the standardized light protocol used in the present study. The shape of the light protocol can be characterized by three parameters, laser power Lp W/cm^2, laser-on period, Lo h, and laser-off period, Lf h.

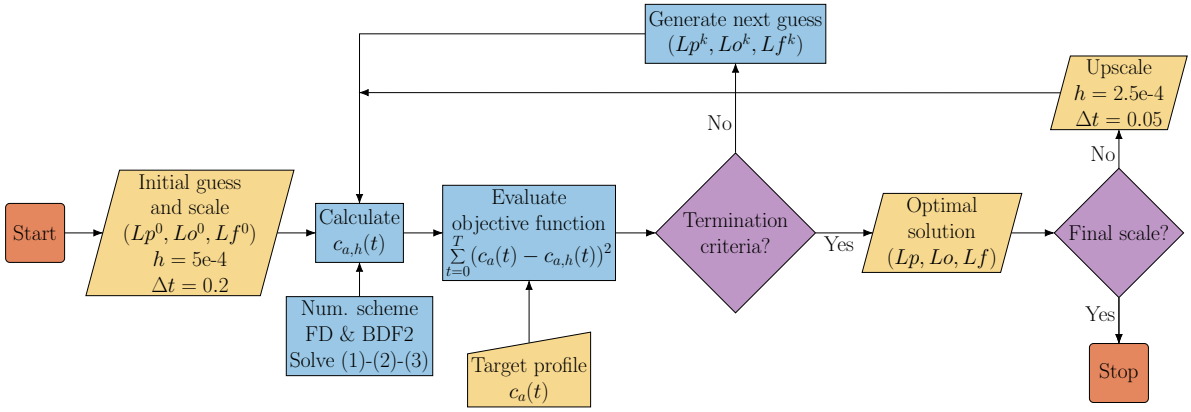

Fig. 4.8 Flowchart of the proposed optimization methodology.

Our goal is to find the light protocol defined by the parameters (Lp, Lo, Lf) such that the associated simulated drug absorption profile, obtained by solving the NIRTDD model (4.4)-(4.6), is in some sense similar to a target drug absorption profile. In particular, we seek to minimize the square of the difference between the profiles, and we formulate the following minimization problem

$$\min_{Lp,Lo,Lf} \quad \sum_{m=0}^{M+1} (c_a(t_m) - c_{a,h}^m)^2$$

with $t_{M+1} = T$ the total simulation time, $c_{a,h}^m$ the simulated drug absorption profile at time t_m, and $c_a(t_m)$ the target absorption drug profile at time t_m.

To solve the minimization problem, we used an implementation of the classic Nelder-Mead downhill simplex algorithm [90].

The minimization algorithm makes successive educated guesses of the parameters (Lp, Lo, Lf) until it finds the combination, i.e., the light protocol, that satisfies a given stopping criteria. For each algorithm iteration we need to solve the NIRTDD model (4.4)-(4.6) to get the simulated drug absorption profile $c_{a,h}^m$. Note that in (4.4)-(4.6) the light protocol is represented by the source term

s in the light equation (4.6). To speed up the minimization process, namely the numerical solution of system (4.4)-(4.6), we employed a multiscale approach, where the optimal solution obtained with the mesh $h = 5 \times 10^{-4}$ cm and the time step $\Delta t = 0.2$ h is used as starting point for the space-time mesh $h = 2.5 \times 10^{-4}$ cm and $\Delta t = 0.05$ h. In Figure 4.8 we give a flowchart with an overview of the proposed optimization methodology.

Next, we test our strategy against two target profiles. We chose two examples with opposing outcomes. The first one illustrates our strategy's good performance and the second its limitations.

Experiment 1: let us consider the target drug absorption profile

$$c_a(t) = 4t, \quad t \in [0, 24]\text{h},$$

represented by a dashed line in Figure 4.9 on the right. In this 24 h target profile, 96% of the drug is absorbed into the systemic circulation at a constant rate of 4 %/h. From a clinical perspective, this profile is convenient to administer drugs that require slow and sustained absorption. We find this need in immunosuppression therapies [91] and in cases of systemic toxicity due to high drug concentration [92].

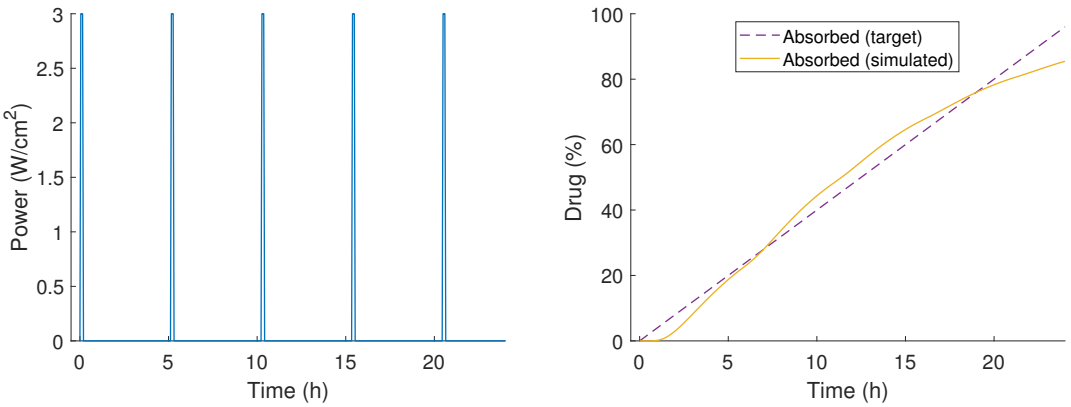

Fig. 4.9 On the left: optimized light protocol with four irradiation periods of 9 min (Lo) with a laser power of 3 W/cm^2 (Lp) followed by a laser-off period of 5.15 h (Lf). On the right: time evolution of drug (%) absorbed into the systemic circulation; target profile, dashed line, and simulated profile, solid line.

After running our optimization, we found the optimal parameters

$$(Lp, Lo, Lf) = (3\,\text{W/cm}^2, 9\,\text{min}, 5.15\,\text{h}),$$

corresponding to the NIR light protocol shown in Figure 4.9 on the left. This light protocol originates the simulated absorption profile of Figure 4.9 on the right. Visually, the agreement between target and simulation profiles is good, as confirmed by a mean absolute error of only 3.471%. A more detailed comparison also reveals that simulation absorption percentages of 30% after 7 h and 70% after 18 h are in line with the target values. Nevertheless, some discrepancies are still present, reflected in a simulated final absorption of 85% against a target of 96%.

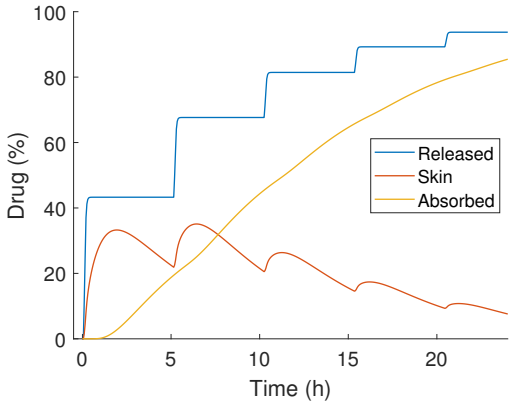

Fig. 4.10 Time evolution of drug (%) released from the polymer, in the skin, and absorbed into the systemic circulation.

In Figure 4.10 we give the time evolution of the three main drug profiles: released, in the skin, and absorbed. The release profile shows that this protocol cleaves the drug in a step-wise fashion. The first laser-on period cleaves around 40% of the drug from the polymeric carrier while the second one, 5.15 h later, releases around 25%. The release percentage surpasses 90% by the end of the simulation. This gradual drug release gives rise to the desired steady and constantly increasing absorption profile. The evolution of the drug in the skin reaches a maximum of 35% around the 1 h time point. Afterward, due to absorption, it decreases until the next laser-on period at the 5 h time point. This dynamic repeats for each laser cycle keeping the percentage of drug in the skin in the interval 8-35%.

Experiment 2: in our second experiment, we consider the target drug absorption profile

$$c_a(t) = 100\sqrt{(t/24)}, \quad t \in [0,24]\text{h},$$

represented with a dashed line in Figure 4.11 on the right. This target profile spans 24 h, and 100% of the drug enters the systemic circulation at a non-constant rate of the order of $1/\sqrt{t}$. This absorption rate is particularly higher in the first few hours, leading to a target absorption of 50% after only 6 h. This absorption profile is convenient to administer drugs that require quick absorption. We find this need in tissue repair therapies [93] and in skin irritation responses [94].

Our optimization algorithm returned the optimal parameters

$$(Lp, Lo, Lf) = (4\,\text{W/cm}^2, 27\,\text{min}, 0\,\text{h}),$$

We note that a value $Lf = 0$ means that we have a single laser-on period, as revealed in Figure 4.11 on the left, where the corresponding NIR light protocol is shown. In Figure 4.11 on the right, we give the corresponding simulated drug absorption profile. There are clear discrepancies between simulated and target profiles, particularly during the initial hours, with the simulated absorption showing a time lag. Nevertheless, as desired, the drug is still quickly absorbed, achieving the target absorption rates of 50% after 6 h and 80% after 19 h. Overall, a mean absolute error of 7.291% can still be considered a relatively small value.

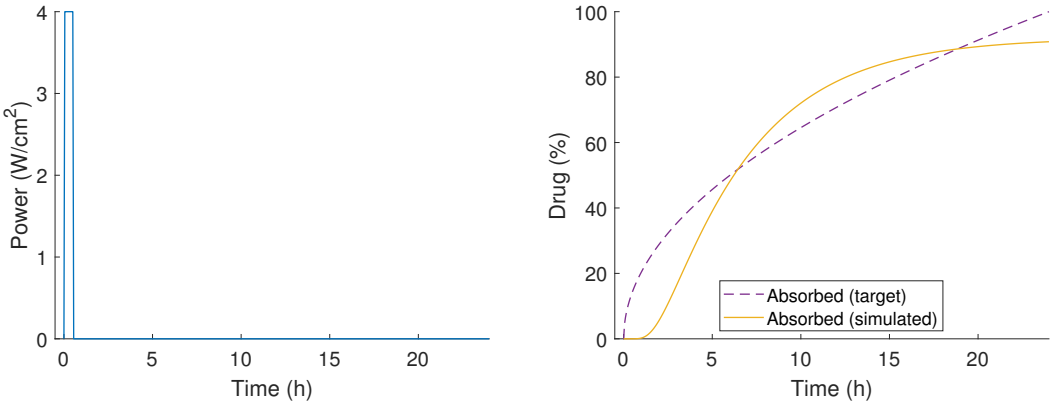

Fig. 4.11 On the left: optimized light protocol with a single irradiation period ($Lf = 0$) of 27 min (Lo) with a laser power of 4 W/cm^2 (Lp). On the right: time evolution of drug (%) absorbed into the systemic circulation; target profile, dashed line, and simulated profile, solid line.

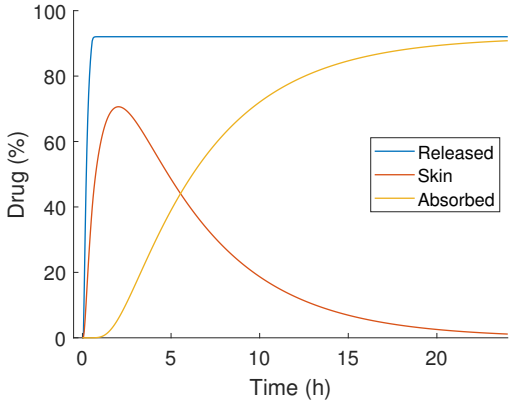

Fig. 4.12 Time evolution of drug (%) released from the polymer, in the skin, and absorbed into the systemic circulation.

In Figure 4.12, we show the time evolution of drug released, drug in the skin, and drug absorbed. The drug dynamics in this experiment are fast, the release is over 90% in less than 1 h, and in less than 2 h, 70% of the drug is in the skin ready to be absorbed. Then, as desired, absorption will occur at a fast pace. By the 10 h time point, the amount of drug in the skin is already less than 18%, and it will drop to less than 3% during the next 10 h.

Discussion

We test our framework with two target absorption profiles motivated by real-life drug therapies. Overall the simulated drug absorption profile was in close agreement with the target profile. The average mean absolute difference between the two experiments was 5.381%. This is a relatively low value, but it may be too high for some drugs with a very narrow therapeutic window. Future work can address some weaknesses of our methodology. For instance,

- NIR light irradiation is known to raise skin temperature and enhance drug diffusion. The addition of this thermal effect to the model would boost its flexibility. For example, it could reduce the initial time lag observed in the simulations. This time lag corresponds to the time

the drug takes to cross the skin by passive diffusion alone. Note that this modification would introduce additional equations and non-linear relations in the NIRTDD model.

- microneedles are an enhancement technique that can be more straightforwardly incorporated into our model. This technique consists of painless micron-sized needles designed to pierce the stratum corneum, delivering the drug directly into the dermis. The bypass of the stratum corneum barrier would allow the simulation of a broader range of drugs.

- other enhancers, such as ultrasound or electric fields, can be added into the model [1, 95]. These enhancers induce a convective drug transport, which increases the model flexibility by allowing the combination of both passive diffusion and convective transport.

- the standardized light protocol can be made more flexible by allowing e.g., laser-on periods with non-constant duration and power. This will increase the number of parameters in the protocol, which would bring additional optimization challenges.

- since drug molecules also interact with light, a more realistic model would make light intensity I dependent on bound drug c_b and free drug c_f. This dependency would appear on equation (4.6) through the optical parameters μ_a and μ_s'.

At last, we refer that in all tests, we used the initial guess $Lp = 1$ W/cm^2, $Lo = 12$ min, and $Lf = 5$ h, and the average execution time was 15 min, suggesting that the optimization procedure is robust and relatively fast. The execution time can be improved by using a non-uniform mesh and by implementing a numerical scheme with a variable time step procedure.

Conclusions

The primary goal of this work was to study numerical methods for systems of partial differential equations that describe drug release from light-responsive hydrogels when the links between the drug particles and the polymeric chains are of the photochemical type. The breakage of these links occurs due to energy absorption.

In Chapter 2: Beer-Lambert approach for light, we consider the Beer-Lambert law to describe the light propagation through the polymeric structure and the IBVP (2.1)-(2.4) for drug release modeling. We start this chapter by studying the semi-discrete approximation defined by (2.6)-(2.9). We analyze stability and convergence in section 2.3 and we prove convergence results considering smooth and nonsmooth solutions in section 2.3.1 and 2.3.2, respectively. We establish the stability and convergence of the IMEX method (2.20)-(2.23) in section 2.4.1.

In Chapter 3: Diffusion approximation for light, we study the IBVP (3.1)-(3.8) from numerical point of view. This system can be used to model drug release from a hydrogel when the light scattering is the dominant phenomenon. Consequently, we can describe light propagation with the diffusion equation (3.1). Section 3.3 is devoted to the stability and convergence analysis of the semi-discrete approximation (3.26)-(3.32). The main results are Proposition 3.3.2 and Theorems 3.3.1 and 3.3.2. We point out that the convergence result, Theorem 3.3.2, is established for smooth solutions. We study the Crank-Nicolson method (3.49)-(3.55) in section 3.4, where we prove stability and convergence: Propositions 3.4.1 and 3.4.2 and Theorems 3.4.1 and 3.4.2.

In Chapter 4: Drug delivery enhanced by light, we use our mathematical tools to simulate light-triggered drug release in two scenarios: drug release from a hydrogel and transdermal drug delivery. The simulation results are compared to in vitro data from [26], for the first scenario, and from [68] for the transdermal drug delivery. We investigate the efficacy of different light protocols to deliver drugs through the skin, using light to control the drug release from a polymeric patch.

To conclude this work, we present some future research directions. Concerning mathematical modeling, a detailed description of all phenomena involved in drug delivery controlled by light requires more realistic and complex differential systems. We mention, for instance, the effect of hydrogel erosion on light attenuation and drug release from the polymeric matrix. The light-induced breakage of the photosensitive bonds of light-responsive hydrogels originates degradation products. On the one hand, those products can increase light attenuation, but degradation causes polymer erosion, which reduces light attenuation. To model this scenario, we can consider a Beer-Lambert law that accounts for the concentration of all the photoactive species, including bound and free drugs ([34]).

Hydrogel erosion also creates a moving front problem and a drug concentration discontinuity. While the bound drug remains trapped with an unchanged initial concentration, the free drug diffuses,

giving rise to concentration jumps. In this case, it would be necessary to track the erosion front and impose appropriate interface conditions for drug concentration through the interface ([96, 97]).

When we consider the polymeric platform in contact with the biological target, the binding and unbinding of free drug to biological tissue occurs. Therefore, we should couple the set of equations introduced before for the drug in the hydrogel with a mathematical description of the behavior of the free drug in the target tissue. In fact, the binding of the free drug to the target, particularly its penetration depth, is critical information about the therapeutic response.

In this work, we consider that the drug release from the polymeric carrier is caused by photochemical processes. However, drug release via thermochemical processes is also reported in experimental literature. To describe the drug release in this scenario, we should take into account the heat propagation and heat effect on the drug transport and on the conversion of bond to free drug. If we consider that hydrogels and live tissues are viscoelastic materials, to describe the drug release from the hydrogel and its transport to the target its crucial to consider the heat impact in both tissues.

For simplicity, in this work, the radiative transfer equation (1.1) is replaced by its diffusion approximation (1.6). However, in a more general setting, we should couple the drug dynamics with the differential system (1.3)-(1.4). This coupling leads to significant challenges, which we would like to address in future research.

Concerning the numerical analysis, the main convergence results proved in Chapter 3 are Theorem 3.4.1 and Theorem 3.4.2, where smoothness of the solution of the IBVP (3.1)-(3.8) is required. In the near future, we would like to study the weakness of these assumptions considering the approach considered for instance in [41] for elliptic problems with Dirichlet boundary problems.

References

[1] J. Ferreira, P. de Oliveira, L. Pinto, Aging effect on iontophoretic transdermal drug delivery, SIAM Journal on Applied Mathematics 80 (2020) 1882–1907. doi:10.1137/19M1247188.

[2] H. Todo, Transdermal permeation of drugs in various animal species, Pharmaceutics 9 (2017) 33. doi:10.3390/pharmaceutics9030033.

[3] H. Takeuchi, M. Ishida, A. Furuya, H. Todo, H. Urano, K. Sugibayashi, Influence of skin thickness on the in vitro permeabilities of drugs through sprague-dawley rat or yucatan micropig skin, Biol. Pharm. Bull 35 (2012) 192–202. doi:10.1248/bpb.35.192.

[4] J. Wang, C. Xu, H. Xiong, Y. Han, A. M. Nilsson, M. Strömberg, T. Edvinsson, G. A. Niklasson, Extraction of backscattering and absorption coefficients of magnetite nanosphere composites from light scattering measurements: Implications for optomagnetic sensing, ACS Appl. Nano Mater 3 (2020) 11172–11183. doi:10.1021/acsanm.0c02309.

[5] J. Araújo, A. Monte, R. Lora-Serrano, W. Iwamoto, A. Antunes, O. Brener, M. Foschini, On the quantitative optical properties of au nanoparticles embedded in biological tissue phantoms, Opt. Mater 114 (2021). doi:10.1016/j.optmat.2021.110924.

[6] F. Marquet, M.-C. Grandclaude, C. C. E. Ferrari, Capacity of an in vitro rat skin model to predict human dermal absorption: Influences of aging and anatomical site, Toxicol. In Vitro 61 (2019). doi:10.1016/j.tiv.2019.104623.

[7] C. A. Ellison, K. O. Tankersley, C. M. Obringer, G. J. Carr, J. Manwaring, H. Rothe, H. Duplan, C. Géniès, S. Grégoire, N. J. Hewitt, C. J. Jamin, M. Klaric, D. Lange, A. Rolaki, A. Schepky, Partition coefficient and diffusion coefficient determinations of 50 compounds in human intact skin, isolated skin layers and isolated stratum corneum lipids, Toxicology in Vitro 69 (2020) 104990. doi:10.1016/j.tiv.2020.104990.

[8] L. Wu, P. Shrestha, M. Iapichino, Y. Cai, B. Kim, B. Stoeber, Characterization method for calculating diffusion coefficient of drug from polylactic acid (PLA) microneedles into the skin, Journal of Drug Delivery Science and Technology 61 (2021) 102192. doi:10.1016/j.jddst.2020.102192.

[9] A. Belamkar, A. Harris, R. Zukerman, B. Siesky, F.Oddone, A. Vercellin, T. A. Ciulla, Sustained release glaucoma therapies: Novel modalities for overcoming key treatment barriers associated with topical medications, Ann Med. 54 (2022) 343–358. doi:10.1080/07853890.2021.1955146.

[10] M. N. Yasin, D. Svirskis, A. Seyfoddin, I. D. Rupenthal, Implants for drug delivery to the posterior segment of the eye: A focus on stimuli-responsive and tunable release systems, Journal of Controlled Release (2014) 208–221doi:10.1016/j.jconrel.2014.09.030.

[11] A. Ernst, J. Bulum, New generation of drug-eluting stents - a brief review, EMJ European Medical Journal 1 (2014) 100–106. doi:10.33590/emjintcardiol/10312250.

[12] P. N. Navya, A. Kaphle, S. Srinivas, S. Bhargava, V. Rotello, H. Daima, Current trends and challenges in cancer management and therapy using designer nanomaterials, Nano Convergence 6 (2019) 23. doi:10.1186/s40580-019-0193-2.

[13] D. Rosenblum, N. Joshi, W. Tao, J. Karp, D. Peer, Progress and challenges towards targeted delivery of cancer therapeutics, Nature Communications 9 (2018) 1410. doi:10.3390/pr9091527.

[14] S. Senapati, A. Mahanta, S. Kumar, P. Maiti, Controlled drug delivery vehicles for cancer treatment and their performance, Signal Transduction and Targeted Therapy 3 (2018) 7. doi:10.1038/s41392-017-0004-3.

[15] R. Kalaydina, K. Bajwa, B. Qorri, A. Decarlo, M. Szewczuk, Recent advances in "smart" delivery systems for extended drug release in cancer therapy, International journal of nanomedicine 13 (2018) 4727–4745. doi:10.2147/IJN.S168053.

[16] S. Hossen, M. Hossain, M. Basher, M. Mia, M. Rahman, M. Uddin, Smart nanocarrier-based drug delivery systems for cancer therapy and toxicity studies: A review, Journal of Advanced Research 15 (2019) 1–18. doi:10.1016/j.jare.2018.06.005.

[17] J. Ferreira, D. Jordão, L. Pinto, Approximating coupled hyperbolic-parabolic systems arising in enhanced drug delivery, Computers & Mathematics with Applications 76 (2018) 81–97. doi:10.1016/j.camwa.2018.04.005.

[18] Y. Shamay, A. Lily, A. Gonen, D. Ayelet, Light induced drug delivery into cancer cells, Biomaterials 32 (2011) 1377–1386. doi:10.1016/j.biomaterials.2010.10.029.

[19] C. Wells, M. Harris, L. Choi, V. Murali, F. Guerra, J. Jennings, Stimuli-responsive drug release from smart polymers, Journal of Functional Biomaterials 10 (2019) 34. doi:10.3390/jfb10030034.

[20] Y. Wang, D. Kohane, External triggering and triggered targeting strategies for drug delivery, Nature Reviews Materials 2 (2017) 17020. doi:10.1038/natrevmats.2017.20.

[21] A. Kasiński, E. O. M. Z.-Pisklak, M. Sobczak, Smart hydrogels - synthetic stimuli-responsive antitumor drug release systems, International Journal of Nanomedicine 15 (2020) 4541–4572. doi:10.2147/IJN.S248987.

[22] Y. Ji, J. Li, J. Zhao, S. Shand, C.-C. Chu, A light-facilitated drug delivery system from a pseudoprotein/hyaluronic acid nanocomplex with improved anti-tumor effects, Nanoscale 11 (2019) 9987–10003. doi:10.1039/C9NR01909J.

[23] M. Tang, D. Svirskis, E. Leung, M. Kanamala, H. Wang, Z. Wu, Can intracellular drug delivery using hyaluronic acid functionalised ph-sensitive liposomes overcome gemcitabine resistance in pancreatic cancer?, Journal of Controlled Release 305 (2019) 89–100. doi:10.1016/j.jconrel.2019.05.018.

[24] I. Tomatsu, K. Peng, A. Kros, Photoresponsive hydrogels for biomedical applications, Advanced Drug Delivery Reviews 63 (2011) 1257–1266. doi:10.1016/j.addr.2011.06.009.

[25] H. Kim, H. Lee, K.-Y. Seong, E. Lee, S. Yang, J. Yoon, Visible light-triggered on-demand drug release from hybrid hydrogels and its application in transdermal patches, Advanced Functional Materials 4 (2015) 2071–2077. doi:10.1002/adhm.201500323.

[26] M. Qiu, D. Wang, W. Liang, L. Liu, Y. Zhang, X. Chen, D. Sang, C. Xing, Z. Li, B. Dong, F. Xing, D. Fan, S. Bao, H. Zhang, Y. Cao, Novel concept of the smart NIR-light-controlled drug release of black phosphorus nanostructure for cancer therapy, Proceedings of the National Academy of Sciences 115 (2018) 501–506. doi:10.1073/pnas.1714421115.

[27] Y. Tao, H. Chan, B. Shi, M. Li, H. Leong, Light: A magical tool for controlled drug delivery, Advanced Functional Materials 30 (2020) 2005029. doi:10.1002/adfm.202005029.

[28] T. Rappa, C. DeForest, Targeting drug delivery with light: a highly focused approach, Advanced Drug Delivery Reviews 171 (2021) 94–107. doi:10.1016/j.addr.2021.01.009.

[29] X. Wang, Z. Xuan, X. Zhu, H. Sun, J. Li, Z. Xi, Near-infrared photoresponsive drug delivery nanosystems for cancer photo-chemotherapy, Journal of Nanobiotechnology 18 (2020) 108. doi:10.1186/s12951-020-00668-5.

[30] W. Zhang, T. Ji, Y. Li, Y. Zheng, M. Mehta, C. Zhao, A. Liu, D. Kohane, Light-triggered release of conventional local anesthetics from a macromolecular prodrugfor on-demand local anesthesia, Nature Communications 11 (2020) 2323. doi:10.1038/s41467-020-16177-w.

[31] J. Siepmann, F. Siepmann, Mathematical modeling of drug delivery, International Journal of Pharmaceutics 364 (2008) 328–343. doi:10.1016/j.ijpharm.2008.09.004.

[32] A. Ishimaru, Wave Propagation ans Scattering in Random Media, Academic Press, 1978.

[33] D. Griffin, J. Patterson, A. Kasko, Photodegradation as a mechanism for controlled drug delivery, Biotechnology and Bioengineering 107 (2010) 1012–1019. doi:10.1002/bit.22882.

[34] M. Tibbitt, A. Kloxin, K. Anseth, Modeling controlled photodegradation in optically thick hydrogels, Journal of Polymer Science 51 (2013) 1899–1911. doi:10.1002/pola.26574.

[35] O. I., S. J., Beer-lambert law for optical tissue diagnostics: current state of the art and the main limitations, J Biomed Opt. 26 (10) (2021). doi:10.1117/1.JBO.26.10.100901.

[36] L. Wang, H. Wu, Biomedical Optics: Principles and Imaging, 1st Edition, John Wiley & Sons, 2007.

[37] W. Sun, Z. Sun, Finite difference methods for a nonlinear and strongly coupled heat and moisture transport system in textile materials, Numerische Mathematik 120 (2012) 153–187. doi:10.1007/s00211-011-0402-3.

[38] L. Chen, Y. Chen, Two-grid method for nonlinear reaction-diffusion equations by mixed finite element methods, Journal of Scientific Computing 49 (2011) 383–401. doi:10.1007/s10915-011-9469-3.

[39] E. Toro, A. Hidalgo, ADER finite volume schemes for nonlinear reaction-diffusion equations, Applied Numerical Mathematics 59 (2009) 73–100. doi:10.1016/j.apnum.2007.12.001.

[40] C. Michoski, A. Alexanderian, C. Paillet, E. Kubatko, C. Dawson, Stability of nonlinear convection-diffusion-reaction systems in discontinuous galerkin methods, Journal of Scientific Computing 70 (2017) 516–550. doi:10.1007/s10915-016-0256-z.

[41] J. Ferreira, R. Grigorieff, Supraconvergence and supercloseness of a scheme for elliptic equations on nonuniform grids, Numerical Functional Analysis and Optimization 27 (2006) 539–564. doi:10.1080/01630560600796485.

[42] J. Ferreira, D. Jordão, L. Pinto, Second order approximations for kinetic and potential energies in maxwell's wave equations, Applied Numerical Mathematics 120 (2017) 125–140. doi:10.1016/j.apnum.2017.05.005.

[43] J. Ferreira, L.Pinto, G.Romanazzi, Supraconvergence and supercloseness in Volterra equations, Applied Numerical Mathematics 62 (2012) 1718–1739. doi:10.1016/j.apnum.2012.06.028.

[44] U. Ascher, S. Ruuth, B. Wetton, Implicit-explicit methods for time-dependent partial differential equations, SIAM Journal on Numerical Analysis 32 (1995) 797–823. doi:10.1137/0732037.

[45] S. Ruuth, Implicit-explicit methods for reaction-diffusion problems in pattern formation, Journal of Mathematical Biology 34 (1995) 148–176. doi:10.1007/BF00178771.

[46] A. Zarzur, H. C. Velho, S. Freitas, S. Stephany, Combined explicit and implicit methods for time integration in partial differential equations, American Society of Thermal and Fluids Engineers (2018) 151–158doi:10.1615/TFEC2018.cfd.021966.

[47] M. Hochbruck, J. Leibold, An implicit-explicit time discretization scheme for second-order semilinear wave equations with application to dynamic boundary conditions, Numerische Mathematik 147 (2021) 869–899. doi:10.1007/s00211-021-01184-w.

[48] A. Preuss, J. Lipoth, R. J. Spiteri, When and how to split? a comparison of two imex splitting techniques for solving advection–diffusion–reaction equations, Journal of Computational and Applied Mathematics 414 (2022) 114418. doi:10.1016/j.cam.2022.114418.

[49] T. Ortega, J. Sanz-Serna, Nonlinear stability and convergence of finite-difference methods for the "good" boussinesq equation, Numer. Math. 58 (1990) 215–229. doi:10.1007/BF01385620.

[50] J. López-Marcos, J. Sanz-Serna, A definition of stability for nonlinear problems, Proceedings of the fourth seminar "NUMDIFF-4" held in Halle. In Numerical treatment of differential equations. Teubner-Texte zur Mathematik. Leipzig (1988).

[51] S. Barbeiro, J. Ferreira, R. Grigorieff, Supraconvergence of a finite difference scheme for solutions in $H^s(0,l)$, IMA Journal of Numerical Analysis 25 (2005) 797–811. doi:10.1093/imanum/dri018.

[52] J. Bramble, S. Hilbert, Estimation of linear functionals on sobolev spaces with application to fourier transforms and spline interpolation, SIAM Journal on Numerical Analysis 7 (1970) 112–124. doi:10.1137/0707006.

[53] S. Barbeiro, S. Bardeji, J. Ferreira, L. Pinto, Non-fickian convection–diffusion models in porous media, Numerische Mathematik 138 (2017) 869–904. doi:10.1007/s00211-017-0922-6.

[54] L. Pinto, Parabolic partial integro-differential equations: Superconvergence estimates and applications, PhD dissertation, University of Coimbra (2013).

[55] P. Forsyth, P. H. Sammon, Quadratic convergence cell-centered grids, Applied Numerical Mathematics 4 (1988) 377–394. doi:10.1016/0168-9274(88)90016-5.

[56] R. Grigorieff, Some stability inequalities for compact finite difference operators, Mathematische Nachrichten 135 (1986) 93–102. doi:10.1002/mana.19881350110.

[57] F. de Hoog, D. Jackett, On the rate of convergence of finite difference schemes on nonuniform grids, Journal Australian Mathematical Society, Serie B (1988) 377–394doi:10.1017/S0334270000004495.

[58] H. O. Kreiss, T. Manteuffel, B. Swartz, B. Wendroff, J. A. B. White, Supraconvergent schemes on irregular grids, Mathematics Of Computation 47 (1986) 537–554. doi:10.2307/2008171.

[59] T. Manteuffel, J. A. B. White, The numerical solution of second order boundary value problems on nonuniform meshes, Mathematics Of Computation 47 (1986) 511–535. doi:10.2307/2008170.

[60] A. Weiser, M. F. Wheeler, On convergence of block-centered finite difference for elliptic problems, SIAM Journal of Numerical Analysis 25 (1988) 351–375.

[61] J. Ferreira, R. Grigorieff, On the supraconvergence of elliptic finite difference schemes, Applied NUmerical Mathematics 28 (1998) 275–292. doi:10.1016/S0168-9274(98)00048-8.

[62] R. Adams, J. Fournier, Sobolev Spaces, 2nd Edition, Vol. 140, Elsevier, 2003.

[63] J. Borges, J. A. Ferreira, G. Romanazzi, E. Abreu, Drug release from viscoelastic polymeric matrices - a stable and supraconvergent fdm, Computers and Mathematics with Applications 99 (2021) 257–269. doi:10.1016/j.camwa.2021.08.007.

[64] J. A. Ferreira, Métodos adaptativos para problemas parabólicos: Estudo da convergência, PhD dissertation, University of Coimbra (1994).

[65] S. Kawashima, Systems of hyperbolic-parabolic composite type with applications of magnetohydrodynamics, PhD dissertation, Kyoto University (1983).

[66] Y. Shizuta, S. Kawashima, Systems of equations of hyperbolic-parabolic type with applications to the discrete boltzmann equation, Hokkaido Mathematical Journal 14 (2) (1985) 249 – 275. doi:10.14492/hokmj/1381757663.

[67] E. Tsyganov, D. Hoff, Systems of partial differential equations of mixed hyperbolic–parabolic type, Journal of Differential Equations 204 (1) (2004) 163–201. doi:10.1016/j.jde.2004.03.010.

[68] M.-C. Chen, M.-H. Ling, K.-W. Wang, Z.-W. Lin, B.-H. Lai, D.-H. Chen, Near-infrared light-responsive composite microneedles for on-demand transdermal drug delivery, Biomacromolecules 16 (2015) 1598–1607. doi:10.1021/acs.biomac.5b00185.

[69] W. Zhan, F. R. y Baena, D. Dini, Effect of tissue permeability and drug diffusion anisotropy on convection-enhanced delivery, Drug Delivery 26 (2019) 773–781. doi:10.1080/10717544.2019.1639844.

[70] I. Mansoor, J. Lai, S. R. et al., A microneedle-based method for the characterization of diffusion in skin tissue using doxorubicin as a model drug, Biomed Microdevices 17 (2015) 61. doi:10.1007/s10544-015-9967-4.

[71] H. Lee, C. Song, S. Baik, D. Kim, T. Hyeon, D.-H. Kim, Device-assisted transdermal drug delivery, Advanced Drug Delivery Reviews 127 (2018) 35–45. doi:10.1016/j.addr.2017.08.009.

[72] D. Ramadon, M. T. C. McCrudden, A. J. Courtenay, R. F. Donnelly, Enhancement strategies for transdermal drug delivery systems: current trends and applications, Drug Delivery and Translational Research (2021) 1–34doi:10.1007/s13346-021-00909-6.

[73] T. Jiang, G. Xu, G. Chen, Y. Zheng, B. He, Z. Gu, Progress in transdermal drug delivery systems for cancer therapy, Nano Research 13 (2020) 1810–1824. doi:10.1007/s12274-020-2664-5.

[74] O. Lee, K. Page, D. Ivancic, I. Helenowski, V. Parini, M. E. Sullivan, J. A. Margenthaler, R. T. Chatterton, B. Jovanovic, B. K. Dunn, B. M. Heckman-Stoddard, K. Foster, M. Muzzio, J. Shklovskaya, S. Skripkauskas, P. Kulesza, D. Green, N. M. Hansen, K. P. Bethke, J. S. Jeruss, R. Bergan, S. A. Khan, A randomized phase II presurgical trial of transdermal 4-hydroxytamoxifen gel versus oral tamoxifen in women with ductal carcinoma in situ of the breast, Clinical Cancer Research 20 (2014) 3672–3682. doi:10.1158/1078-0432.ccr-13-3045.

[75] Z. Zhao, A. Ukidve, A. Dasgupta, S. Mitragotri, Transdermal immunomodulation: Principles, advances and perspectives, Advanced Drug Delivery Reviews 127 (2018) 3–19. doi:10.1016/j.addr.2018.03.010.

[76] D. Gabriel, T. Mugnier, H. Courthion, K. Kranidioti, N. Karagianni, M. C. Denis, M. Lapteva, Y. Kalia, M. Möller, R. Gurny, Improved topical delivery of tacrolimus: A novel composite hydrogel formulation for the treatment of psoriasis, Journal of Controlled Release 242 (2016) 16–24. doi:10.1016/j.jconrel.2016.09.007.

[77] M.-C. Chen, Z.-W. Lin, M.-H. Ling, Near-infrared light-activatable microneedle system for treating superficial tumors by combination of chemotherapy and photothermal therapy, ACS Nano 10 (2015) 93–101. doi:10.1021/acsnano.5b05043.

[78] Y. Yang, J. Aw, B. Xing, Nanostructures for NIR light-controlled therapies, Nanoscale 9 (2017) 3698–3718. doi:10.1039/c6nr09177f.

[79] M. L. B. Kaoui, G. Pontrelli, Mechanistic modelling of drug release from multi-layer capsules, Computers in Biology and Medicine 93 (2018) 149–157. doi:10.1016/j.compbiomed.2017.12.010.

[80] S. K. P. P. R. Yadav, L. J. Dobson, D. B. Das, Swellable microneedles based transdermal drug delivery: Mathematical model development and numerical experiments, Chemical Engineering Science 247 (2022). doi:doi:10.1016/j.ces.2021.117005.

[81] D. J. Bora, R. Dasgupta, Numerical simulation of iontophoresis for in-silico prediction of transdermal drugs in the dermal layers using skin impedance values, Computer Methods and Programs in Biomedicine 214 (2022). doi:10.1016/j.cmpb.2021.106551.

[82] K. McLean, W. Zhan, Mathematical modelling of nanoparticle-mediated topical drug delivery to skin tissue, International Journal of Pharmaceutics 611 (2022). doi:10.1016/j.ijpharm.2021.121322.

[83] J. E. D. Sebastia-Saez, A. Burbidge, M. Ramaioli, New trends in mechanistic transdermal drug delivery modelling: Towards an accurate geometric description of the skin microstructure, Computers and Chemical Engineering 141 (2020). doi:10.1016/j.compchemeng.2020.106976.

[84] A. M. Barbero, H. F. Frasch, Effect of stratum corneum heterogeneity, anisotropy, asymmetry and follicular pathway on transdermal penetration, Journal of Controlled Release 260 (2017) 234–246. doi:10.1016/j.jconrel.2017.05.034.

[85] M. Schweiger, S. R. Arridge, The finite-element method for the propagation of light in scattering media: Frequency domain case, Medical Physics 24 (1997) 895–902. doi:10.1118/1.598008.

[86] B. W. Pogue, M. S. Patterson, Frequency-domain optical absorptionspectroscopy of finite tissue volumes using diffusion theory, Physics in Medicine & Biology 39 (1994) 1157–1180. doi:10.1088/0031-9155/39/7/008.

[87] S. McGinty, A decade of modelling drug release from arterial stents, Mathematical Biosciences 257 (2014) 80–90. doi:10.1016/j.mbs.2014.06.016.

[88] Y. Gu, Q. Gu, Q. Yang, M. Yang, S. Wang, J. Liu, Finite element analysis for predicting skin pharmacokinetics of nano transdermal drug delivery system based on the multilayer geometry model, International Journal of Nanomedicine Volume 15 (2020) 6007–6018. doi:10.2147/ijn.s261386.

[89] C. Ash, M. Dubec, K. Donne, T. Bashford, Effect of wavelength and beam width on penetration in light-tissue interaction using computational methods, Lasers in Medical Science 32 (2017) 1909–1918. doi:10.1007/s10103-017-2317-4.

[90] J. A. Nelder, R. Mead, A simplex method for function minimization, The Computer Journal 8 (1965) 27–27. doi:10.1093/comjnl/8.1.27.

[91] D. X. Nguyen, Development of thermosensitive injectable hydrogel and transdermal controlled release formulations for tacrolimus, PhD dissertation, Oregon State University (2018).

[92] S. Shaikh, A. Birdi, S. Qutubuddin, E. Lakatosh, H. Baskaran, Controlled release in transdermal pressure sensitive adhesives using organosilicate nanocomposites, Annals of Biomedical Engineering 35 (2007) 2130–2137. doi:10.1007/s10439-007-9369-8.

[93] P. Singh, A. Carrier, Y. Chen, S. Lin, J. Wang, S. Cui, X. Zhang, Polymeric microneedles for controlled transdermal drug delivery, Journal of Controlled Release 315 (2019) 97–113. doi:10.1016/j.jconrel.2019.10.022.

[94] P. Anantaworasakul, W. Chaiyana, B. B. Michniak-Kohn, W. Rungseevijitprapa, C. Ampasavate, Enhanced transdermal delivery of concentrated capsaicin from chili extract-loaded lipid nanoparticles with reduced skin irritation, Pharmaceutics 12 (2020) 463. doi:10.3390/pharmaceutics12050463.

[95] J. Ferreira, D. Jordão, L. Pinto, Drug delivery enhanced by ultrasound: Mathematical modeling and simulation, Computers & Mathematics with Applications 107 (2022) 57–69. doi:10.1016/j.camwa.2021.12.008.

[96] A. Hossein, Z. Kalkhorana, O. Vahidia, S. Naghib, A new mathematical approach to predict the actual drug release from hydrogels, European Journal of Pharmaceutical Sciences 111 (2018) 303–310. doi:10.1016/j.ejps.2017.09.038.

[97] J. Ferreira, M. Grassi, E. G. no, P. de Oliveira, A 3D model for mechanistic control drug release, SIAM Journal on Applied Mathematics 74 (2014) 620–633. doi:10.1137/130930674.